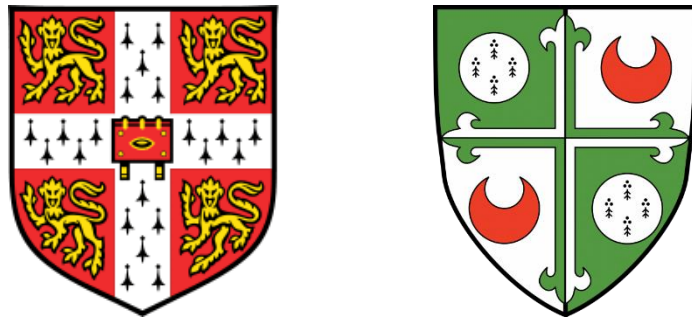


The Lipid-Facing M4 Helix of $\alpha 4\beta 2$ nACh and 5-HT_{3A} Receptors



Susanne Marie Mesøy

Supervisor: Professor Sarah Lummis

Department of Biochemistry

University of Cambridge

This dissertation is submitted for the degree of

Doctor of Philosophy

Girton College

December 2021

To Kate Carlsen, who taught me so much, and loved me even more

Acknowledgments

My great thanks go to the Lummis lab, which has been a fantastically warm, exciting, and supportive place to do my PhD work. My supervisor, Professor Sarah Lummis, has guided my journey into the world of both pLGICs and scientific thinking and experiment design. She has given me opportunities to learn and try new things and grow as a scientist at every step of the way, and the space and encouragement to develop my skills in research, presentation, communication, and science enthusiasm! Steve Devenish, Kerry Price, and Jenny Jeffreys were the best lab I could have wished for to learn from; they welcomed me with open arms, taught me the ways of the lab, checked many an early presentation for missteps, and endlessly encouraged my witty wordplay. I owe you all so much, and cannot thank you enough. Tea is on me, any time. James Mocatta was my first student, and Merryn Hughes, Anya Weber, Kathleen Bowman, Dorottya Fricska and Kate Crowther followed over time in his footsteps as supervisees in the lab, and I thank them for their patience with my overexcitedness, and their excellent science. I thank Emily Capes for crises averted and endless tubes taken/put/spun/frozen/thawed, and teaching me many secrets of the department.

I am grateful to AstraZeneca for their financial support. Their backing far exceeded just the financial aspect, and I am extremely thankful for the wide and fascinating range of AZ events I was able to attend. The annual PhD seminar provided fantastic opportunities for learning and presentation, and the opportunity to reach outside academia and interact so deeply with so many interesting people was invaluable. Particular thanks to Mike Snowden for being unrelentingly inspiring, and Micheal Tonge for enthusiasm and endless administrative and practical support. My excellent AstraZeneca supervisor, Matthew Bridgland-Taylor, brought many new perspectives to my work, gave me much insight, and always encouraged me to consider other points of view than my own, for which I am very thankful.

The second half of my PhD was all made possible by a fantastic collaboration with Alessandro Crnjar and Carla Molteni at King's College London. Many thanks to Alessandro for hours of scientific dialogue, challenging me on so many assumptions, providing me with so much data to play with, and for finding the next steps in a project I'd met the wall with, which led to really interesting places.

Massive thanks to Skylab for being the best neighbors and friends a lab could wish for. Sam Salvage in particular for, beyond friendship, teaching me the technique I needed to prove my discoveries were real, to Samir for encouraging me right from the beginning, and David for his in-Jenny-ous wordplay. Skylab kept me going through many a late night or rough week, and I will always treasure my time there and the people I got to share it with. The Hopkins tea room was a haven of warmth and cool people. My unending thanks to the good people of the tea room who provided tea and sausage rolls and a friendly face on the hardest of days.

Sitting down with the tea allowed me to widen my experience of the Department beyond my nearest neighbor labs, and this provided for many a helpful scientific conversation, interesting facts learned, and great people met. Barney, Isabel, Adrian, Paolo, and the rest of the Howe lab welcomed me around their tea table. Katy is the best symposium co-planner, breakout room creator, and all-round inspire-er. I would like to especially thank Martin Welch for a judicious mix of good advice, generous support, and sarcastic commentary.

The lively openness of the Biochemistry Department gave me many opportunities to practice not only good science, but a range of science communication, from open days to school and artist visits. Particular thanks to my Advisor Tony Jackson and my Graduate Thesis Panel, Ben Luisi and Bill Broadhurst, for excellent advice and warm encouragement along the way. Beyond the concrete interactions we had, knowing that I had someone to talk to if needed was a constant reassurance. Thanks to Juan Mata for leading my first PRG and his enthusiasm in all our interactions. The University provided a rich and fruitful place for my work, with excellent training and resources. Many thanks to Florian Pein from the Statistical Laboratory at the Centre for Mathematical Sciences for helping me get my stats right.

Girton College has truly been a home away from home for me, and provided support and resources throughout my time there. The opportunities to mix with other students and attend the fascinating fellows' talk evening, and meet people from all corners of academia and find the strangest overlaps between our work have been incomparable. The pastoral support has been steady and solid, and I would particularly like to thank my tutor Hilary Marlowe. Tim Boniface helped me immeasurably, and I am endlessly grateful to all the administrative staff whose efficiency and kindness made my student time so easy. The porters have also been unfailingly kind and helpful in so many ways, and I thank them for that.

Throughout my time at Cambridge I have been inexpressibly lucky for so many good friends in the UK who have made my time here a dream. My warmest thanks to: Lizzie and Jonny

for a haven and a spare bed wherever you've lived, and for having such spacious furniture with so many nooks and crannies. Tom and Helena, for dinners galore and teaching me new words for 'hill'. My fantastic HUB group: Sam, Lizzie, James, Cesar, Sarah, Becky, Tom, and other HUB group members throughout the years, to Vic for truly unfailing generosity, and to StAG for being my family in Cambridge. My housemates at 101 Beaumont Road: Jenny, Sam, Zoe, Amy, Becky, and Sarah, for food and warmth and food, also food. To Hannah, Colin, Helen, Olivia, Nick, Sarah, Ned, Bob, Joss, Fred, Joe, Mati, Matthew, Lewis, Baskaran, and many others for company and commiseration. To the swing and folk dancing people of Cambridge, to the Round, and to all my argentine tango friends.

My family and friends in Norway have both shaped me as a person and a scientist, and supported me through my PhD. Thanks to Henrik, Sigrun, Ellen, Magnus, Ingrid, and Signe for making Norway feel like home even before I lived there. To Pål and Janne and Maiken and Atle, for such happy summer times together. To Fredrik and Dagrun and Marit and Håkon for warm welcomes up north. To Kate and Kurt and Harald and Kari, my incomparable grandparents, who have always supported me in everything. To Jens and Kjersti and Egil and Anne for much joy. To Torkild, Inger, Farfar, Maria, Ellisiv, Sondre, Eva, Marie (Landsem), Heidi, Marie (Lyngmo), Ole Fredrik, Katrina, Alf og Torill, for so much. To Torleif and Kirsti for such warmth. To Nan, for being there from the very beginning. To teachers through the years, including Sally Lazanas, Leif Thore Jelmert, Astrid Dick, Bibbi, Håkon Skånland, Arnhild Mindrebø, Kristin Finstad, Moritz Røyr, and many more for enthusiasm and encouragement

A very special thanks goes to my partner Matthew, whose gentle encouragement has lifted me up in more ways than I thought possible. Thanks to his parents, David and Brigitte, for enthusiastic support, especially hosting me for the last two weeks of thesis writing. Merry Christmas 2021!

Finally, I would like to thank my parents. My mother, for sharing with me her creativity and joy and people skills, and for proof-reading this entire (!) dissertation. My father, for teaching me precise and careful thinking, and how to evaluate and prioritise. You have both shown me so much support, and your love for me gave me the security and space and freedom to find myself, to appreciate my skills and talents, and that has formed the backbone of how I did most of the work that follows here, and so many other things. Thank you.

Declaration

This thesis is the result of my own work and includes nothing which is the outcome of work done in collaboration except as declared in the Preface and specified in the text. I further state that no substantial part of my thesis has already been submitted, or, is being concurrently submitted for any such degree, diploma or other qualification at the University of Cambridge or any other University or similar institution except as declared in the Preface and specified in the text. It does not exceed the prescribed word limit for the relevant Degree Committee

Susanne Marie Mesøy

December 2021

The Lipid-Facing M4 Helix of $\alpha 4\beta 2$ nACh and 5-HT_{3A} Receptors

Susanne Marie Mesøy

Summary

Pentameric ligand-gated ion channels (pLGICs) are expressed throughout the human nervous system, and contribute to a range of muscle, gut, and neurological functions. Elucidating their mechanism of action and how it might be modulated would improve our understanding of the nervous system, and contribute to building tools to treat diseases arising from dysregulated pLGICs.

The outermost lipid-facing transmembrane helix (M4) and the lipids surrounding it have recently emerged as important factors in pLGIC function. To investigate the role of the M4 helix in cation-selective mammalian pLGICs, I studied the effects of mutations in the M4 helices of the 5-HT_{3A} and $\alpha 4\beta 2$ nACh receptors. I used a membrane potential-sensitive fluorescent dye, two-electrode voltage clamp and manual patch-clamp for functional characterisation of mutant receptors in HEK293 cells and *Xenopus* oocytes, and radioligand binding and immunofluorescence to assess ligand binding and receptor expression.

I show that 1 out of 28 alanine mutations in the 5-HT_{3A}R M4 and 8 out of 28 double alanine mutations in the $\alpha 4\beta 2$ nAChR abolish receptor function in HEK cells without ablating ligand binding, indicating that the M4 helices of these cation-selective pLGICs are involved in, and can modulate, receptor function. I explored the mechanism of action of these key M4 residues by characterising prospective interaction partners, and identified a potential chain of interactions going from the outermost M4 helix all the way to the channel pore.

I also show that eight of the nine 5-HT_{3A}R and $\alpha 4\beta 2$ nAChR mutants that showed ligand binding but no receptor function in HEK cells, showed WT-like function when expressed in *Xenopus* oocytes. In addition, M4 mutations that altered the function of receptors expressed

in HEK cells had different effects on receptors expressed in oocytes. Together this shows that the role of the M4 helix in cation-selective pLGIC function depends on the expression system.

For comparison, I investigated another peripheral helix in the 5-HT_{3A}R; the N-terminal helix, which rests above the extracellular domain of mammalian pLGICs, and showed that it is important for correct receptor expression.

Overall, this work shows that the M4 helix of cation-selective pLGICs is an attractive target for receptor modulation by small-molecule binding, as this helix is both accessible, poorly conserved between pLGICs, and intimately involved in receptor function. It has also laid the groundwork for further understanding the functional mechanism of pLGICs, especially the interactions of the M4 helices and with the rest of the transmembrane helical bundle. Finally, it has highlighted the dependency on the expression system of both pLGIC function and of the role of the M4 helix, and emphasises the need to understand the native environment of these receptors and how that modulates function.

Table of Contents

List of figures	xiii
List of tables	xv
Papers arising from this PhD	xvi
Nomenclature	xvii
Chapter 1 Introduction	1
1.1 Pentameric ligand-gated ion channels	1
1.1.1 Structure	2
1.1.2 Mechanism of receptor function	6
1.1.3 Cation-selective pLGICs in human health	9
1.2 Role of M4 in pLGICs	15
1.2.1 Role of the M4 helix in bacterial pLGICs	16
1.2.2 Role of the M4 helix in anion-selective pLGICs	18
1.2.3 Role of the M4 helix in cation-selective pLGICs	19
1.2.4 Site-directed mutagenesis as a tool for understanding pLGIC function	23
1.3 Expression systems for studying pLGICs	24
1.3.1 HEK293 cells	24
1.3.2 <i>Xenopus</i> oocytes	25
1.3.3 Membrane composition	25
1.4 Trafficking of cation-selective pLGICs	28
1.4.1 Improving functional expression of cation-selective pLGICs	29
1.5 Aims summary	31
Chapter 2 Materials and methods	32
2.1 DNA and RNA	32
2.2 HEK293 cells	33
2.2.1 HEK cell culture and receptor expression	33
2.2.2 Fluorescent membrane potential assay	33
2.2.3 Electrophysiology	34
2.2.4 Radioligand binding	35
2.3 <i>Xenopus</i> oocytes	36
2.3.1 Oocyte harvesting and receptor expression	36
2.3.2 Current recordings	36
2.4 Computational methods	37
Chapter 3 The role of the M4 helix in the 5-HT _{3A} receptor	38
3.1 Introduction	38

3.2 Results	38
3.2.1 Characterisation of 5-HT _{3A} Rs with M4 alanine substitutions	38
3.2.2 Potential interaction partners of Y4.7	53
3.2.3 Molecular dynamics and mechanism of action of Y4.7	56
3.3 Discussion	66
3.3.1 Role of D4.0 in 5-HT _{3A} R function.....	66
3.3.2 Role of W4.25 and aromatic residues in M4 in 5-HT _{3A} R function	68
3.3.3 Role of Y4.7 in 5-HT _{3A} R function.....	68
3.4 Conclusions	76
Chapter 4 The role of the M4 helix in the $\alpha 4\beta 2$ receptor	77
4.1 Introduction	77
4.2 Results	78
4.2.1 Characterisation of $\alpha 4\beta 2$ nAChRs with M4 alanine substitutions.....	78
4.2.2 Characterisation of $\alpha 4\beta 2$ nAChRs with M4 non-alanine substitutions	85
4.2.3 Potential interaction partners of key M4 residues.....	87
4.3 Discussion	90
4.3.1 Expression of non-responsive mutant receptors	90
4.3.2 Potential roles of key M4 residues.....	91
4.3.3 Potential interaction partners of key M4 residues.....	96
4.4 Conclusions	97
Chapter 5 The role of the M4 helix in cation-selective pLGICs depends on the environment	98
5.1 Introduction	98
5.2 Results	99
5.2.1 Single-cell assays of 5-HT _{3A} receptors	99
5.2.2 Single-cell assays of $\alpha 4\beta 2$ nACh receptors	105
5.3 Discussion	108
5.3.1 Most mutations that abolish 5-HT _{3A} or $\alpha 4\beta 2$ receptor function in HEK293 cells have little effect in <i>Xenopus</i> oocytes	109
5.3.2 Most M4 mutations that alter 5-HT _{3A} or $\alpha 4\beta 2$ receptor function in HEK cells have different effects in <i>Xenopus</i> oocytes	116
5.4 Conclusion.....	117
Chapter 6 The N-terminal helix of the 5-HT _{3A} receptor.....	119
6.1 Introduction	119
6.1.1 Ligand binding near the N-terminal helix.....	119
6.1.2 The N-terminal helix in other pLGICs.....	121
6.1.3 The N-terminal helix in the 5-HT _{3A} receptor.....	123
6.2 Results	124

6.2.1	Characterisation of 5-HT _{3A} Rs with NTH alanine and aspartic acid substitutions.....	124
6.2.2	Characterisation of NTH mutant 5-HT _{3A} Rs in <i>Xenopus</i> oocytes	129
6.3	Discussion	130
6.3.1	N-terminal helix 5-HT _{3A} mutant receptors in HEK293 cells.....	130
6.3.2	N-terminal helix 5-HT _{3A} mutant receptors in <i>Xenopus</i> oocytes	132
6.4	Conclusions	132
Chapter 7	Discussion	133
7.1	Consequences	133
7.1.1	Determining the role of M4 in pLGICs	133
7.1.2	Differences in pLGIC function between HEK cells and oocytes	134
7.2	Limitations and future work.....	135
References.....		137

List of figures

Figure 1.1: pLGIC subunits and composition.....	3
Figure 1.2: Structures of pentameric ligand-gated ion channels from selected organisms	5
Figure 1.3: Comparing closed and agonist-bound structures of the 5-HT _{3A} R.....	8
Figure 1.4: Distribution of cation-selective pLGIC subunits in human tissues.....	12
Figure 1.5: Schematic of a 5-HT _{3A} receptor indicating known and predicted ligand binding sites	14
Figure 1.6: Sequence alignment of selected pLGIC M4 helices	16
Figure 3.1 Typical responses of 5-HT _{3A} receptors in HEK293 cells.....	40
Figure 3.2: Single-point radioligand binding relative to WT of nonresponsive M4 mutants..	44
Figure 3.3: Potential interaction partners of D4.0.....	47
Figure 3.4: Aromatic residues on M4	49
Figure 3.5: Radioligand binding curves.....	52
Figure 3.6: Single-point radioligand binding.....	53
Figure 3.7: Potential interaction partners of Y4.7.....	54
Figure 3.8: Responses of 5-HT _{3A} receptors with Y441-adjacent mutations.....	56
Figure 3.9: Two proposed mechanisms of action for Y4.7.....	57
Figure 3.10: Suggested lipid-dependent structural rearrangements of M4.....	58
Figure 3.11: M4 characteristics in molecular dynamics simulations.....	61
Figure 3.12: Horizontal effects of Y4.7A.	63
Figure 3.13: D238 C γ -K255 terminal nitrogen distance over time	64
Figure 3.14: Sequence alignment of selected pLGIC M1, M2 and M3 helices.....	71
Figure 3.15: Comparing closed and open states of the 5-HT _{3A} receptor.....	75
Figure 4.1: Typical responses of α 4 β 2 nACh receptors in HEK293 cells.....	79
Figure 4.2: Key α 4 β 2 nAChR M4 residues..	82
Figure 4.3: Single-point radioligand binding relative to 'WT of non-responsive M4 mutants.	84
Figure 4.4: Potential M4-M3-M2 link in the α 4 β 2 receptor	88
Figure 4.5: Single-point radioligand binding relative to 'WT of M1/M3 mutants.....	89

Figure 4.6: Potential interaction partners of key M4 residues	94
Figure 5.1: Typical responses of 5-HT _{3A} receptors in Xenopus oocytes.....	99
Figure 5.2: Typical current recordings of 5-HT _{3A} receptors on addition of 3 μM 5-HT.....	100
Figure 5.3: WT and mutant 5-HT _{3AR} responses to 3 μM 5-HT in Xenopus oocytes.....	103
Figure 5.4: Typical responses of 5-HT _{3A} receptors in HEK293 cells with single-cell patch clamp.....	104
Figure 5.5: Typical responses of α4β2 nACh receptors in Xenopus oocytes	106
Figure 5.6: ‘WT and mutant α4β2 receptors in Xenopus oocytes	107
Figure 5.7: Snapshots from MD simulations of the 5-HT _{3A} receptor	113
Figure 5.8: Cholesterol moieties in the 6cnj PDB structure	114
Figure 5.9: Representative snapshot of cholesterol binding representing examples of cholesterol observed in coarse-grained MD simulations	115
Figure 5.10: Changes in EC ₅₀ of α4β2 nACh (top) and 5-HT _{3A} (bottom) receptor mutants in HEK cells and oocytes	117
Figure 6.1: N-terminal helix of the 5-HT _{3A} receptor	120
Figure 6.2: Small molecule binding near the NTH of the GlyR.....	121
Figure 6.3: Sequence alignment of selected pLGICs around the 5-HT _{3AR} NTH.....	122
Figure 6.4: Typical responses of 5-HT _{3A} receptors in HEK293 cells.....	125
Figure 6.5: WT and mutant 5-HT _{3AR} responses in Xenopus oocytes	130

List of tables

Table 1.1: Effects of alanine and aromatic substitutions in pLGIC M4 helices	22
Table 3.1: Parameters of 5-HT _{3A} receptors with M4 alanine substitutions	42
Table 3.2: Parameters of 5-HT _{3A} M4 alanine mutant receptors coexpressed with RIC-3.....	43
Table 3.3: Parameters of 5-HT _{3A} receptors with substitutions of D4.0	45
Table 3.4: Parameters of 5-HT _{3A} receptors with substitutions of potential interaction partners of D4.0	47
Table 3.5: Parameters of 5-HT _{3A} receptors with aromatic substitutions in M4.....	50
Table 3.6: Parameters of 5-HT _{3A} receptors with substitutions of potential interaction partners of Y4.7	54
Table 3.7: Parameters of 5-HT _{3A} receptors with substitutions of K255	65
Table 4.1: Parameters of α4β2 nACh receptors with M4 alanine substitutions (next page) ...	80
Table 4.2: Parameters of α4β2 nACh single M4 mutant receptors.....	83
Table 4.3: Parameters of α4β2 nACh receptors with non-alanine substitutions of key M4 residues	86
Table 4.4: Parameters of α4β2 nACh receptors with alanine substitutions in M1, M2, or M3	89
Table 5.1: Parameters of 5-HT _{3A} receptors in <i>Xenopus</i> oocytes.....	100
Table 5.2: Parameters of 5-HT _{3A} receptors with alanine substitutions in M1-M3 in <i>Xenopus</i> oocytes	102
Table 5.3: Parameters of α4β2 nACh receptors with M4 alanine substitutions	107
Table 5.4: Parameters of additional α4β2 nACh receptors with M4 alanine substitutions ...	108
Table 6.1: Parameters of 5-HT _{3A} receptors with NTH alanine substitutions	126
Table 6.2: Parameters of 5-HT _{3A} receptors with NTH aspartic acid substitutions	127
Table 6.3: Parameters of 5-HT _{3A} receptors with selected NTH substitutions	128

Papers arising from this PhD

Published papers

1. ***Characterization of Residues in the 5-HT₃ Receptor M4 Region That Contribute to Function.** Susanne Mesoy, Jennifer Jeffreys, and Sarah C. R. Lummis *ACS Chemical Neuroscience*, 2019, 10 (7), 3167-3172 doi:10.1021/acschemneuro.8b00603
2. ***M4, the Outermost Helix, is Extensively Involved in Opening of the α 4 β 2 nACh Receptor.** Susanne M. Mesoy and Sarah C. R. Lummis *ACS Chemical Neuroscience*, 2021 12 (1), 133-139 doi: 10.1021/acschemneuro.0c00618
3. ***A Single Mutation in the Outer Lipid-Facing Helix of a Pentameric Ligand-Gated Ion Channel Affects Channel Function Through a Radially-Propagating Mechanism.** Alessandro Crnjar, Susanne M. Mesoy, Sarah C. R. Lummis, Carla Molteni *Frontiers in Molecular Biosciences* 2021 8, 644720 doi: 10.3389/fmolb.2021.644720
4. ***Mutations of the nAChR M4 helix reveal different phenotypes in different expression systems: could lipids be responsible?** Susanne M. Mesoy, Matthew Bridgland-Taylor and Sarah C. R. Lummis.

First author papers indicated by *

Nomenclature

5-HT	5-hydroxytryptamine, serotonin
5-HT ₃ R	5-HT ₃ receptor
ACh	Acetylcholine
AChBP	Acetylcholine binding protein
AU	Arbitrary units
B	Specific binding
C _{ij}	Time-averaged dynamical correlation
CTD	C-terminal domain
EC ₅₀	Half maximal effective concentration
ECD	Extracellular domain
EGFP	Enhanced green fluorescent protein
ELIC	<i>Erwinia chrysanthemi</i> ligand-gated ion channel
ER	Endoplasmatic reticulum
F	Fluorescence
GABA _A R	GABA _A receptor
GLIC	<i>Gloeobacter violaceus</i> ligand-gated ion channel
GlyR	Glycine receptor
ICD	Intracellular domain
K _d	Dissociation constant
MRF	Maximum recorded fluorescence
NACHO	Novel acetylcholine receptor chaperone
nAChR	Nicotinic acetylcholine receptor
n _H	Hill coefficient
NTH	N-terminal helix
pEC ₅₀	-log half maximal effective concentration
pH ₅₀	Half maximal effective pH
PLGIC	Pentameric ligand-gated ion channel

POPE	Phosphatidylethanolamine
POPC	Phosphatidylcholine
PTM	Post-translational modification
RIC-3	Resistance to inhibitors of cholinesterase 3
RMSF	Root mean square fluctuation
SEM	Standard error of the mean
TMD	Transmembrane domain
UT	Untransfected cells
WT	Wild-type
WT+	Wild-type coexpressed with relevant chaperones (RIC-3 or RIC-3 and NACHO)
‘WT	WT $\alpha 4\beta 2$ with an L9’A (L257A) mutation in the $\alpha 4$ subunit
‘WT+	WT $\alpha 4\beta 2$ with an L9’A (L257A) mutation in the $\alpha 4$ subunit coexpressed with RIC-3 and NACHO

PDB structures

6be1	Mouse 5-HT ₃ AR in apo state (Cryo-EM)
6dg8	Mouse 5-HT ₃ AR in serotonin-bound state, state 2 (Cryo-EM)
5kxi	2 α :3 β human $\alpha 4\beta 2$ nAChR with nicotine bound (X-Ray)
6cnj	2 α :3 β human $\alpha 4\beta 2$ nAChR with antibody fragments and nicotine bound (Cryo-EM)

Chapter 1 Introduction

An electrical impulse going along a nerve cell is the fastest long-range form of communication in the human body. When it reaches the synapse, this signal is converted into the form of a physical molecule (the neurotransmitter) that must diffuse across the neuronal junction to the postsynaptic membrane, where it binds to and activates a receptor, carrying the signal into the next nerve cell. Crossing the synapse is a rate-limiting step in nervous communication, and any defect in this process can adversely affect muscle, brain, and gut functions.

A major family of neurotransmitter-gated receptors in humans are the pentameric ligand-gated ion channels (pLGICs), which are expressed throughout the central and peripheral nervous systems and are involved in memory, addiction, pain sensation and anxiety, among other functions. Mutations in pLGICs are correlated with a range of neurological disorders, including epilepsy, schizophrenia, and depression. In this work, I explore the functional mechanism of two pLGICs, the 5-HT_{3A} receptor and the $\alpha 4\beta 2$ nicotinic acetylcholine receptor. In particular, I have focussed on the role of the outermost lipid-facing transmembrane helix, M4. M4 is the most accessible and least conserved of the four pLGIC transmembrane helices. If it is involved in receptor function, it would offer excellent opportunities for specific, targeted modulation of pLGICs, which would be relevant to a range of human and animal diseases.

1.1 Pentameric ligand-gated ion channels

Pentameric ligand-gated ion channels are found in organisms from bacteria to humans and mediate the effects of many common neurotransmitters. The mammalian anion-selective pLGICs are the γ -aminobutyric acid receptors (GABA_{ARs}) activated by GABA and the glycine receptors (GlyRs) activated by glycine. Their activation hyperpolarizes the postsynaptic membrane, inhibiting neuronal signalling. The mammalian cation-selective

pLGICs, which are the focus of this work, include the 5-HT₃ receptors (5-HT₃Rs) activated by serotonin, and the nicotinic acetylcholine receptors (nAChRs) activated by acetylcholine (ACh). Their activation initiates an excitatory postsynaptic potential, promoting neuronal signal initiation.

1.1.1 Structure

pLGICs consist of five monomers arranged in a homo-or hetero-pentamer around the central ion channel pore. Within each family there are several individual subunits, which can combine to form a range of pentamers (Figure 1.1). The principles of assembly are not yet fully understood, though some rules have emerged: the 5-HT₃ receptor appears to require some A subunits to assemble into functional receptors (Holbrook et al. 2009; Niesler et al. 2007), so can form 5-HT_{3A} homopentamers and AB, AC, AD and AE heteropentamers, and potentially more complex combinations. The muscle-type nAChRs at the neuromuscular junction occur in $(\alpha 1)_2\beta 1\delta\epsilon$ or $(\alpha 1)_2\beta 1\delta\gamma$ stoichiometries, while the neuronal nAChRs with their wider range of available subunits are found in various combinations throughout the nervous system (Figure 1.4).

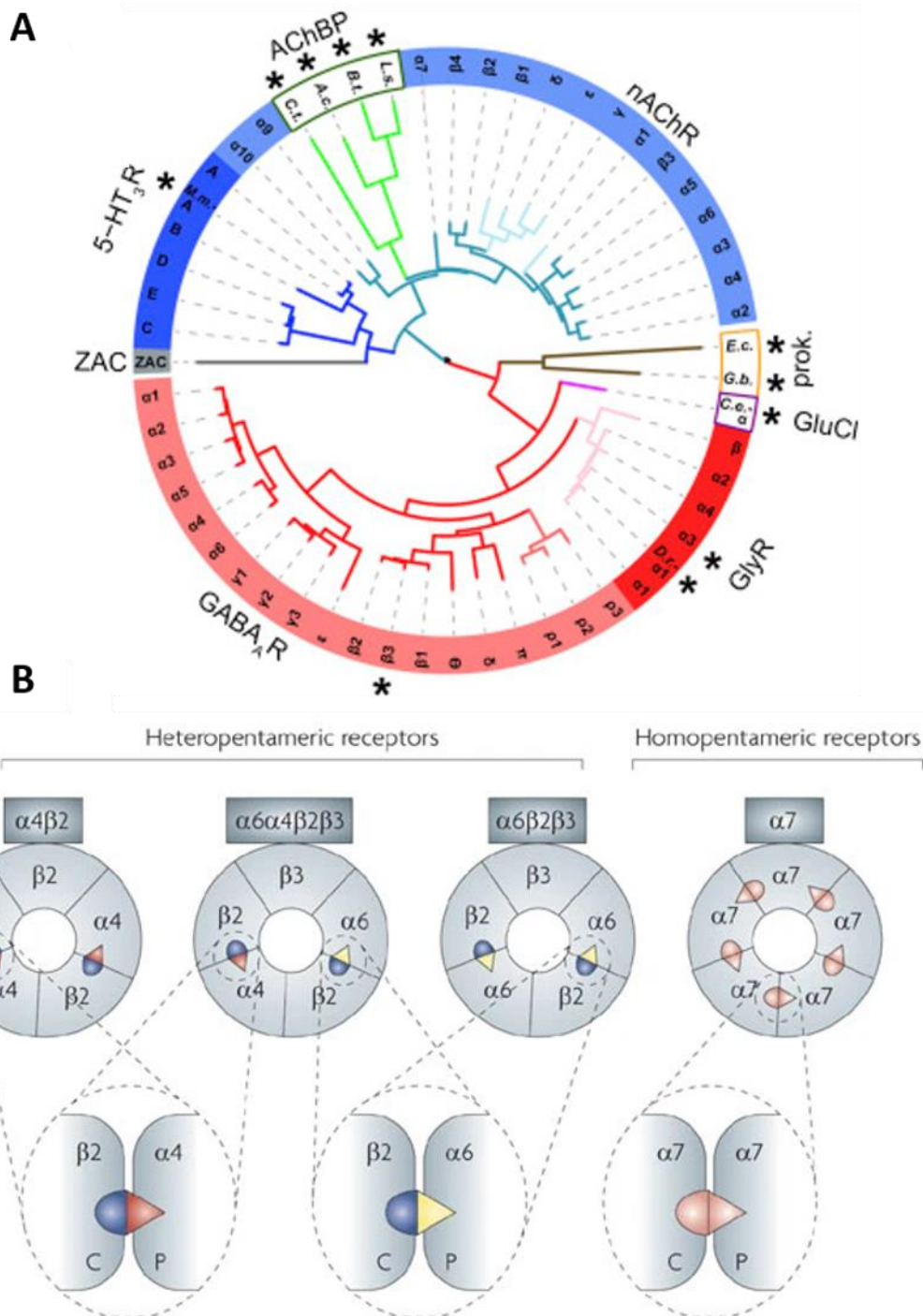


Figure 1.1: pLGIC subunits and composition. A) Subunit diversity of the four major mammalian pLGIC families and selected other receptors. (Reprinted from Neuron, 90, Nemecz Á, Prevost MS, Menny A, Corringer P-J, Emerging Molecular Mechanisms of Signal Transduction in Pentameric Ligand-Gated Ion Channels, 19, Copyright (2016), with permission from Elsevier.) B) Selected nAChR subunit combinations showing relative contributions to the orthosteric ligand binding site. (Reprinted by permission from Springer Nature: Springer Nature, Nature Reviews Drug Discovery, Nicotinic receptors: Allosteric transitions and therapeutic targets in the nervous system, Taly A., Corringer PJ., Guedin D., Lestage P., Changeux JP., Copyright (2009).)

All pLGIC subunits studied so far have the same basic structure (Figure 1.2). The extracellular domain (ECD) predominantly consists of β -sheets, and contains the ligand binding domain in the interface between two subunits. Not all subunits can bind ligand, and the contribution to the ligand binding sites from the primary subunit is different from the complementary subunit (Figure 1.2G). Subunit composition therefore determines ligand binding stoichiometries (Figure 1.1B). The transmembrane domain (TMD) of each monomer contains four α -helices, including the pore-lining helix M2 which contributes to channel gating and ion selectivity (Corringer et al., 1999), helices M1 and M3 which surround the M2 helices, and the lipid-facing helix M4. Some pLGICs also contain an intracellular domain (ICD) formed by a long loop between M3 and M4, which can affect receptor modulation and ion conductance levels (Kelley, Dunlop, et al., 2003).

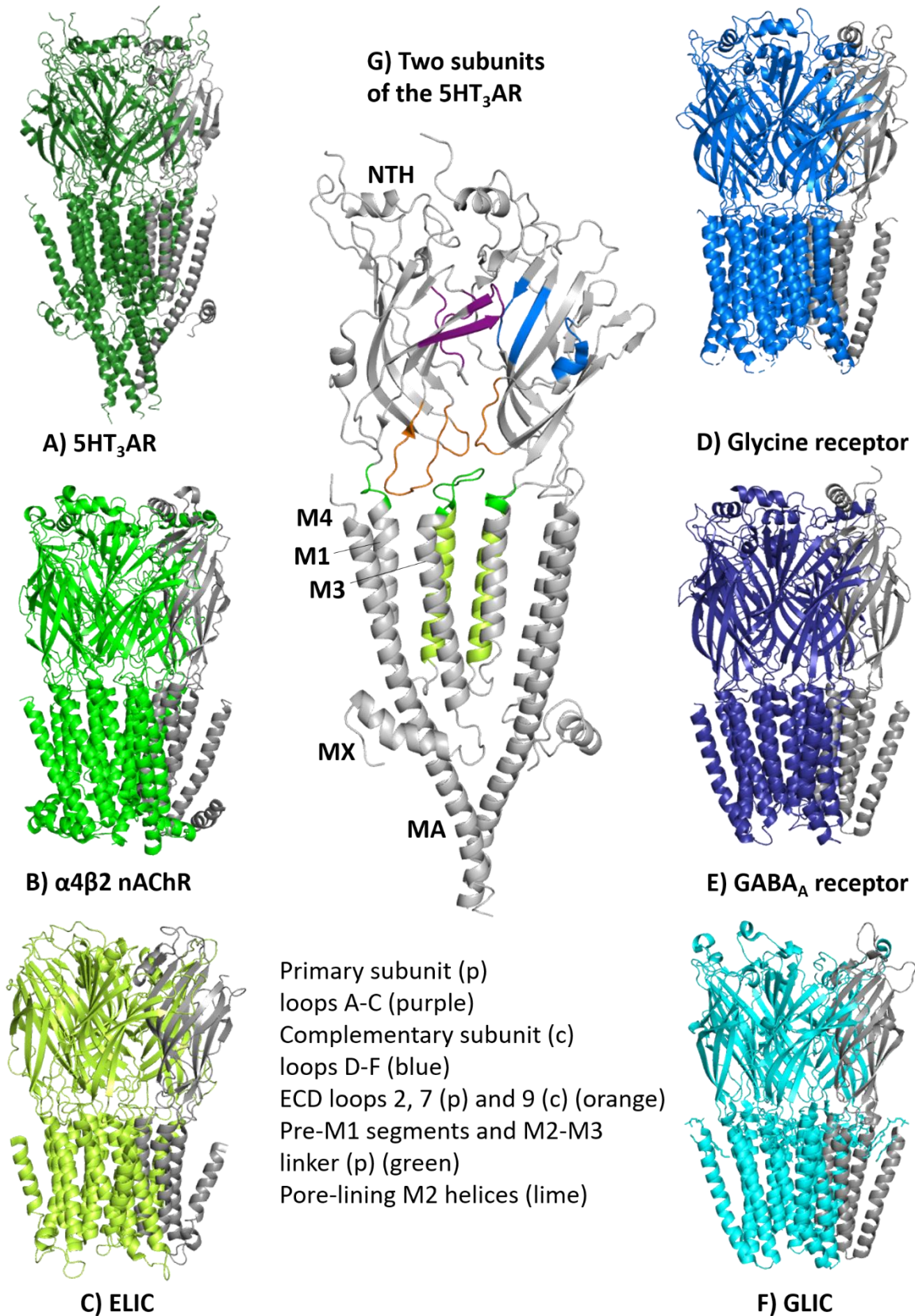


Figure 1.2: Structures of pentameric ligand-gated ion channels from selected organisms. A) *Mus musculus* 5-HT_{3A}R (6be1). B) *Homo sapiens* α4β2 nAChR (5kxi). C) *Erwinia chrysanthemi* ligand-gated ion channel (ELIC, 2yn6). D) *Danio rerio* α1 glycine receptor (3jad). E) *Homo sapiens* β3 GABA_A receptor (4cof). F) *Gloeobacter violaceus* ligand-gated ion channel (GLIC, 3p4w). A-F) single subunit shown in grey. G) Two subunits of the 5-HT_{3A}R highlighting important regions for receptor function, with all helices labelled. The ICD is shortened or not visible in most of these structures.

Signal transduction from the ligand-binding site in the ECD to the channel pore-forming TMD relies on loops reaching down from the ECD, particularly loops 2, 7 and 9 (also known as the Cys-loop), and loops coming up from the TMD, particularly the pre-M1 segment and the M2-M3 loops, and in some cases the CTD (C-terminal domain) of the M4 helix.

1.1.2 Mechanism of receptor function

The neurotransmitter binds to a cleft in the extracellular domain of pLGICs formed by loops A, B and C on the principal subunit, and loops D, E and F on the complementary subunit (Figure 1.2G). Movements that occur on ligand binding to cause channel opening have been deduced from comparing closed and open - or as near to open as can be obtained - structures of the same receptor. Much channel opening mechanism modelling has been based on early bacterial and anionic pLGIC structures. Nemecz et al. (2016) reviews the movements on channel opening in GLIC, the GluCl α receptor, and the GlyR α 1. In short: ligand binding causes an 'un-blooming' movement of the ECD, involving a clockwise rotation and closer packing of the subunits. The M2 helices in the TMD undergo an anticlockwise rotation and either a kinking or tilting motion away from the pore, opening the hydrophobic gates at the levels of residues 9' and 16'. The residues of the M2 helix are numbered from 0' (a highly conserved positively charged residue at the intracellular end of the pore), with positive numbers towards the extracellular end, and negative numbers further down. The 2', 6', 9', 13' and 16' residues line the pore of most pLGICs. The movements of the M2-M3 loops in these structural transitions implicate it in communicating the ligand-binding signal to the TMD.

Later structures and work in cation-selective receptors have added nuance to these observations and allow for predictions of potential differences between anion-selective and cation-selective receptor mechanisms. The recent structures of inhibited and proposed active and pre-active or desensitized mouse 5-HT_{3A} receptors (Basak, Gicheru, Rao, et al., 2018; Basak, Gicheru, Samanta, et al., 2018; Polovinkin et al., 2018) have given much insight into the mechanism of action of the 5-HT_{3A}R.

The open structure from Basak, Gicheru, Rao, et al. (2018) (yellow and blue, Figure 1.3) shows an anti-clockwise rotation of the ECD on opening compared to the closed structure from Basak, Gicheru, Samanta, et al. (2018) (pink, Figure 1.3). There is a clockwise rotation of the TMD, including the TMD helices expanding away from the channel pore, all accompanied by the M2-M3 loop moving outwards, away from the pre-M1 region. In this structural comparison the M4 helix straightens markedly on opening, going from the top tilted outwards to almost perpendicular to the membrane, and the MX helix moves 23Å away from the receptor. This contrasts with the observed closed-open transition for GLIC, where the M4 does not move much, and no MX helix has been observed (Nemecz et al., 2016).

The Polovinkin et al. (2018) structural comparisons show an anticlockwise twist and expansion of the whole TMD on ligand binding, with M4 sliding up compared to the rest of the TMD, changing its relative position dramatically, and the MX helix again moving away from the rest of the protein. The FPF motif on loop 9 (the Cys-loop) is close to M2 in the closed structure, and nearer M1 and M4 in the proposed open structure, where it also pushes close to the M2-M3 loop, implicating roles for all these segments in cation-selective pLGIC channel opening.

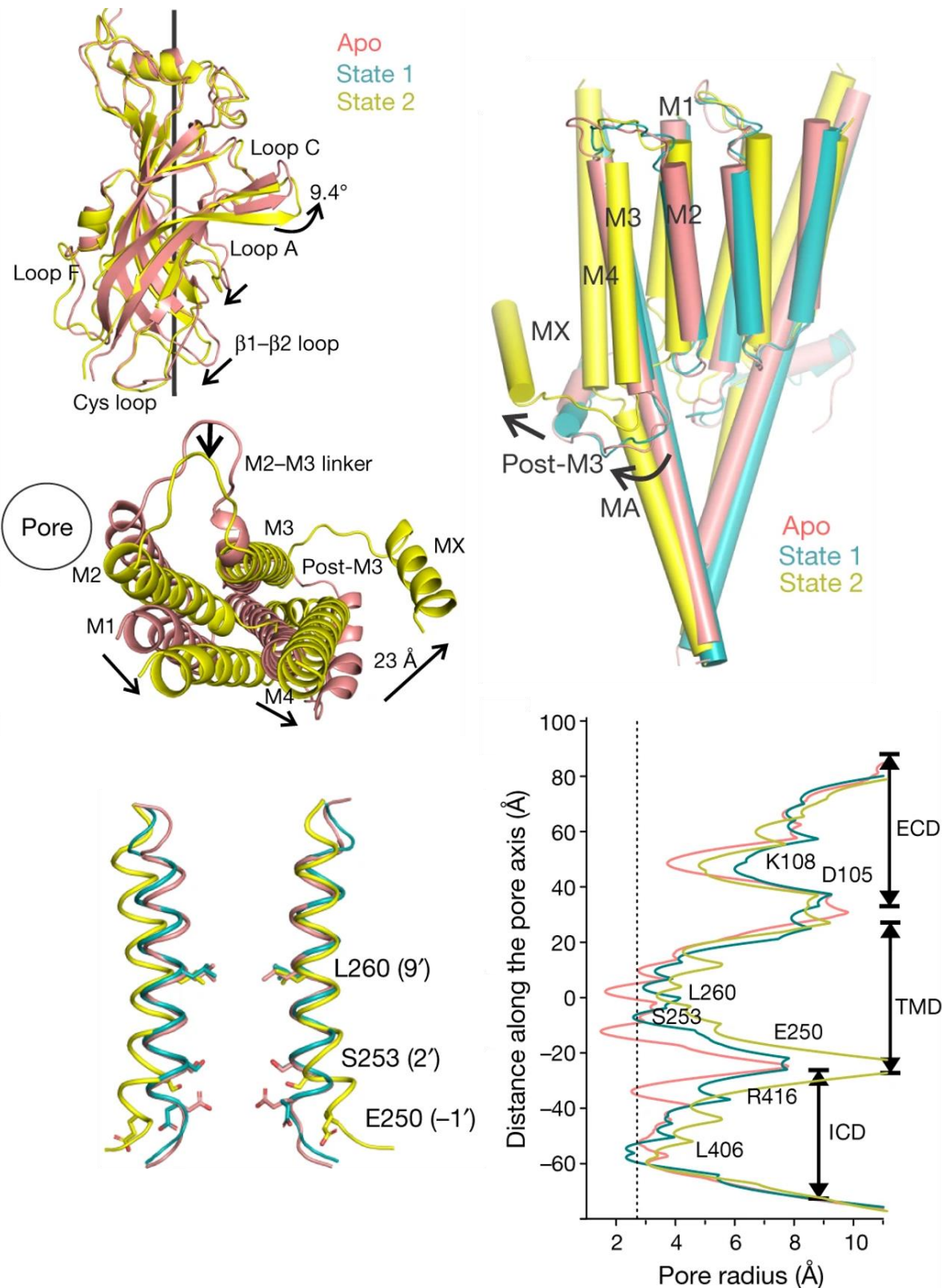


Figure 1.3: Comparing closed and agonist-bound structures of the 5-HT₃AR. Closed (apo) structure in pink, and the agonist-bound structure with the widest channel pore (state 2) in yellow. Another agonist-bound structure (state 1) in blue. (Reprinted by permission from Springer Nature: Springer Nature, Cryo-EM reveals two distinct serotonin-bound conformations of full-length 5-HT_{3A} receptor, Basak S, Gicheru Y, Rao S, Sansom MSP, Chakrapani S, Copyright (2018).)

Recent structures of the $\alpha 7$ nAChR in resting, open, and desensitized states show an anti-clockwise twist and compaction ('unblooming') of the ECD on the resting-open transition (Noviello et al., 2021). In the transmembrane domain, this transition shows an outward movement of the M2 helices, and no clockwise rotation of the other transmembrane helices, but instead a marked change in their tilt angles relative to the membrane. In addition to this, the M4 helix moves 'upwards' by about one helical turn (as in the 5-HT₃R). This movement does not disrupt the salt bridge between the intracellular ends of M4 and M2 (D445-K238), which indicates that the tilting and movement of M1, M3, and especially M4, could contribute to the outwards movement of the intracellular end of M2 in channel opening. In the ICD, receptor opening causes a partial unwinding of the α -helix at the MA-M4 junction (as the M4 helix moves away from the MA helix, also seen in the 5-HT₃R), and a counter clockwise movement of the MX helix away from the M4 (the MX helix does move 'upwards' in tandem with the M4, so it remains at the same height relative to the M4 helix).

1.1.3 Cation-selective pLGICs in human health

1.1.3.1 Functional roles and distribution of cation-selective pLGICs

The 5-HT₃R controls parts of the vomiting/nausea pathway, as evidenced by the range of 5-HT₃R antagonists that are highly effective anti-emetics, e.g. ondansetron and granisetron, (Theriot and Ashurst, 2019). Initial studies of 5-HT_{3A} receptor knockout mice showed normal feeding, motor function and sexual behaviour, but did find reduced sensitivity to chronic, but not acute, injury-induced pain sensation in the knockout mice (Zeitz et al., 2002). Further studies found that the knockout mice displayed reduced anxiety (Kelley, Bratt, et al., 2003),

with some effects being sex-dependent (Bhatnagar et al., 2004), and impaired social behaviour (Smit-Rigter et al., 2010).

Single nucleotide polymorphisms in 5-HT₃ receptor-coding genes are also informative: for example, Y129S mutation in the 5-HT_{3B} receptor has been found to be associated with protection against major depression in females in a Japanese population (Yamada et al., 2006), and with protection against nausea under treatment with paroxetine in a mixed Japanese population (Sugai et al., 2006). This mutation has been shown to substantially increase maximal receptor response to serotonin compared to WT (wild-type) receptors, without measurably affecting their EC₅₀ values as measured by either a fluorescent membrane potential-sensitive dye, an intracellular Ca²⁺ assay, or whole-cell electrophysiological recordings of HEK293 cells (Krzywkowski et al., 2008). This was not due to changes in expression levels, but rather slowed deactivation and desensitization as measured by both whole-cell electrophysiology and single-channel measurements.

The expression levels of 5-HT₃ receptors also appears to tune their function: a single nucleotide polymorphism (C178T) in the 5' untranslated region of the 5-HT_{3A} gene that was shown to increase translation of the downstream gene, is associated with bipolar disorder in a German population (Niesler et al., 2001). Frank et al., (2004) also finds a 3 bp deletion in the 5' untranslated region of the 5-HT_{3B} gene is underrepresented in bipolar affected patients compared to controls. This variant is also correlated with higher chemotherapy induced emesis (Tremblay et al., 2003).

Further research indicates a potentially broader role for these receptors, finding that they are involved in depression, body weight control, memory deficit disorders, and irritable bowel syndrome (Fakhfouri et al., 2019), as well as schizophrenia, autism, eating disorders and bipolar affective disorder (Walstab et al., 2010). Drug studies support putative roles for 5-HT₃ receptors in pain, GI disorders, addiction and appetite modulation, as described in more detail in section 1.1.3.2.

mRNA for the 5-HT_{3A} subunit is widely distributed in adult human brain and internal organ tissues, and has been found in a range of immune system cells (Fiebich et al., 2004; Miyake et al., 1995). mRNA of the 5-HT_{3B} subunit has been found in several areas of human brain

(Davies et al., 1999). mRNA of 5-HT_{3D} has been found to be restricted to kidney, colon and liver, and 5-HT_{3E} mRNA to colon and intestine alone in Niesler et al. (2003) (Figure 1.4A), though Holbrook et al. (2009) find the E subunit mRNA widely distributed throughout human tissues, including various brain areas (Figure 1.4C).

Knockout studies in mice have indicated that neuronal nAChRs are involved in nociception (particularly the $\alpha 4\beta 2$ receptor), nicotine addiction (particularly $\beta 2$ -containing receptors), aging, and learning (Cordero-Erausquin et al., 2000; Marubio et al., 1999). Naturally occurring mutations in humans implicate neuronal nAChRs in some forms of epilepsy, Alzheimer's disease, and schizophrenia (Changeux and Edelstein, 2001). The different nAChR subunits are expressed in various combinations throughout the brain (Figure 1.4B).

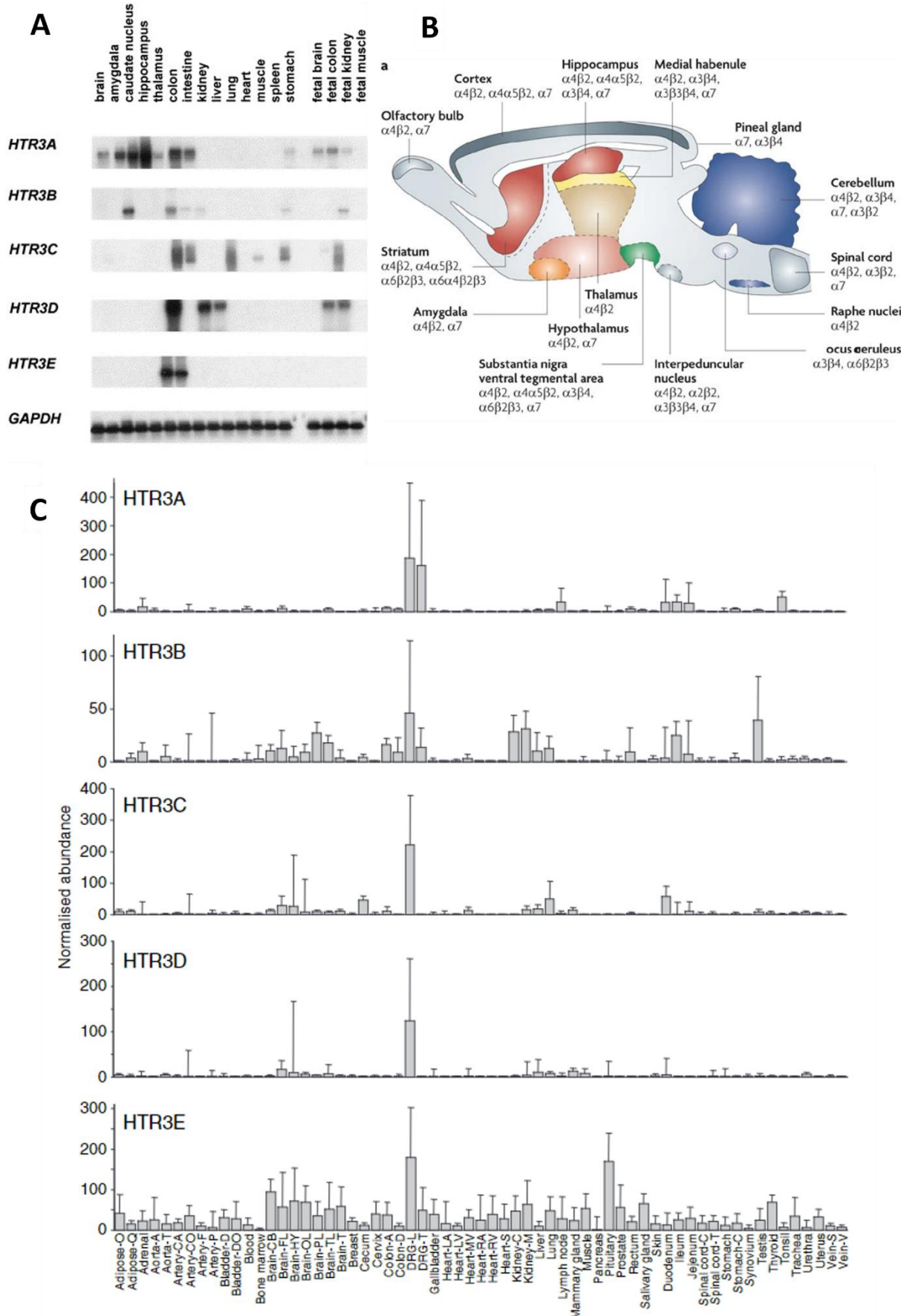


Figure 1.4: Distribution of cation-selective pLGIC subunits in human tissues. A) RT-PCR analysis of 5-HT₃R genes in 18 human tissues. (Reprinted from GENE, 310, Niesler B, Frank B, Kapeller J, Rappold GA, Cloning, physical mapping and expression analysis of the human 5-HT₃ serotonin receptor-like genes HTR3C, HTR3D and HTR3E, 101-111, Copyright (2003), with permission from Elsevier.) B) Distribution of neuronal nAChR binding sites in the human brain. (Reprinted by permission from Springer Nature: Springer Nature, Nature Reviews Drug Discovery, Nicotinic receptors: Allosteric transitions and therapeutic targets in the nervous system, Taly A., Corringer PJ., Guedin D., Lestage P., Changeux JP., Copyright (2009).) C) Expression profiles of 5-HT₃R subunits in human tissues, assessed by RT-PCR. DRG: dorsal root ganglion. (Reprinted with permission from Journal of Neurochemistry, Characterisation of 5-HT_{3C}, 5-HT_{3D} and 5-HT_{3E} receptor subunits: Evolution, distribution and function, Holbrook, JD; Gill, CH; Zebda, N; Spencer, JP; Leyland, R; Rance, KH; Trinh, H; Balmer, G; Kelly, FM; Yusaf, SP; Courtenay, N; Luck, J; Rhodes, A; Modha, S; Moore, SE; Sanger, GJ; Gunthorpe, MJ, Copyright (2009).)

1.1.3.2 Pharmacology of cation-selective pLGICs

In addition to the highly effective ‘setrons’ (5-HT₃R antagonists used as anti-emetics), a range of compounds bind to 5-HT₃ receptors and modulate function (Figure 1.5). The common side effects of 5-HT₃R agonists, including nausea, have so far rendered them unattractive for clinical use, so most compounds of interest are either antagonists or allosteric modulators.

Ondansetron, an anti-emetic 5-HT₃R antagonist, has been shown to be helpful in reducing drinking in alcohol-dependent adolescents (Dawes et al., 2005). Treatment with ondansetron decreases binge-eating and vomiting in patients with bulimia (as well as alleviating depressive symptoms in the same patients) (Faris et al., 2006), and ondansetron, tropisetron, and other 5-HT₃R antagonists reduce the normal degree of anorectic responses of rats to an anorexigenic diet (Hammer et al., 1990; Jiang & Gietzen, 1994), indicating the involvement of the 5-HT₃ receptor in these processes.

Injection or topical application of serotonin causes pain that is attenuated by some 5-HT₃R antagonists (Richardson et al., 1985), and some 5-HT₃R antagonists have been shown to reduce or ameliorate pain caused by e.g. fibromyalgia, chronic pain, arthritis and injections, as reviewed in (Faerber et al., 2007). In rats, ondansetron can prevent the development of chronic pain (Suzuki et al., 2004).

Alosetron is a 5-HT₃R antagonist used for treatment of irritable bowel syndrome in women, increasing fluid absorption in the small intestine and delaying post-prandial colonic transit (Barman Balfour et al., 2000).

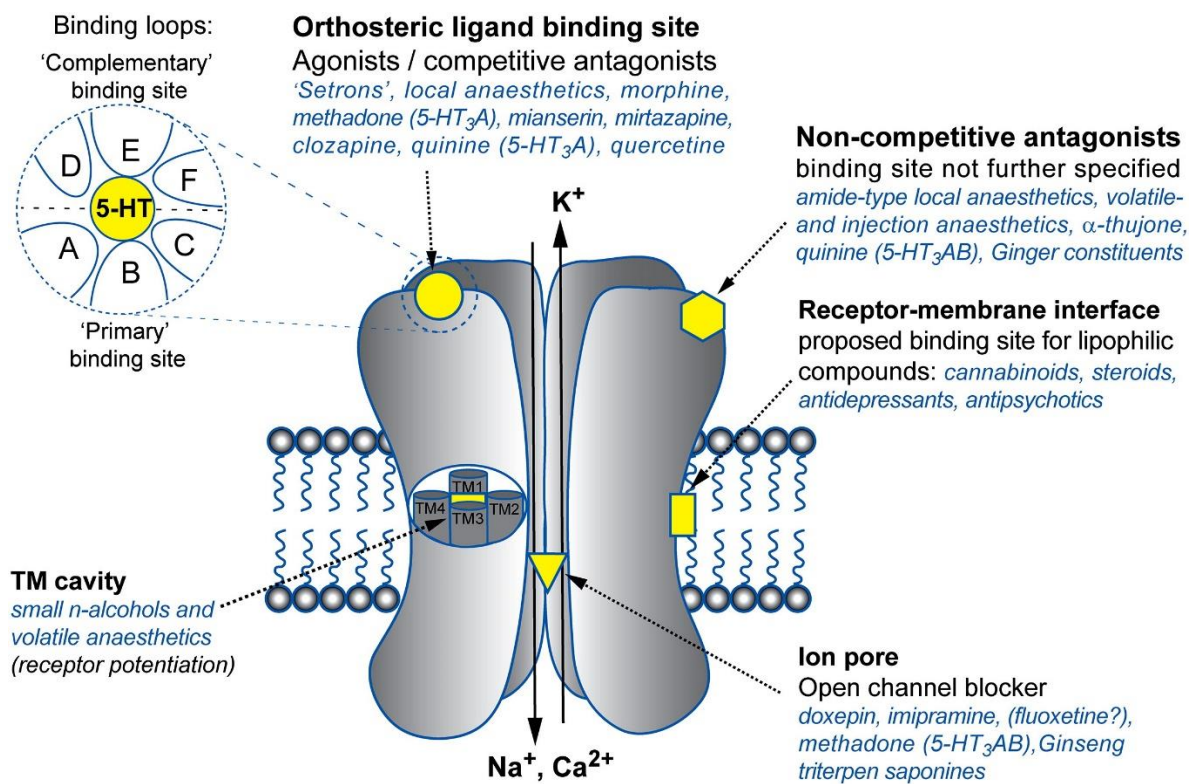


Figure 1.5: Schematic of a 5-HT_{3A} receptor indicating known and predicted ligand binding sites. One subunit removed to show channel pore. (Reprinted from Pharmacology & Therapeutics, 128, Walstab J, Rappold G, Niesler B, 5-HT₃ receptors: Role in disease and target of drugs, 24, Copyright (2010), with permission from Elsevier.)

Allosteric binding sites in the neuronal nAChRs include the non-orthosteric ligand binding sites (between subunits that do not form orthosteric ligand binding sites, e.g. $\beta 2:\beta 2$ in the $\alpha 4\beta 2$ nAChR, Figure 1.1B), the ECD-TMD interface, the lipid-accessible M4 helix, as well as crevices formed by M1 and M3, and the intracellular domain.

Varenicline, a smoking cessation drug (Cahill et al., 2016), is an $\alpha 4\beta 2$ partial agonist, and an $\alpha 7$ full agonist (Coe et al., 2005; Mihalak et al., 2006). Additionally, several widely used antidepressants (including Prozac, Zoloft, Paxil and Cipramil) inhibit neuronal nAChRs at clinically relevant concentrations (Fryer & Lukas, 1999; García-Colunga et al., 1997; Hennings et al., 1999). ABT-418, a nAChR agonist, improves memory performance in spontaneously hypertensive rats (an animal model for ADHD), where it also causes increased expression of hippocampal $\alpha 4$ and cortical $\alpha 4$ and $\beta 2$ nAChR subunits (Guo et al., 2012). A small human trial also showed efficacy of ABT-418 against ADHD symptoms. ABT-418 has also been shown to improve total recall, spatial learning, and memory in human patients with Alzheimer's disease (Potter et al., 1999).

The large variation in subunit composition and distribution of neuronal nAChRs makes targeting specific subunits an attractive option (Figure 1.4). These and other active nAChR modulators are reviewed in Taly et al. (2009).

1.2 Role of M4 in pLGICs

The M4 is at first glance a peripheral helix on the edge of the TMD, distant from key sites like the ligand binding domain or the channel pore. However, the work described in sections 1.2.1-1.2.3 has shown that the M4 helix is intimately involved in pLGIC function and, in some cases at least, it couples ligand binding to channel opening. How this occurs, and how it varies between pLGICs, are key questions in understanding pLGIC function, and answering

them could potentially open the way to better distinguishing between structurally similar pLGICs. In addition to the sequence alignment of selected M4 helices (Figure 1.6), an overview table of all the mutations discussed here is provided at the end of section 1.2.3 (Table 1.1).

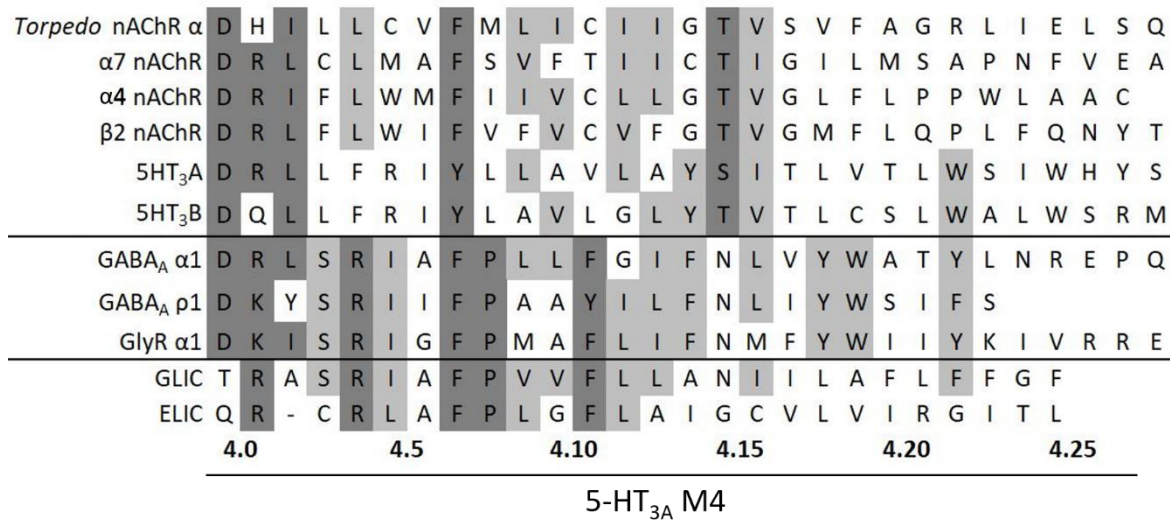


Figure 1.6: Sequence alignment of selected pLGIC M4 helices. Uniprot numbers are in order: P02710, P36544, P09483, P12390, P23979, Q9JHJ5, P62813, P24046, P23415, Q7NDN8, P0C7B7. Residues coloured by high (dark grey) and medium (light grey) conservation of sidechain properties. The numbering system for the M4 helix (extent in the 5-HT₃AR shown by the line beneath the numbering) starts at the highly conserved intracellular Asp (D434 in the 5-HT₃AR), and is added to provide an easy way of comparing M4 residues between pLGICs.

1.2.1 Role of the M4 helix in bacterial pLGICs

The M4 helix has been thoroughly characterised in two bacterial pLGICs, ELIC and GLIC, where it plays markedly different roles in function.

26 out of 31 alanine mutations in the ELIC M4 cause decreased EC₅₀s (half maximal effective concentration of ligand), while the remaining five have no measurable effect (Hénault et al., 2015). While all 26 affective mutations have fairly modest effects (all <5-fold

change in EC₅₀, all but two <3-fold change in EC₅₀), mutations of inwards-facing (towards the rest of the helical bundle) residues generally have the largest effects (e.g. F303A which causes the largest change (4.9-fold) in EC₅₀). Deletion of the seven last residues of ELIC together has no effect on receptor function, indicating that the C-terminal domain is unrelated to function here. Interestingly, while all the M4 aromatic-alanine mutations caused decreased EC₅₀s in ELIC, adding other aromatic residues to the M4-M1/M3 interface also caused decreased EC₅₀s, and adding more than one aromatic residue to this interface at a time further decreased EC₅₀ (Carswell et al., 2015)

In GLIC in contrast, 15 out of 25 alanine mutations in the M4 increase the concentration of protons required to cause channel opening (i.e. decrease pH₅₀, the equivalent to EC₅₀ in GLIC), (Hénault et al., 2015). The largest changes in pH₅₀ were caused by alanine mutation of aromatic residues, indicating that they are particularly important to GLIC function. Finally, deletion of the three C-terminal residues of M4 starkly reduces receptor function, and any further deletion abolishes it completely, demonstrating that these residues are crucial to receptor expression and/or function.

Together, these data indicate that the ELIC M4 helix is only loosely interacting with the rest of the transmembrane helices, while the GLIC M4 appears to be tightly bound to the M1/M3 interface. Based on structural comparisons and sequence alignments, Therien and Baenziger (2017) suggests that the GLIC and ELIC M4 helices might be two different ‘archetypes’ for the M4 helices of mammalian pLGICs. The authors predicted that most anion-selective pLGICs would fall into the GLIC category (with strong M4-M1/M3 interactions, generally involving aromatic residues, the M4 CTD being crucial to receptor function, and M4 alanine mutations generally being detrimental to receptor function), and that most cation-selective pLGICs would fall into the ELIC category (weak or poor M4-M1/M3 interactions, few aromatic interactions at the M4-M1/M3 interface, CTD not involved in receptor function, and M4 alanine mutations generally being beneficial to receptor function).

1.2.2 Role of the M4 helix in anion-selective pLGICs

The M4 helices of anion-selective pLGICs investigated so far do resemble the GLIC M4: 7 out of 21 alanine mutations in the $\alpha 1$ glycine receptor M4 helix reduce or ablate receptor function (Haeger et al., 2010), six of which are aromatic-to-alanine mutations. A closer investigation of these aromatic residues reveals that most of them can be substituted with other aromatic residues without loss of function (Tang and Lummis, 2018), emphasising the importance of aromatic interactions here. The M4 helix has also been shown to contribute to the different agonist efficacies in the $\alpha 1$ and $\alpha 3$ glycine receptors (Chen et al., 2009): $\alpha 1$ and $\alpha 3$ receptors show very different response profiles to β -alanine and taurine applied individually or with glycine. $\alpha 1$ receptors with the $\alpha 3$ M4 recapitulate the $\alpha 3$ response profile very closely. $\alpha 3$ receptors with an $\alpha 1$ M4 give a response profile that resembles that of the $\alpha 1$ receptor, except in the case of taurine application, where the $\alpha 3$ receptor with an $\alpha 1$ M4 helix gives an intermediate response between those of $\alpha 1$ and $\alpha 3$ receptors. Interestingly, $\alpha 3$ receptors with the $\alpha 1$ M1-M3 segment show a completely $\alpha 3$ -like response profile, and $\alpha 1$ receptors with the $\alpha 3$ M1-M3 segment show a completely $\alpha 1$ -like response profile. More particularly, individual M4 mutations cannot replicate the dramatic shift in agonist efficacy that occurs on switching the $\alpha 1$ and $\alpha 3$ M4 helices, and the orientations of the two M4 helices are markedly different (Han et al., 2013), indicating that it is the action of the whole M4, or at least cooperative action between multiple sections of it, that affects receptor function this way. Finally, when the glycine receptor M4 is expressed as a separate construct from the rest of the subunit, the receptor still forms competent pentamers *in vivo*, highlighting the strength and specificity of the M4-M1/M3 interactions in this receptor (Haeger et al., 2010).

In the GABA ρ receptor, alanine mutation of six of the seven M4 aromatic residues reduces or ablates receptor function (Cory-Wright et al., 2017), again highlighting the importance of M4 aromatic residues in an anion-selective pLGIC. Deletion of the four C-terminal M4 residues has little effect on receptor function, but extending this deletion to the fifth residue (W475) results in receptors that are expressed at the cell surface, but are non-responsive in the functional assay (Reyes-Ruiz et al., 2010), demonstrating the key role of the GABA ρ M4 CTD for receptor function. Further investigation shows that the interaction of W475 with L207 in the Cys-loop is critical to receptor function (Estrada-Mondragón et al., 2010). The

M4 of the GABA_A $\alpha 1\beta 2\gamma 2$ receptor has been probed by assaying the effect of tryptophan substitutions of all the residues in a segment of the $\alpha 1$ M4 helix (Jenkins et al., 2002). One of these ablated receptor function, two decreased EC₅₀, three increased EC₅₀, and five had no measurable effect on EC₅₀. While this data cannot straightforwardly be compared to that of the alanine mutations in the other pLGIC M4s (as the impact of substituting in a tryptophan vs an alanine is different along several different axes, including size, polarity, and aromaticity), this study also showed that some of these tryptophan mutations abolished GABA_AR sensitivity to some general anaesthetics: T414W abolished receptor modulation by isoflurane but not halothane or chloroform, L416W ablated modulation by halothane and chloroform, without affecting isoflurane modulation, and Y411W blocked the effects of halothane and isoflurane without affecting chloroform action. This demonstrates that the M4, whether through direct interactions or indirect effects, is key not only to receptor function, but also modulation of receptor function.

Taken together, this supports a model where the M4 helices of anion-selective pLGICs play a role in receptor function, and some M4 residues are required to allow receptor function in response to ligand binding. These M4 helices have many aromatic residues at the M4-M1/M3 interface that are important for receptor function. Additionally, the CTD of these M4 helices is required for function, in one case acting through an interaction with a residue in the extracellular Cys-loop.

1.2.3 Role of the M4 helix in cation-selective pLGICs

When I started my PhD, some work had been done on the 5-HT_{3A}R M4 helix, and the *Torpedo* nAChR M4 had been fairly extensively studied, as described below.

In the 5-HT_{3A} receptor, deletion of the C-terminal residues of the human 5-HT_{3A} M4 helix abolishes receptor export to the plasma membrane as measured by immunocytochemistry or detection of an N-terminal GFP tag (Butler et al., 2009; Pons et al., 2004), and as with the glycine receptor, when coexpressing the receptor without M4 and the M4 helix separately, it can reassemble *in vivo* to form functional receptors (Haeger et al., 2010). These initial data were somewhat counterindicative of the prediction that the 5-HT_{3A} would follow the ELIC

M4 archetype, where the M4 CTD is of little importance, and M4-M1/M3 interactions are weak and poorly optimised.

The M4 helix of the *Torpedo californica* nAChR M4 has been more extensively studied. The most recent investigation was a study of alanine mutations in and around the M4 of the α subunit (Thompson et al., 2020). Of 36 alanine mutations in this region, eight increased EC₅₀ and five reduced EC₅₀, though the changes are mostly minor (all but one are smaller than 5-fold changes from WT). Two of the mutations that increased EC₅₀ are ‘below’ (N-terminal to) the D4.0 that I used as the start of the M4 helix, though the exact point of transition between the intracellular MA helix and the M4 helix is not well defined.

Deletion of the four C-terminal residues of the of the *Torpedo californica* nAChR α M4 had no measurable effects. Further deletions from residue five to eleven caused gradual increases in EC₅₀, and deleting the C-terminal twelve residues ablated receptor expression. Together this indicates that CTD-ECD interactions are not key to receptor function in the *Torpedo* nAChR. In comparison to the effects of alanine mutations, three tryptophan substitutions in the α subunit M4 (C418W, G421W, V425W) reduce EC₅₀ (Lasalde et al., 1996; Lee et al., 1994; Li et al., 1992), eight somewhat increase EC₅₀, and one ablates receptor expression as measured by α -bungarotoxin binding (Tamamizu et al., 2000). Conversely, two alanine mutations (C418A and T422A) increase EC₅₀ (Roccamo et al., 1998).

The α C418W mutation causes slow-channel myasthenic syndrome in humans (Shen et al., 2006), where it increases channel open times. This potentiation has been shown not to be caused through interaction between the M4 CTD with the Cys-loop, but rather involves an energetic link with two polar residues on M1 (Domville and Baenziger, 2018). This study also showed that while the M4 CTD of the human muscle nAChR is involved in receptor expression, deletion of the last 11 residues has only a small effect on receptor function. Interestingly, the M4 of the *Torpedo* nAChR can be completely replaced with a hydrophobic helix from a different protein without ablating receptor function (Tobimatsu et al., 1987). Extensive analysis of single-molecule kinetics indicate that the α M4 of the mouse muscle nAChR likely moves as a single block in channel gating events, after the α ECD and M2-M3 linker, but before the δ M2 helix (Mitra et al., 2004). In the γ subunit of the *Torpedo*

californica nAChR, four out of eleven tryptophan substitutions tested decrease EC₅₀ and one increases it (Ortiz-Acevedo et al., 2004). This was also the first receptor where an ‘uncoupled state’ (where the receptor binds ligand but does not open in response without being in the desensitized state) was investigated; this is discussed further in section 1.3.3.1.

During the period of my PhD, the M4 helix of the $\alpha 7$ nAChR was also thoroughly investigated (da Costa Couto et al., 2020). 9 out of 24 alanine mutations here slightly lower EC₅₀, one ablates receptor expression (measured by binding of fluorescently tagged α -bungarotoxin), and the remaining 14 have no measurable effect. In addition, substituting an aromatic residue into the M1/M3-facing side of the M4 lowers EC₅₀ in three of four positions assessed. This pattern is fairly similar to that of the ELIC M4, with M4 alanine mutations or inwards-facing aromatic substitutions mostly promoting receptor function.

Overall, these data do not give a consistent pattern of M4 role for cation-selective pLGICs. Alanine mutations have varying effects, and the CTD appears crucial to function in some receptors, but incidental in others.

Table 1.1: Effects of alanine and aromatic substitutions in pLGIC M4 helices

M4	ELIC ^{a,b}	GLIC ^{a,b}	Torpedo α nAChR ^{c,d}	$\alpha 7$ nAChR ^e	GABA _A pR ^f	GABA _A $\alpha 1 R^g$	GlyR ^h
4.0	Q297	T292	D407	D446			
4.1	R298	R293	H408		R447		
4.2		A294	I409		L448	Y458	W F
4.3	C299	S295	L410		C449		
4.4	R300	R296	L411		L450		R392
4.5	L301	I297	G412	C→W	M451		I393
4.6	A302	A298	V413		452		G394
4.7	F303	F299	F414		F453	F463 Y W	F395
4.8	P304*	P300	M415	W	S454		P396
4.9	L305	V301	L416	W	V455		M397
4.10	G306	V302	V417	I→W	F456		F399 Y
4.11	F307	F303	C418	W	T457	Y467 W F	L400
4.12	L308	W	L304	W	I419	W	I401
4.13	A309	L305	I420	W	I459		I406W F402 Y
4.14	I310	A306	G421	W	C460	F470 Y W	F407W N403
4.15	G311	N307	T422	W	T461		N408W M404
4.16	C312	I308	L423	V→W	I462		L409W F405 Y
4.17	V313	I309	A424	S→W	G463		V410W Y406
4.18	L314	L310	V425	W	I464	Y474 W F	Y411W W407
4.19	V315	A311	F426		L465	W475 Y F	W412W I408
4.20	I316	F312	427		M466		A413W I409
4.21	R317	L313	G428		S467		T414W Y410
4.22	G318	F314	R429		468	F478 Y W	Y415W K411
4.23	I319	F315	L430		P469		L416W I412
4.24	T320	G315	I431		N470		N417W V413
4.25	L321	F317	E432		F471		
4.26			L433				
4.27			N434				
4.28			Q435				
4.29			Q436				
4.30			G437				

Effect of mutating a residue to alanine on receptor function (EC_{50}) shown in colour of each residue, with effect of other substitutions at the same or equivalent position shown in additional columns (except for the GABA_A $\alpha 1 R$, where only the effects of tryptophan substitutions are shown). Blue: gain of function (lowered EC_{50} or pH50 closer to 7), red: loss of function (increased EC_{50} or lowered pH50), no colour: no statistically significant

effect on EC₅₀ measured, grey: no response to ligand in functional assay, black: receptor not expressed. ^a(Hénault et al. 2015), ^b(Carswell et al., 2015), ^c(Thompson et al. 2020), ^d(Tamamizu et al., 2000): as the paper did not show statistical analysis of the EC₅₀ values, I performed a 2-way ANOVA, using n=6 (the paper states n=6-35 for calculation of n_H), ^e(da Costa Couto et al., 2020), ^f(Cory-Wright et al., 2017), ^g(Jenkins et al., 2002), ^h(Tang and Lummis, 2018). *indicates altered desensitisation kinetics. First column is a comparative numbering system for pLGIC M4 helices, introduced in Figure 1.6.

1.2.4 Site-directed mutagenesis as a tool for understanding pLGIC function

As the preceding sections show, site-directed mutagenesis is a flexible strategy for learning about the roles and functions of individual residues in complex protein structures.

Substitution of different amino acids into the same position of a protein can inform on the particular requirements on that position for protein expression and/or function (depending on the assay in question): e.g. substituting in a leucine, aspartic acid and asparagine at the same position would test whether the degree of polarity/charge at that position affects protein function, without appreciably changing the size of the residue in question. Similar tactics can be used to probe the effect of positive vs negative charge, backbone flexibility, positioning of charge/polarity, residue size, at any given position on protein function. The addition of unnatural amino acids to this technique has greatly broadened the scale of what is possible to test for, and how precisely the preferences and requirements at a position can be determined, as described in e.g. Dougherty (2000).

I selected alanine-based site-directed mutagenesis (colloquially known as ‘alanine scanning’) for the initial interrogations of the M4 helices of the 5-HT_{3A} and α4β2 nACh receptors for two main reasons. Firstly, this would let me directly compare my results to the wealth of work already done by alanine site-directed mutagenesis of other pLGICs, and allow for reasonably straightforward analysis of similar datasets for a range of different pLGIC M4s. Secondly, even without the context of other pLGIC studies, alanine site

directed mutagenesis offers a reasonably unbiased and informative initial approach to a not well-studied domain of a protein. Performing the same substitution at all positions in a section of protein removes possible bias in human understanding of which residues are more or less ‘interesting’ based on structure (a judgement which is still imperfect). The choice of alanine for substituting in, as initially described in Cunningham & Wells, (1989), arises from alanine being relatively ‘neutral’ in regards to many of the chemical aspects being probed here: it is neither charged, polar, or aromatic, and though it is hydrophobic, the sidechain is small and energetically inoffensive in a larger range of environments than large hydrophobic sidechains like leucine or valine. Unlike glycine or proline, it does not perturb the conformational dynamics of the backbone. Alanine is also one of the most common amino acids in recorded proteins (Eitner et al., 2010).

In this work, I obtained initial information on the protein domains I studied by systematic site-directed mutagenesis, and used that to direct my studies towards specific residues or functional patterns within each domain.

1.3 Expression systems for studying pLGICs

For functional studies of pLGICs without protein purification and reconstitution, the most common expression systems are HEK293 cells and *Xenopus laevis* oocytes. A wide variety of pLGICs have been expressed and characterised in both HEK cells and oocytes, demonstrating that they are both broadly permissive to pLGIC expression and function. Therefore relevant differences between these two systems must generally either have no measurable effect on pLGIC function, or modulate receptor function (as opposed to abolishing or preventing it). Each expression system has its own advantages for receptor expression, and I used both for different purposes in my PhD work.

1.3.1 HEK293 cells

HEK293 cells are an immortalised cell line that was generated from human embryonic kidney cells (Graham et al., 1977). Not only are HEK cells particularly easy to transfect and

culture, they have also been shown to express several proteins typically found in immature neurons, and in many ways resemble neurons more than kidney cells (Shaw et al., 2002). Together these properties make HEK cells well suited for studying pLGICs. The main disadvantage of HEK cells for this type of study is that they natively express muscarinic acetylcholine receptors (e.g. (Luo et al., 2008)), so some nAChR ligands may have off-target effects in these cells.

1.3.2 *Xenopus* oocytes

Xenopus laevis oocytes have a long history as biochemical model systems, and many advantages for pLGIC study. They can translate exogenous microinjected RNA, making receptor expression straightforward, and have been shown to be able to functionally express a range of different channel proteins from a variety of eukaryotes (a good review of the functionality of oocytes, including an overview of successfully expressed channel proteins is Lin-Moshier and Marchant (2013)). Copy numbers of $\sim 5 \times 10^8$ of heterologously expressed proteins have been detected in oocytes (Sigel, 1990), demonstrating the ease of protein expression here. Oocytes have also been found to be more permissive to pLGIC expression than HEK293 cells, perhaps due to being kept at 16°C, which may promote slower and more accurate protein expression (Denning et al., 1992). Many post-translational modifications can be added to endogenous or exogenous proteins in oocytes, including acetylation, hydroxylation, phosphorylation, glycosylation, removal of signal sequences, S-S bond formation and non-covalent assembly (Colman et al., 1984), making them suitable hosts for pLGICs, which require glycosylation and non-covalent assembly. Their large size also makes many functional assays straightforward to perform.

1.3.3 Membrane composition

One aspect that is markedly different between these two expression systems is the composition and characteristics of their plasma membranes. They have different transmembrane proteins as well as different lipid compositions in the bilayer. The largest difference in membrane composition is in the phosphatidylcholine content: phosphatidylcholine makes up 65% of total phospholipid content in oocyte membranes

compared to only 35% in HEK cells. This is made up for by a greater diversity of other glycerophospholipids in HEK cells. There is also more sphingomyelin in HEK cells (10-15% of total phospholipid content compared to 5% in oocytes), and less cholesterol than in oocytes. The cholesterol:phospholipid molar ratio is 0.6-0.7 in oocytes compared to just under 0.5 in HEK cells, assuming an average phospholipid weight of 744 g/mol (Dawaliby et al., 2016; Opekarová and Tanner, 2003). It must be noted that the lipid content of these two model systems was measured by different methods: that of HEK cells by mass spectrometry, and that of oocytes by spectrophotometry (Santiago et al., 2001) and evaporative light scattering (Stith et al., 2000), and therefore are not perfectly comparable.

1.3.3.1 Membrane composition affects pLGIC function

Membrane composition has been shown to affect the function of several pLGICs, and altering it can modulate receptor activity.

Of the prokaryotic pLGICs, ELIC has been shown to require a specific lipid composition to function correctly. When reconstituted into a membrane without cholesterol and anionic lipids, ELIC shows a complete lack of receptor function, even though it still binds ligand. Adding aromatic residues to the M4-M1/M3 interface restores ELIC function in membranes without cholesterol and anionic lipids, indicating that the effects of membrane composition and M4-M1/M3 interactions are closely intertwined (Carswell et al., 2015). GLIC does not show the same sensitivity, and its function is unaffected by the removal of anionic lipids and cholesterol (Labriola et al., 2013).

The dependency of *Torpedo* nAChR activity on membrane composition has been extensively documented, and both the transition from resting to active, and active to desensitized states, are dependent on lipid composition. In particular, both cholesterol and negatively charged phospholipids are generally required in reconstituted membranes for channel opening to occur on ligand binding (Benziger et al., 2000; Fong and McNamee, 1986). Of the anionic lipids, those with smaller headgroups are most effective at promoting a functional receptor state when added to phosphatidylcholine (POPC) membranes (DaCosta et al., 2009). However, thicker and more hydrophobic membrane compositions can allow the receptor to

open even in the absence of cholesterol and anionic lipids, and thinner POPC membranes prevent channel opening (Dacosta et al., 2013). The number of functional nAChRs in reconstituted membranes increases with increasing percentage of cholesterol in the lipid bilayer up to a C/P molar ratio of 0.42 (Rankin et al., 1997). In oocytes, depleting almost half the endogenous cholesterol from the oocyte has no effect on wild-type (WT) nAChR receptors, but promotes the activity of α C418W mutants. Conversely, increasing cholesterol inhibits the activity of both the WT and the α C418W mutant (though only the latter recovers function on depletion of this excess cholesterol) (Santiago et al., 2001). Adding steroids and free fatty acids to *Torpedo* membranes in the absence of agonist causes receptors to enter a desensitized state (Nievias et al., 2008). Thorough reviews of protein-lipid interactions of the nAChR are Baenziger et al. (2015); Barrantes (2007, 2015); Hénault et al. (2015); Thompson and Baenziger (2020).

Recent work indicates that lipid-inactivated nAChRs are not in the desensitized state, but in an 'uncoupled' state which binds ligand (though less tightly than the desensitized state) but does not open on ligand binding. DaCosta and Baenziger (2009) shows three pieces of evidence for this. Firstly, measurements of ethidium fluorescence, which increases in the desensitized state: the ethidium fluorescence increases on addition of carbamylcholine (an agonist) in the WT receptor, but not in the lipid-uncoupled receptor, indicating that the uncoupled receptor is not entering the desensitized state even when binding carbamylcholine. Secondly, ligand binding is not tighter in the uncoupled receptor than the WT, as one would expect from the desensitized state. Thirdly, a pore-binding allosteric modulator affects the ligand binding site in WT receptors, but not in the lipid-uncoupled receptors.

Sun et al. (2017) suggests that the low affinity of uncoupled nAChR for ligand indicates that the ECD is in a resting-like state, not a desensitized state. They also propose that several ELIC structures may in fact be showing the receptor in an uncoupled state, as the last residues of M4 are unresolved, the ECD-TMD interactions are few and weak, and there are no changes in the pore between agonist-bound and non-agonist structures. In addition to this, the ELIC pore is more restricted than in other closed pLGICs, leading to the proposal that the TMD of the uncoupled state is distinct from both the resting and the desensitized pore structure. They show that the uncoupled state of the *Torpedo* nAChR does not bind pore

blockers, indicating that, as in many ELIC structures, the pore of the uncoupled state may be more restricted than the resting and the desensitized pore.

1.4 Trafficking of cation-selective pLGICs

A significant part of my PhD work relies on distinguishing between receptors correctly inserted into the plasma membrane but unable to perform channel function in response to ligand binding, and receptors that have defects in folding, assembly, or export from the ER, and do not reach the cell surface.

The progress of pLGICs from synthesis to fully-formed oligomers (in the correct heteromeric assemblies, where appropriate) at the cell surface requires many coordinated steps, including (in no particular order) subunit folding, insertion into the membrane, oligomerisation, correct additions of post-translational modifications (e.g. crucial N-linked glycosylations (Monk et al., 2004; Wanamaker & Green, 2005), and the previously eponymous cystine in the ECD (Gelman & Prives, 1996)), and stepwise quality control passes throughout the endoplasmatic reticulum (ER) and Golgi on the way to the cell surface.

The progression of this journey has been followed by tracking fluorescently labelled 5-HT_{3A} receptors by microscopy. Cotransfection with fluorophores targeted to either the ER or the Golgi revealed that 5-HT_{3A} receptors were reaching the ER three hours after transfection, the Golgi apparatus around four hours after transfection, and the cell surface about 30 minutes after that again (the latter confirmed by binding of a fluorescently labelled 5-HT_{3A}R antagonist) (Ilegems et al., 2004). Further facets of 5-HT_{3A} receptor trafficking are well reviewed in Connolly (2009).

Studies of nAChRs have shown that cell-surface expression levels of nAChRs are more dependent on subunit composition than total cell expression levels (Harkness & Millar, 2001, 2002). Sections of the N-terminal domain, the intracellular domain, the transmembrane domains and hydrophobic residues in the M3-M4 loop have all been implicated in parts of subunit folding, assembly, export from the ER, and cell-surface expression (Cooper & Millar,

2002; Dineley & Patrick, 2000; Gee et al., 2007; Kracun et al., 2008; Ren et al., 2005; Sumikawa, 1992; Vicente-Agulló et al., 1996).

1.4.1 Improving functional expression of cation-selective pLGICs

To promote folding, assembly, and/or cell-surface expression of mutant receptors in my work, I make extensive use of the chaperone proteins RIC-3 (resistance to inhibitors of cholinesterase 3) and NACHO (novel acetylcholine receptor chaperone), which in many cases are useful tools to disambiguate between a lack of channel function and a lack of cell-surface expression.

Originally identified in a *Caenorhabditis elegans* screen for genes involved in acetylcholine receptor activity (Nguyen et al., 1995), RIC-3 is a membrane protein expressed in both muscles and neurons with a role in acetylcholine receptor folding, assembly and/or trafficking (Halevi et al., 2002). The human homolog, hRIC-3, also enhances $\alpha 7$ nAChR activity in *Xenopus* oocytes (Halevi et al., 2003) and both activity and ligand binding at the plasma membrane of the $\alpha 7$ nAChR in HEK293 cells (Williams et al., 2005). However, the exact levels of RIC-3 may be important to its function, with indications that higher levels of RIC-3 may promote ER retention rather than cell-surface expression, of the $\alpha 7$ receptor (Alexander et al., 2010).

While RIC-3 inhibits the functional responses of $\alpha 4\beta 2$ receptors in *Xenopus* oocytes (likely by affecting cell-surface expression levels) (Halevi et al., 2003), it significantly enhances expression levels of the $\alpha 4\beta 2$ nAChR in mammalian cells (Lansdell et al., 2005), though it appears to have no measurable effect on $\alpha 4\beta 2$ nAChR subunit assembly (Dau et al., 2013). With regards to the 5-HT_{3A} receptor, RIC-3, while not essential for cell-surface expression, does enhance both receptor transport to the plasma membrane and function in COS-7 cells (Cheng et al., 2005), but suppresses it in *Xenopus* oocytes (Castillo et al., 2005; Halevi et al., 2003). The exact effects of a range of RIC-3 homologs and isoforms on receptor expression and/or functional response levels has since been shown to be dependent on the expression system used (Lansdell et al., 2008).

In 2016 another mediator of $\alpha 7$ expression, NACHO, was found by screening for $\alpha 7$ nAChR activity in HEK cells heterologously expressing $\alpha 7$ nAChRs (Gu et al., 2016). NACHO is an intracellular protein found in neurons but not astrocytes (Gu et al., 2016), and markedly increases cell-surface expression of both $\alpha 7$ and $\alpha 4\beta 2$ nAChRs, and its cotransfection allowed detectable levels of $\alpha 7$ nAChR function, and increased $\alpha 4\beta 2$ nAChR responses in HEK cells (it also promotes the 2($\alpha 4$):3($\beta 2$) stoichiometry of the $\alpha 4\beta 2$ receptor in a related mammalian cell line (Mazzaferro et al., 2021). However, no significant effect on 5-HT₃ receptors, either on cell-surface expression levels or function, was found in this study. Co-immunoprecipitation and proteomics data indicate that NACHO may be associated with the ER oligosaccharyltransferase machinery, suggesting that it might play a role in promoting correct glycosylation of nAChRs (Kweon et al., 2020). Coexpression of NACHO appears to have no measurable effect on the expression levels of 5-HT_{3ARs} (Kweon et al., 2020).

Cotransfection of RIC-3 and NACHO together causes a greater increase in cell-surface expression of $\alpha 7$ nAChRs than either alone, though permeabilization shows that total $\alpha 7$ nAChR levels are similar with or without the chaperones, indicating that their effect involves promotion of intracellular receptors to the cell surface (Gu et al., 2016).

A range of other proteins have also been found to interact with and affect nAChR assembly in the ER (well reviewed in Colombo et al. (2013), including BiP, ERp57, and calnexin). 14-3-3 η is an intracellular protein that increases surface-level $\alpha 4\beta 2$ nAChR expression in tsA201 cells compared to a non-interacting mutant receptor, without significantly affecting the measured acetylcholine EC₅₀ in oocytes (Jeanclos et al., 2001). Beyond chaperone proteins, chemical chaperones can also have great effects on pLGIC expression levels, including e.g. 4-phenylbutyric acid and valproic acid for the $\alpha 7$ nAChR (Kuryatov et al., 2013), or nicotine for the $\alpha 4\beta 2$ nAChR (Nashmi et al., 2003) (though co-expression with RIC-3 may mask/prevent this effect of nicotine (Dau et al., 2013)).

1.5 Aims summary

The aim of this work was to characterise the role of the outermost lipid-facing helix of two cation-selective pLGICs, elucidating their mechanisms of action, with the long-term goal of finding ways to differentiate between mammalian pLGICs for specific receptor modulation.

In Chapter 3, I characterised the M4 helix of the serotonin-gated 5-HT_{3A} receptor in HEK293 cells, and showed that while most mutations here had no effect on receptor function, one mutation completely abolished receptor function without affecting ligand binding. This indicates that the M4 helix of the 5-HT_{3A} receptor is crucial to the process of receptor function occurring in response to ligand binding. Using further mutational analysis based on a collaboration providing molecular dynamics simulations, I examined likely interaction partners for the key M4 residue, and determined which of these were also involved in promoting channel opening in response to ligand binding. In Chapter 4, I characterised the M4 helix of the acetylcholine-gated α4β2 nACh receptor in HEK293 cells, and showed that eight mutations here abolished receptor function without decreasing ligand binding. In Chapter 5 I further investigated the key M4 mutants from Chapters 3 and 4 using single-cell assays in *Xenopus* oocytes. Surprisingly, I found that of the one 5-HT_{3A} and eight α4β2 M4 mutants that abolished receptor function but not ligand binding in HEK cells, the 5-HT_{3A} mutant and seven of the eight α4β2 mutants were perfectly functional in oocytes. Finally, in Chapter 6, I showed that the N-terminal helix of the 5-HT_{3A} receptor, which sits above the extracellular domain, is crucial to receptor expression.

Together this shows that the M4 helix of cation-selective pLGICs has a different functional role than predicted, and that the local environment of these receptors has a sizeable effect on function, highlighting the importance of understanding their native contexts.

Chapter 2 Materials and methods

2.1 DNA and RNA

All DNA mutations were made by QuikChange site-directed mutagenesis of mouse or human 5-HT₃R genes or rat α4 or β2 nAChR genes in pcDNA3.1 (for mammalian expression) or pGEMHE (for oocyte expression) vectors (both from Invitrogen). This involves designing a PCR primer with the codon for the desired mutation flanked by DNA sequences that match the gene sequence in the vector everywhere except at the mutation target codon (calculating the melting temperature for the primers without the mismatching bases), and the reverse complement of that sequence as the reverse primer. PCR was performed with Pfu Turbo Polymerase (Agilent 600252), 50 ng vector, 125 ng of each primer, 0.2 μM dNTP mix (Agilent 200415) and 1.5 μl dimethyl sulfoxide (Sigma) in a total volume of 50 μl. DNA was melted at 98°C, followed by 18 cycles of (98°C for 30s, 55°C for 1 min, 68°C for 1 min/kb of plasmid length), with another 1 min/kb of plasmid length at the end for final extensions. This was followed by 1 hr digestion with 1 μl DpnI (NEB R0176S) at 37°C.

4 μl of the PCR reaction was transformed into E. coli (Library Efficiency DH5α, ThermoFisher) by electroporation (0.2 cm cuvettes in a BIORAD electroporator, according to manufacturer's instructions) and harvested by mini-prep (QIAprep spin kit 27106 or NEB Monarch Plasmid Miniprep kit T1010S) or midi-prep (QIAfilter kit 12243) and sequenced to confirm identity.

For RNA production, pGEMHE DNA was linearised with NheI (for 5-HT₃AR DNA) or SbfI (for α4 and β2 nAChR DNA), and cRNA was transcribed with an mMESSAGE mMACHINE T7 kit (ThermoFisher, AM1344) according to manufacturer's instructions.

2.2 HEK293 cells

2.2.1 HEK cell culture and receptor expression

HEK293 cells were grown at 37°C in 7% CO₂ in Dulbecco's modified Eagle's medium/Nutrient Mix/F12 + Glutamax (DMEM/F12, ThermoFisher 31331-028) with 10% foetal bovine serum (FBS, ThermoFisher 10270106), and kept at 10-90% confluence.

Transfection was performed using PEI, as in Raymond et al., (2011). Briefly, 5 µg of m5-HT_{3A} or h5-HT_{3A-E} (A:B-E ratio 1:2 by molarity for the heteropentamers) or α4 and β2 DNA (α4:β2 ratio 1:2 by molarity, as in Morales-Perez et al. (2016)) was incubated with 30 µg 25 kDa linear polyethyleneimine (PEI (Polysciences), pH 7.0) in 1 ml DMEM/F12 for 10 min (with the PEI added after the DNA), added to HEK293 cells at 40-60% confluence in 9 ml DMEM/F12+FBS, and left 48-72h before any assays. Some DNA was also cotransfected with 500 ng each of human RIC-3 DNA (for the 5-HT_{3AR}) and human NACHO and human RIC-3 DNA (for the α4β2 nAChR) in pcDNA3.1. RIC-3 and NACHO are chaperone proteins which enhance cell-surface expression of 5-HT_{3A} and α4β2 nACh receptors (Dau et al., 2013; Matta et al., 2017; Walstab et al., 2010), and these genes were obtained from the Lester Research Group at Caltech.

2.2.2 Fluorescent membrane potential assay

One day after transfection, HEK293 cells were transferred to three columns of a poly-lysine coated 96-well plate to allow for three technical replicates to be performed together, and incubated overnight. They were then washed with 200 µl flex buffer (115 mM NaCl, 1 mM CaCl₂, 1 mM MgCl₂, 1 mM KCl, 10 mM HEPES, 10 mM D-glucose, pH 7.2) and incubated with 100 µl of fluorescent membrane potential dye (blue FLIPR, Molecular Devices R8034) for 45 min at 37°C before assaying responses to 5-HT (5-hydroxytryptamine, 5-hydroxytryptamine creatinine sulfate complex, SIGMA H-7752, lot 63H0844) or nicotine ((-)-Nicotine, Fluka Analytical 36733, lot 5ZBA119XV) on a Flexstation 3 machine (Molecular Devices). Readings were taken with an excitation wavelength of 525 nm, an emission wavelength of 565 nm, and a cutoff of 550 nm, reading every well every two seconds, for

times indicated in figures (generally 200s for 5-HT₃Rs and 150s for α4β2 nAChRs). Fluorescent responses were normalised to the maximum response at maximum concentration, and concentration-response curves were generated by iterative fitting in GraphPad Prism 7 with the equation $\frac{b-a}{1+10^{(n_H(\log EC_{50}-x))}}$, where y is the fluorescent response, x is log[ligand], a is the minimum response, b is the maximum response, and n_H is the Hill slope.

2.2.3 Electrophysiology

Electrophysiology conditions were based on Thompson et al. (2006). HEK293 cells were transfected as above with an additional 500 ng of EGFP (enhanced green fluorescent protein) in pcDNA3.1 (or EGFP and RIC-3 alone), transferred onto glass coverslips, and assayed 48h after transfection. Single cells expressing EGFP were selected visually on an Olympus IX71 inverted microscope. Experiments were performed at room temperature in voltage-clamp mode, and recordings were taken with an Axopatch 200B amplifier (Axon Instruments) and a Digidata 1322A digitizer (Axon Instruments). Cells were kept in extracellular bath solution (140 mM NaCl, 5.4 mM KCl, 0.5 mM CaCl₂, 1 mM MgCl₂, 10 mM HEPES, 10 mM D-glucose, pH 7.2). Patch pipettes (1.5-2.5 MΩ) were made from borosilicate glass capillaries (Harvard Apparatus Ltd.) in a horizontal pipette puller (P-87, Sutter Instruments) and filled with intracellular solution (140 mM CsCl, 1.0 mM MgCl₂, 1.0 mM CaCl₂, 10.0 mM EGTA, 10 mM HEPES; pH 7.2).

Using a micromanipulator, the pipette was positioned above a single cell that was positive for EGFP fluorescence and was not touching any other cells. Light positive pressure was applied to the pipette, and then it was lowered until it formed a small dimple on the cell. Negative pressure was applied to form a small rupture in the cell membrane, and then it was left to settle and allow a seal to form between the pipette tip and the cell membrane. On confirmation of a viable seal, the cell membrane potential was set to -60 mV. 10 μM 5-HT in extracellular solution was added to the cells from gravity-driven reservoirs at a constant flow rate, and resultant currents recorded. Number of replicates listed always indicates biological replicates.

2.2.4 Radioligand binding

This was performed as described in Thompson and Lummis (2013). Briefly, 80-90% confluent HEK293 cells were collected at 4°C by washing twice with PBS (ThermoFisher 70011-036), harvesting into 1 ml assay buffer (10 mM HEPES pH 7.4 for 5-HT₃R membranes, 50 mM Tris-HCl pH 7.4 for nAChR membranes) with a cell scraper, and stored at -20°C. Subsequently the cells were thawed, spun down (3500 g, 6 min) and resuspended in 1 ml ice-cold assay buffer, using a needle to break up the membranes. Membranes were incubated with ligands for 1h at 4°C for cells expressing 5-HT₃Rs or 4 hours at 4°C for cells expressing nAChRs: single-point radioligand binding assays used final concentrations of 1 nM [³H]GR65630 (83.6 Ci/mmol, PerkinElmer, lot 2390168) for 5-HT₃R and 1 nM [³H]epibatidine (6.62 Ci/mmol, PerkinElmer, lot 1651420) for nAChR. Saturation binding curves were performed with a wider range of ligand concentrations as indicated in individual figures. Nonspecific binding was determined using final concentrations of 1 μM quipazine for 5- HT₃R and 300 μM nicotine for nAChR.

5-HT₃R membranes were harvested with a Brandel cell harvester and nAChR membranes manually using vacuum suction, onto GF/B filter paper (soaked in 0.3% branched polyethyleneimine, Fluka Analytical) and washed twice with ice-cold assay buffer. Filters were incubated in scintillation fluid for 3h before the radioactivity was measured by scintillation counting (5 min per sample, Beckman LS6000sc). For saturation binding curves, the resulting data was analysed in GraphPad Prism 7, using the equation $y = \frac{B_{max} \cdot x}{K_d + x}$, where y is the specific binding, x is the concentration of [³H]ligand, B_{max} is the total number of available binding sites, and K_d is the ligand concentration at which half of the ligand binding sites are occupied (the dissociation constant). Number of replicates listed always indicates biological replicates.

2.3 *Xenopus* oocytes

2.3.1 Oocyte harvesting and receptor expression

Stage V-VI *Xenopus laevis* oocytes were acquired either defolliculated from EcoCyte Biosciences or by manual harvesting. After manual harvesting, stage V-VI oocytes were prepared as in da Costa Couto et al. (2020): rinsed first in calcium-free ND96 (96 mM NaCl, 2 mM KCl, 1 mM MgCl₂, 5 mM HEPES, pH 7.5), then in calcium-free Barth's solution (88 mM NaCl, 2.4 mM NaHCO₃, 1 mM KCl, 0.82 mM MgSO₄·7H₂O, 5 mM Tris-HCl, pH 7.4). Oocytes were defolliculated in 1.5 mg/ml collagenase for 2h at 4°C, confirmed by visual inspection. Oocytes were then rinsed in Barth's solution and selected healthy oocytes were transferred into injection media (Barth's solution with added 300 µM Ca(NO₃)₂·4H₂O). Oocytes were injected with 5-25 ng cRNA (1:2 ratio for α4:β2 RNA) and left in injection media (88 mM NaCl, 2.4 mM NaHCO₃, 1 mM KCl, 0.82 mM MgSO₄·7H₂O, 5 mM Tris-HCl, 0.33 mM Ca(NO₃)₂·4H₂O, 0.41 mM CaCl₂·2H₂O, 2.51 mM sodium pyruvate, 0.12 mg/ml theophylline, 0.05 mg/ml gentamicin, pH 7.5) at 16°C for 24h before recording.

2.3.2 Current recordings

Two-electrode voltage-clamp measurements were performed on a Roboocyt (multichannel systems), clamping the oocytes at -60 mV with pipette resistance kept between 100 and 2000 kΩ, and electrodes filled with 1 M KCl, 1.5 M KAc. During recording, oocytes expressing nAChRs were kept in ND96 medium (96 mM NaCl, 2 mM KCl, 1 mM MgCl₂·6H₂O, 1.8mM CaCl₂·2H₂O, 5mM HEPES, pH 7.5), and oocytes expressing 5-HT₃Rs were kept in Ca²⁺-free ND96. Oocytes were perfused with the same ND96 or drug solutions in the same ND96 at 1 mL/min, and currents were recorded at 50 Hz. Oocytes were initially tested with 30 µM 5-HT, 1 µM nicotine or 3 µM acetylcholine to detect receptor expression, and then assayed with concentration ranges as indicated on individual figures, with 120 s perfusion of ND96 after each drug solution. Currents were normalised to the maximum current for that oocyte, and these values were iteratively fitted in GraphPad Prism 7 to the four-parameter logistic equation $y = a + \frac{b-a}{1+10^{(n_H(\log EC_{50})-x)}}$ where y is the current, x is

$\log[\text{ligand}]$, a is the minimum response, b is the maximum response, and n_H is the Hill slope.
Number of replicates listed always indicates biological replicates.

2.4 Computational methods

DNA sequences were aligned using Clustal Omega (Madeira et al., 2019), and percent identity and conservation scores assigned in Jalview (Waterhouse et al., 2009). The alignments were visualised in Excel. Protein structures were visualised in PyMOL (The PyMOL Molecular Graphics System, Schrödinger, LLC).

Chapter 3 The role of the M4 helix in the 5-HT_{3A} receptor

3.1 Introduction

The aim of this work was to determine the functional role of the M4 helix in the 5-HT_{3A} receptor, firstly to characterise the mode of action of the 5-HT_{3A} receptor, and more widely to start determining the role of the M4 helix in cation-selective pLGICs. This would allow for comparisons between anion-selective and cation-selective pLGICs, and assessment of the M4 (as the least conserved of the transmembrane helices) as a potential target for specific receptor modulation.

Prior to the start of my PhD I had mutated each residue in the 5-HT_{3A} M4 helix to alanine and shown that, contrary to expectations that the 5-HT_{3A} M4 helix would play a similar role to that of the ELIC M4 (section 1.2.1), five mutations here each abolished channel function. This work is described in section 3.2.1.2, which is included to give context to my PhD work.

In sections 3.2.1.3 and onwards I first characterise the five non-functional mutants in more detail, and then explore the mode of action of one of these residues in channel opening.

3.2 Results

3.2.1 Characterisation of 5-HT_{3A}Rs with M4 alanine substitutions

To examine the role of the M4 helix in the 5-HT_{3A} receptor, I mutated each residue in the helix to alanine, expressed the WT and resultant mutants in HEK293 cells, and assayed their function using a membrane-potential sensitive fluorescent dye and their cell-surface expression by radioligand binding.

3.2.1.1 Characterisation of WT 5-HT_{3A} receptors

I characterised the WT receptor in HEK293 cells by incubating it with a membrane potential-sensitive dye and assaying the response to addition of 5-HT (Figure 3.1, section 2.2.2). In short, the distribution of the membrane-permeable dye across the plasma membrane changes with the voltage across the membrane: on depolarisation more dye enters the plasma membrane, where its fluorescent signal increases. Conversely, on repolarisation the dye moves out of the membrane, and the fluorescent signal decreases. This gave an EC₅₀ of 0.17 µM, i.e. a pEC₅₀ (-log half maximal effective concentration) of 6.76 ± 0.01 M (Figure 3.1), consistent with previously published data (Lummis et al., 2011). I also coexpressed the WT with the chaperone RIC-3, which promotes folding and/or assembly of cation-selective pLGICs (Cheng et al., 2005). Coexpression with RIC-3 had no statistically significant effect on the recorded parameters of WT receptor function in HEK293 cells (Table 3.2, Figure 3.1), and is hereafter denoted by a + sign (e.g. WT+).

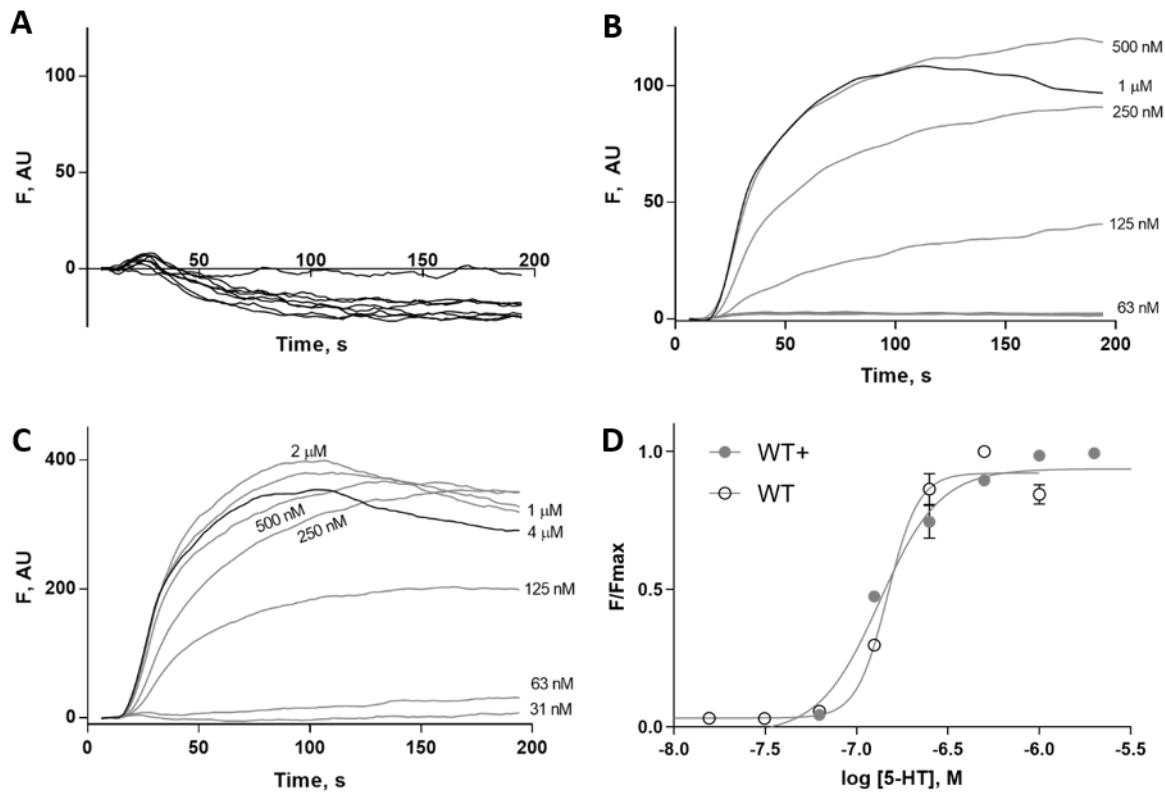


Figure 3.1 Typical responses of 5-HT_{3A} receptors in HEK293 cells. Fluorescent responses (F in arbitrary units, AU) on addition of 5-HT at 20 s in A) mock transfected cells, B) cells expressing WT 5-HT_{3A}R, C) cells expressing WT 5-HT_{3A}R and RIC-3. D) Concentration-response curve from WT data. Data are mean \pm SEM (standard error of the mean), $n \geq 3$.

3.2.1.2 5 out of 28 5-HT_{3A}R M4 alanine mutations abolished receptor function¹

4 of the 28 residues in the 5-HT_{3A} M4 helix had already been investigated in the lab when I started, and it was found that alanine mutations of each (Y441A, Y448A, W456A and W459A) abolished function (later published in Mesoy et al. (2019)). I assayed alanine

¹ All experimental work in section 3.2.1.2 was performed before the beginning of my PhD.

mutants of the remaining 24 residues in the 5-HT_{3A} M4. 23 of these gave WT-like responses to ligand, and one (D434A) did not respond. In sum, alanine mutations of 23 out of 28 5-HT_{3A} M4 residues had no measureable effect beyond small changes in EC₅₀ (<5-fold changed from WT), and alanine mutations of the remaining five completely abolished function (Table 3.1). To simplify comparisons with other pLGIC subunits later, I added a positional numbering system for M4 (column 2 of Table 3.1), based on the alignment of pLGIC sequences (Figure 1.6), starting at the highly conserved aspartic acid residue D434 (D4.0A).

Table 3.1: Parameters of 5-HT_{3A} receptors with M4 alanine substitutions

Position	Mutant	pEC₅₀ (M)	EC₅₀ (μM)	n_H	MRF	n
D434	UT	NF				3
	WT	6.76 ± 0.01	0.17	3.7 ± 0.3	273 ± 16	12
D434	D4.0A	NF				3
R435	R4.1A	6.54 ± 0.02	0.32	3.8 ± 0.5	361 ± 37	4
L436	L4.2A	7.05 ± 0.02	0.09	3.1 ± 0.3	381 ± 15	4
L437	L4.3A	6.58 ± 0.03	0.27	3.6 ± 0.6	169 ± 6	6
L438	L4.4A	6.54 ± 0.05	0.29	2.0 ± 0.5	260 ± 9	6
R439	R4.5A	6.86 ± 0.06	0.19	2.8 ± 0.5	279 ± 19	4
I440	I4.6A	6.49 ± 0.05	0.32	3.3 ± 0.8	258 ± 22	4
Y441	Y4.7A	NF				9
L442	L4.8A	6.45 ± 0.05	0.35	4.9 ± 1.6	220 ± 19	6
L443	L4.9A	6.53 ± 0.04	0.29	4.2 ± 1.5	352 ± 19	6
A444	A4.10	WT				
V445	V4.11A	6.48 ± 0.02	0.33	3.8 ± 0.9	206 ± 7	6
L446	L4.12A	6.41 ± 0.05	0.23	3.1 ± 0.7	363 ± 10	6
A447	A4.13	WT				
Y448	Y4.14A	NF				9
S449	S4.15A	6.46 ± 0.02	0.34	4.4 ± 1.2	189 ± 16	4
I450	I4.16A	6.82 ± 0.03	0.14	2.8 ± 0.4	274 ± 12	4
T451	T4.17A	6.73 ± 0.04	0.18	2.6 ± 0.3	279 ± 12	4
L452	L4.18A	6.37 ± 0.01	0.42	3.7 ± 0.4	69 ± 21	4
V453	V4.19A	6.91 ± 0.05	0.12	3.0 ± 0.5	345 ± 39	4
T454	T4.20A	6.73 ± 0.04	0.19	3.3 ± 0.9	364 ± 30	4
L455	L4.21A	6.44 ± 0.05	0.36	2.7 ± 0.7	310 ± 16	4
W456	W4.22A	NF				9
S457	S4.23A	6.23 ± 0.02	0.59	3.8 ± 0.5	248 ± 9	3
I458	I4.24A	6.45 ± 0.02	0.35	2.5 ± 0.3	303 ± 13	6
W459	W4.25A	NF				9
H460	H4.26A	6.38 ± 0.01	0.42	6.0 ± 0.6*	192 ± 16	6
Y461	Y4.27A	6.85 ± 0.03	0.15	3.7 ± 0.8	375 ± 17	3
L455	L4.21STOP	NF			11 ± 3	3

Data are mean ± SEM. NF = non-functional at concentrations up to 1 mM 5-HT. MRF is maximum recorded fluorescence. Typical MRF values for NF receptors were between 0 and 20. *n_H significantly different from WT or pEC₅₀ significantly different from WT and >5-fold change, p < 0.05, 2-way ANOVA. Column 1 is the standard residue numbering, column 2 is my comparative numbering starting at a highly conserved aspartate residue.

n=3x indicates 3 technical replicates of x biological replicates, n=4 indicates two biological replicates. Results in italics were collected by Jennifer Jeffreys before I joined the lab.

3.2.1.3 2 out of 5 non-functional 5-HT_{3A}R M4 mutant receptors could be rescued by coexpression with a chaperone

To test whether any of the five non-responsive mutants had issues with folding, assembly and/or export, I coexpressed the non-functional receptors with the chaperone RIC-3. Two of the previously non-responsive mutant receptors (Y4.14A and W4.22A) now showed WT-like responses (Table 3.2), indicating that those mutations affect receptor folding and/or export, and have no measurable effect on channel function. However, three mutant receptors (D4.0A, Y4.7A, and W4.25A) still showed no activity in response to ligand addition. I further probed these mutants by assaying radioligand binding.

Table 3.2: Parameters of 5-HT_{3A} M4 alanine mutant receptors coexpressed with RIC-3

Mutant	pEC ₅₀ (M)	EC ₅₀ (μM)	n _H	MRF	n
RIC-3 only	NF				3
WT	6.76 ± 0.01	0.17	3.7 ± 0.3	273 ± 16	12
WT+	6.89 ± 0.04	0.13	2.5 ± 0.4	349 ± 35	3
D4.0A+	NF				3
Y4.7A+	NF				3
Y4.14A+	6.93 ± 0.02	0.12	2.1 ± 0.2	334 ± 18	5
W4.22A+	6.71 ± 0.03	0.19	2.1 ± 0.3	334 ± 21	4
W4.25A+	NF				3

Data are mean ± SEM. + indicates coexpression with chaperone RIC-3, MRF is maximum recorded fluorescence, NF = non-functional at concentrations up to 1 mM 5-HT. Typical MRF values for NF receptors were between 0 and 20. No pEC₅₀ or n_H values were significantly different from WT/WT+ and ≥5-fold change, p < 0.05, 2-way ANOVA. n=3x indicates 3 technical replicates of x biological replicates, n=4 indicates two biological replicates.

3.2.1.4 Radioligand binding showed 1 out of 3 non-responsive mutant receptors was capable of ligand binding at the plasma membrane

The absence of response from the non-functional M4 mutants could arise from three main failure points: the receptors could 1) be at the plasma membrane but unable to bind ligand (and therefore unable to open), 2) be at the plasma membrane and able to bind ligand, but unable to gate the pore or 3) have failed to reach the plasma membrane. To determine whether these three M4 mutants reached the plasma membrane, I performed radioligand binding with the selective antagonist [³H]GR65630 (Figure 3.2, section 2.2.4). The radioligand used ([³H]GR65630) mainly accesses receptors at the plasma membrane, as evidenced by permeabilised cells binding almost twice the amount of [³H]GR65630 as non-permeabilised cells (Ilegems, Pick, Deluz, et al., 2004). All mutants were coexpressed with RIC-3 to promote cell-surface expression.

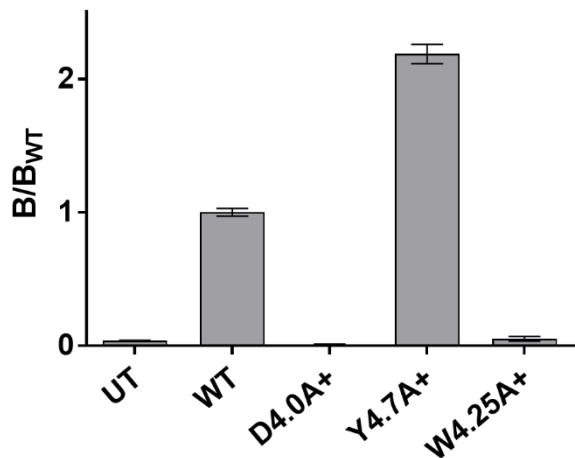


Figure 3.2: Single-point radioligand binding relative to WT of nonresponsive M4 mutants. B is specific binding of [³H]GR65630 to transfected cell membranes. Data are mean \pm SEM, n \geq 3, + indicates coexpression with chaperone RIC-3, UT is untransfected cells.

The Y4.7A mutant receptor was shown to bind radioligand at levels comparable to the WT. This demonstrates that Y4.7A only prevented channel function, not ligand binding, at the plasma membrane. Thus Y4.7 must be required for channel function to occur in response to ligand binding, which was unexpected for a residue so far removed from the binding site, the channel pore, and the space between those two. In contrast, no binding was detected for either the D4.0A or W4.25A mutant receptors above the level of binding of untransfected cells. This suggests that D4.0 and W4.25 are required for receptor expression to the plasma

membrane, and their importance in channel function when correctly expressed and exported cannot be deduced from the behaviour of these alanine mutants. I further investigated all three of these positions on the M4 helix.

3.2.1.5 Further characterisation of non-functional 5-HT_{3A}R M4 mutant receptors

3.2.1.5.A D4.0

To probe the role of D4.0, I assayed different substitutions at this position (Table 3.3). Changing the position of the negative charge (D4.0E) appeared to be detrimental to receptor expression; this mutant receptor showed WT-like response to ligand on some days (though with reduced MRF values), and no response to ligand at all on other days. Changing the degree of negative charge (D4.0N) abolished receptor function. In both these cases however, coexpression with RIC-3 rescued receptor function, indicating that these changes were affecting receptor expression more than function. The effects of the other substitutions tested (A, L, V, S, R) could not be overcome by coexpression with a chaperone. Together this indicates that some negative polarity, and its position, are both key to the role of D4.0 in protein assembly or export.

Table 3.3: Parameters of 5-HT_{3A} receptors with substitutions of D4.0

Mutant	pEC ₅₀ (M)	EC ₅₀ (μM)	n _H	MRF	n
WT	6.76 ± 0.01	0.17	3.7 ± 0.3	273 ± 16	12
WT+	6.89 ± 0.04	0.13	2.5 ± 0.4	349 ± 35	3
D4.0A+	NF				3
D4.0L+	NF				3
D4.0V+	NF				3
D4.0S+	NF				3
D4.0E	Inconsistent responses				12
D4.0E+	6.51 ± 0.12	0.31	5.2 ± 4.9	223 ± 5	4
D4.0R+	NF				6
D4.0N	NF				4
D4.0N+	6.46 ± 0.05	0.34	3.8 ± 1.1	166 ± 3	4

Data are mean \pm SEM. + indicates coexpression with RIC-3, MRF is maximum recorded fluorescence, NF = non-functional at concentrations up to 1 mM 5-HT. Typical MRF values for NF receptors were between 0 and 20. No pEC₅₀ or n_H values were significantly different from WT/WT+ and \geq 5-fold change, p < 0.05, 2-way ANOVA. n=3x indicates 3 technical replicates of x biological replicates, n=4 indicates two biological replicates.

I also looked for potential interaction partners of D4.0. The residues with a sidechain within 5 Å of D4.0 (not including residues on the same helix) in the closed structure (6be1) and/or a serotonin-bound structure (6dg8) are F242, P245, P246, R251, E300 and I304 (Figure 3.3). As proline and isoleucine are hydrophobic, and likely do not interact with D4.0, I selected E300 (on M3) and R251 (on M2, the pore-lining helix) as the most likely candidates for functional partners for D4.0, and F242 (on M1) as a candidate for potentially stabilising one of the putative polar interactions. R251 and E300 are less than 4Å from each other, leading me to consider that in addition to either alone being able to form polar/charge interactions with D4.0, these three residues (D4.0, R251 and E300) could form a network of polar/charge interactions. F242 sits above this system in the closed structure (6be1), with the potential to form an anion-pi, cation-pi or polar-pi interaction with D4.0, R251 and/or E300. In the open structure (6dg8), F242 is likely too far above the D-R-E trio for any interaction to occur.

I assayed alanine mutations of these three residues (Table 3.4), and found that E300A had no measurable effect and F242A only caused a small increase in EC₅₀, indicating that they are likely not the functional interaction partners of D4.0 in its role in receptor assembly and/or export. In contrast, R251A abolished channel responses in the functional assay, as D4.0A had previously done. R251 is therefore an excellent candidate for being functionally connected to D4.0 in the WT receptor.

To probe the importance of the D4.0-R251 interaction to channel assembly, I assayed the double mutant R251D/D4.0R (Table 3.4). This mutant gave no response, and further mutations (Table 3.4) showed that position 251 is highly selective, with even the R251K mutant receptor coexpressed with RIC-3 being inactive. I also assayed R251K in *Xenopus* oocytes (which can be more permissive to receptor expression than HEK293 cells) with two-

electrode voltage clamp and found it non-responsive to ligand. Altogether these data indicate that D4.0 and R251 are both key to receptor expression and/or function.

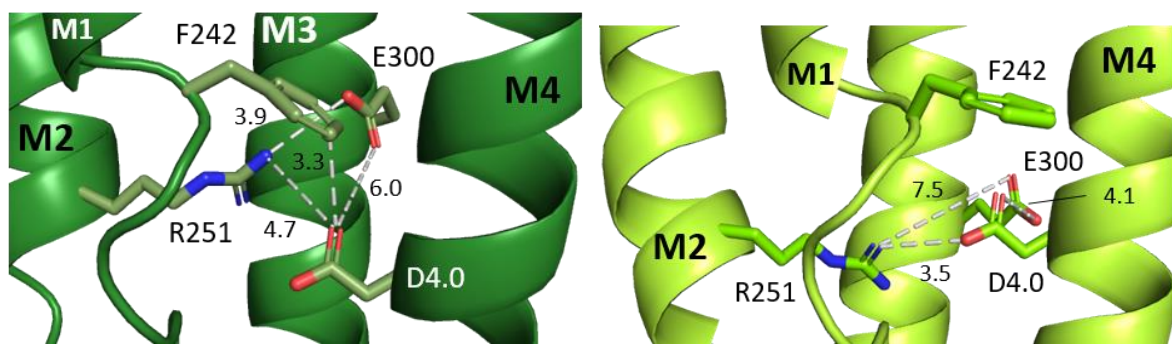


Figure 3.3: Potential interaction partners of D4.0. Distances in marked by dashed lines. 6be1 (closed structure) in dark green and 6dg8 (open structure) in light green.

Table 3.4: Parameters of 5-HT_{3A} receptors with substitutions of potential interaction partners of D4.0

Mutant	pEC ₅₀ (M)	EC ₅₀ (μM)	n _H	MRF	n
WT	6.76 ± 0.01	0.17	3.7 ± 0.3	273 ± 16	12
WT+	6.89 ± 0.04	0.13	2.5 ± 0.4	349 ± 35	3
R251A+	NF				3
R251K+	NF				3
R251E+	NF				3
R251D+	NF				3
E300A	6.71 ± 0.04	0.19	2.4 ± 0.4	219 ± 14	3
E300D	6.37 ± 0.03	0.43	3.7 ± 1.3	78 ± 9	6
E300Q	6.50 ± 0.02	0.32	5.5 ± 0.8	206 ± 14	3
R251D/D4.0R	NF				3
E300Q/D4.0N	NF				6
F242A	6.54 ± 0.03	0.28	2.8 ± 0.5	105 ± 16	3

Data are mean \pm SEM. MRF is maximum recorded fluorescence, + indicates coexpression with chaperone RIC-3, NF = non-functional at concentrations up to 1 mM 5-HT. Typical MRF values for NF receptors were between 0 and 20. No pEC₅₀ or n_H values were significantly different from WT/WT+ and \geq 5-fold change, p < 0.05, 2-way ANOVA. n=3x indicates 3 technical replicates of x biological replicates, n=4 indicates two biological replicates.

3.2.1.5.B W4.25 and aromatic residues in M4

The other mutation that abolished detectable ligand binding (even on coexpression with RIC-3) was W4.25A (Table 3.2). Further mutations (Table 3.5) indicated that an aromatic residue was sufficient for channel function at this position, although both the W4.25F and W4.25Y mutant receptors required coexpression with RIC-3 to reach WT-like MRF values. W4.25 is well positioned for a π - π interaction with the critical Cys-loop residue F144 (Figure 3.4), and I posit that this interaction may be key to 5-HT_{3A} assembly/export in HEK cells.

I also further probed the effects of Y4.14A and W4.22A by assaying the double mutant Y4.14A/W4.22A (Table 3.5). When coexpressed with RIC-3, it showed WT-like function, demonstrating that even the lack of both these aromatic residues at once did not hinder channel function (beyond some effect on channel expression, overcome by coexpression with RIC-3).

To investigate whether any of the other positions with an aromatic residue showed selectivity between different aromatic residues, I performed further substitutions at those positions (Table 3.5). All aromatic residues could be substituted with a different aromatic residue without disturbing receptor function.

Finally, to assess the effect of adding an aromatic residue at the M4-M1/M3 interface (which consistently lowers EC₅₀ in ELIC ((Hénault et al. 2015), section 1.2.1), I substituted in aromatic residues for A4.10, V4.11 and A4.13 individually. V4.11 faces inwards between Y4.7 and Y4.14, and the two alanine positions are either side of V4.11 (Figure 3.4). However none of these aromatic substitutions had any measurable effect on channel activity (Table

3.5), showing that unlike in ELIC, adding aromatic residues to the 5-HT_{3A} M4-M1/M3 interface does not promote channel opening.

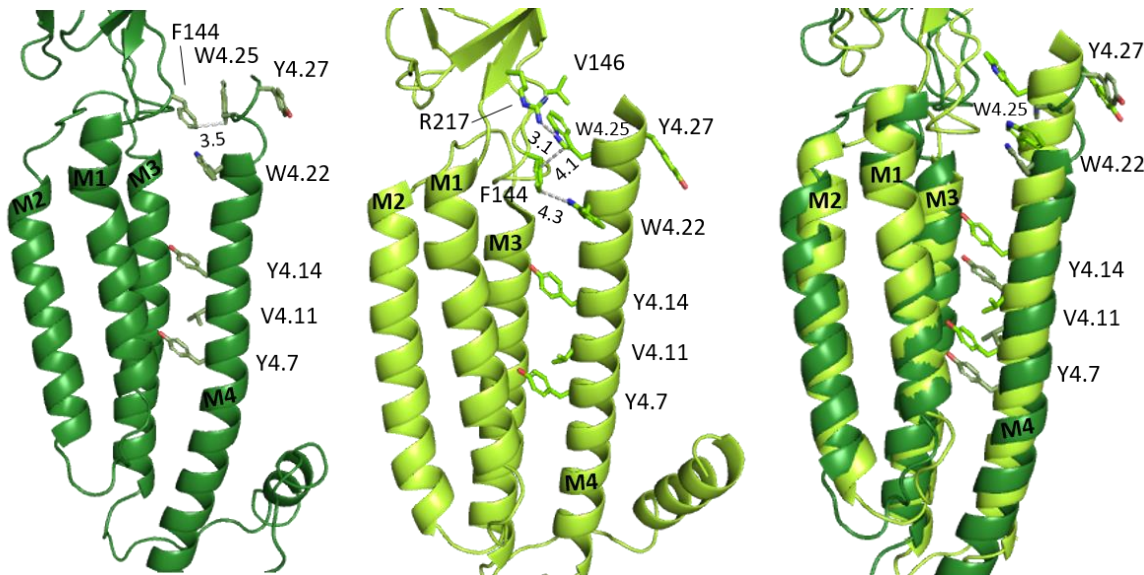


Figure 3.4: Aromatic residues on M4. Single subunit of 5-HT_{3A} in A) the closed (6bel, dark green) and B) the open (6dg8, light green) conformation, showing key aromatic residues, selected potential interaction partners of W4.25, and V4.11. C) Alignment of the two transmembrane domains, showing how M4 moves 'upwards' compared to the rest of the TMD on channel opening.

Table 3.5: Parameters of 5-HT_{3A} receptors with aromatic substitutions in M4

Mutant	pEC ₅₀ (M)	EC ₅₀ (μM)	n _H	MRF	n
WT	6.76 ± 0.01	0.17	3.7 ± 0.3	273 ± 16	12
WT+	6.89 ± 0.04	0.13	2.5 ± 0.4	349 ± 35	3
Y4.7A+	NF				3
Y4.7F	6.40 ± 0.08	0.40	2.0 ± 0.6	118 ± 27	4
Y4.7L+	NF				3
Y4.7S+	NF				3
Y4.14A	NF				9
Y4.14A+	6.93 ± 0.02	0.12	2.1 ± 0.2	334 ± 40	5
Y4.14F	6.49 ± 0.02	0.32	3.0 ± 0.5	275 ± 16	6
W4.22A	NF				9
W4.22A+	6.71 ± 0.03	0.19	2.1 ± 0.3	334 ± 47	4
W4.22Y	6.64 ± 0.04	0.23	3.1 ± 0.5	242 ± 14	4
W4.25A	NF				9
W4.25A+	NF				3
W4.25Y	6.25 ± 0.04	0.56	3.9 ± 0.7	71 ± 3	6
W4.25F	6.45 ± 0.03	0.35	2.6 ± 0.7	71 ± 7	6
W4.25F+	6.64 ± 0.11	0.23	3.5 ± 1.3	197 ± 9	3
Y4.27A	6.85 ± 0.03	0.15	3.7 ± 0.8	375 ± 17	3
Y4.27F	6.85 ± 0.03	0.14	2.5 ± 0.4	323 ± 17	3
Y4.14A/W4.22A+	7.08 ± 0.02	0.08	2.4 ± 0.3	613 ± 21	3
A4.10G	6.43 ± 0.02	0.37	2.3 ± 0.4	195 ± 5	3
A4.10V	6.32 ± 0.04	0.48	2.9 ± 0.6	253 ± 10	3
V4.11Y	6.41 ± 0.05	0.39	4.0 ± 1.4	237 ± 13	3
V4.11F	6.42 ± 0.02	0.38	3.7 ± 0.6	165 ± 2	3
V4.11W	6.55 ± 0.03	0.28	2.9 ± 0.5	255 ± 4	3
L4.12V	6.75 ± 0.03	0.18	3.8 ± 0.5	254 ± 6	3
A4.13I	6.66 ± 0.03	0.22	2.2 ± 0.3	378 ± 18	3
A4.13L	6.68 ± 0.04	0.21	2.0 ± 0.3	337 ± 16	3

Data are mean \pm SEM. + indicates coexpression with chaperone RIC-3, MRF is maximum recorded fluorescence, NF = non-functional at concentrations up to 1 mM 5-HT. Typical MRF values for NF receptors were between 0 and 20. No pEC₅₀ or n_H values were significantly different from WT/WT+ and \geq 5-fold change, p < 0.05, 2-way ANOVA. n=3x indicates 3 technical replicates of x biological replicates, n=4 indicates two biological replicates. Results in italics were collected by Jennifer Jeffreys before I joined the lab.

3.2.1.5.C Y4.7A

The Y4.7A mutant receptor gave no response in the functional assay (Table 3.1), but was expressed and capable of binding ligand at the plasma membrane (Figure 3.2). To determine whether Y4.7A was causing any change in ligand binding affinity, I performed saturation binding (Figure 3.5, section 2.2.4), which showed no measurable reduction in B_{max} or K_d in the Y4.7A mutant compared to the WT receptor. Thus the lack of response must be due to the channel failing to open upon ligand binding, rather than any defect in the ligand binding itself. This striking result shows that while most residues on the M4 are individually incidental to channel function (23 out of 28 5-HT₃AR M4 alanine mutations had no detectable effect on function, section 3.2.1.2), or are required for expression (2 alanine mutations affected expression, sections 3.2.1.3 and 3.2.1.4), Y4.7 plays a pivotal role in allowing channel opening on ligand binding.

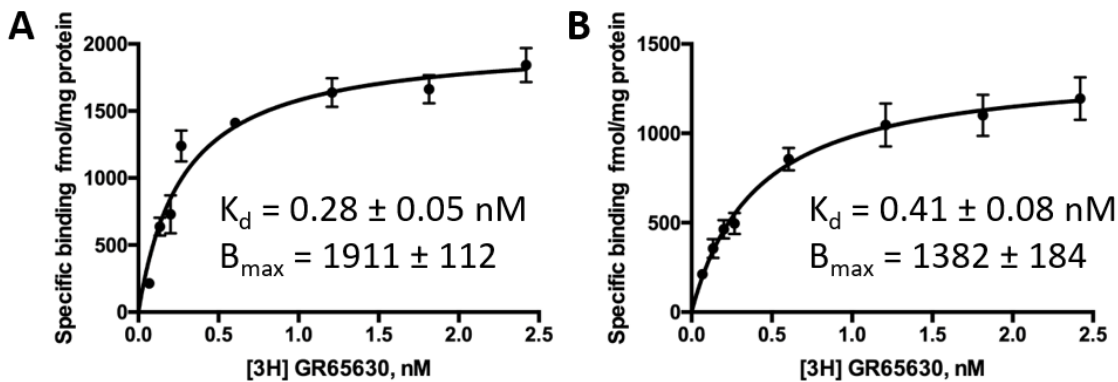


Figure 3.5: Radioligand binding curves of A) the WT 5-HT_{3A} and B) Y4.7A mutant receptors. Data = mean \pm SEM, B_{max} measured in fmol/mg protein. (Adapted with permission from Mesoy, S., Jeffreys, J., & Lummis, S. C. R. (2019). Copyright 2019 American Chemical Society.)

To determine how Y4.7 might be acting to allow channel opening on ligand binding, I tested the effects of substituting other residues at this position (Table 3.5). Y4.7F allowed WT-like function, while mutations to a large hydrophobic non-aromatic residue (Y4.7L) or to non-aromatic residues with hydroxyl groups (Y4.7S, Y4.7D) all abolished function. This indicates that the aromatic ring of Y4.7 is functionally key, and the hydroxyl group is not.

To determine whether Y4.7 is equally important in all 5-HT₃R subunits, I assessed the effect of Y4.7F and Y4.7A mutations in human 5-HT_{3A-AE} (5-HT_{3A}, 5-HT_{3AB}, 5-HT_{3AC}, 5-HT_{3AD}, and 5-HT_{3AE}) receptors on function and ligand binding. HEK cells transfected with h5-HT_{3A-AE} DNA gave robust responses to 5-HT in the functional assay (average MRF = 406 ± 36), with EC₅₀s around 0.2 μ M, except for 5-HT_{3AB} which gave an EC₅₀ of 0.8 μ M. This is consistent with previous work showing that 5-HT_{3AB} receptors have a higher EC₅₀ for 5-HT than other 5-HT₃ receptors (Price et al., 2017). HEK cells transfected with h5-HT_{3A-AE} DNA with Y4.7F mutations in all subunits all also gave robust responses to ligand (average MRF = 235 ± 17). However, none of the h5-HT_{3A-AE} receptors with Y4.7A mutations in all subunits showed any response in the functional assay, even when co-expressed with RJC-3 (average MRF = 30 ± 5).

Although all the h5-HT_{3A} Y4.7A mutant receptors were non-functional, none of them showed different radioligand binding from the same WT receptor, p<0.05, 2-way ANOVA (Figure 3.6). This indicates that Y4.7 plays an important role in receptor function in response to ligand binding in all 5-HT₃ subunits, or at least in the A subunit even in heteropentamers. To further investigate the specific role of Y4.7, I returned to the m5-HT_{3A} receptor.

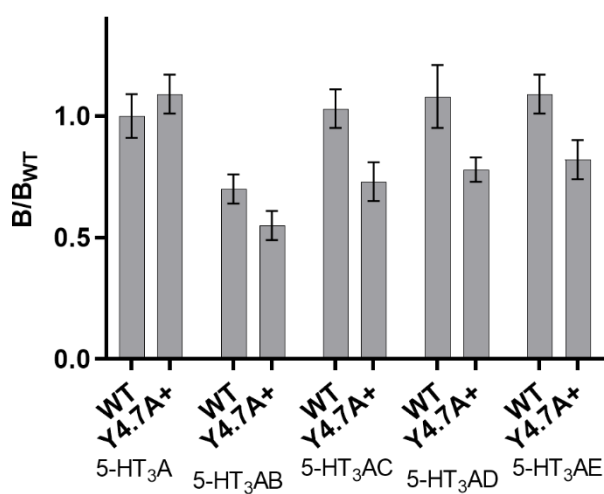


Figure 3.6: Single-point radioligand binding relative to WT h5-HT_{3AR} of 5-HT_{3AB-AE} receptors and Y4.7A 5-HT_{3AB-AE} receptor mutants. B is specific binding of [³H]GR65630 to transfected cell membranes. Data are mean ± SEM, n = 3, + indicates coexpression with chaperone RIC-3.

3.2.2 Potential interaction partners of Y4.7

There are 7 residue sidechains from residues not in M4 within 5 Å of Y4.7 in the closed m5-HT_{3A} structure 6be1 (M235, D238, I239, F242, L293, L294 and S297), and 4 in the open structure 6dg8 (L234, D238, C290 and L293) (Figure 3.7). From their positioning and side chain characteristics, I initially judged M235, D238, C290 and S297 to be the best candidates for potential interaction partners for Y4.7. To probe the roles of these residues, I mutated each to alanine and assayed function and in some cases ligand binding affinity (Table 3.6). I had also already probed F242 (Table 3.4), which is a plausible candidate for a π-π interaction with Y4.7, so included that in my analysis. Some mutants showed small changes in function relative to WT, but only one showed a similar effect to Y4.7A. I will discuss these two groups separately.

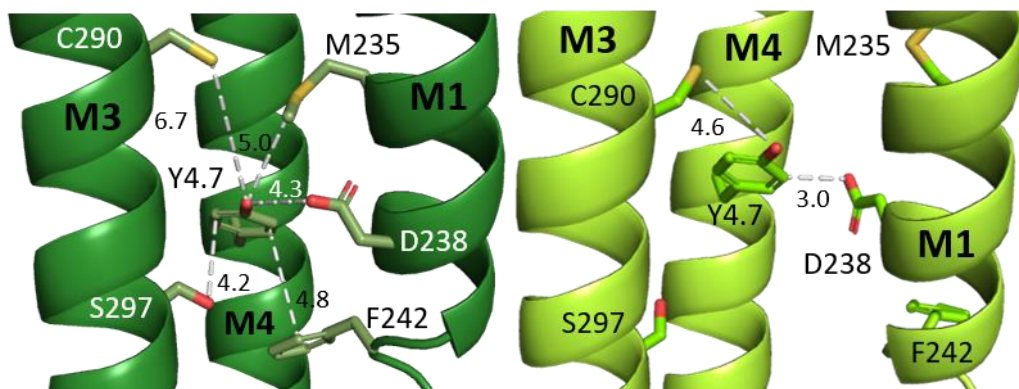


Figure 3.7: Potential interaction partners of Y4.7. Distances in Å marked by dashed lines, 6be1 (closed structure) in dark green, 6dg8 (open structure) in light green.

Table 3.6: Parameters of 5-HT_{3A} receptors with substitutions of potential interaction partners of Y4.7

Mutant	pEC ₅₀ (M)	EC ₅₀ (μM)	n _H	MRF	K _d (nM)	B _{max} (pmol/mg protein)
WT	6.76 ± 0.01	0.17	3.7 ± 0.3	273 ± 16	0.28 ± 0.05	1.9 ± 0.1
M235A	7.19 ± 0.06	0.07	2.4 ± 0.6	116 ± 23	0.70 ± 0.09*	2.4 ± 0.4
D238A	NF					
D238A+	NF				0.50 ± 0.07	1.8 ± 0.4
F242A	6.54 ± 0.03	0.28	2.8 ± 0.5	105 ± 16		
C290A	7.79 ± 0.05*	0.02	1.2 ± 0.2*	153 ± 17	0.85 ± 0.10*	3.8 ± 0.3
S297A	6.34 ± 0.03	0.46	3.5 ± 0.8	172 ± 12		

Data are mean ± SEM, n≥3. + indicates coexpression with chaperone RIC-3, MRF is maximum recorded fluorescence, NF = non-functional at concentrations up to 1 mM 5-HT. Typical MRF values for NF receptors were between 0 and 20. *n_H or K_d significantly different from WT/WT+, or pEC₅₀ significantly different from WT/WT+ and ≥5-fold change, p < 0.05, 2-way ANOVA. n≥3 technical replicates for the fluorescence assay, n≥3 biological replicates for the radioligand binding.

3.2.2.1 One mutation near Y4.7 had the same effect on receptor function as Y4.7A

One mutation had the same effect as Y4.7A, showing no response in the functional assay, yet WT-like capacity for ligand binding: D238A (Table 3.6). This indicates that D238 may interact with Y4.7, and that their interaction could be key to channel opening in response to ligand binding.

While D238 appears well positioned for a hydrogen bond with the hydroxyl group of Y4.7, this cannot be the functionally pivotal interaction, as Y4.7F gave WT-like function (Table 3.5) without the hydroxyl group. Attempting to prove the importance of the Y4.7-D238 interaction by switching the residues (Y4.7D/D238Y) resulted in a non-functional receptor, indicating that the positioning of the residues may be important, or that surrounding residues may be affecting the interaction in an asymmetric fashion.

3.2.2.2 Two mutations near Y4.7 affected receptor function

Of the other mutations near Y4.7, C290A caused an almost 10-fold decrease in EC₅₀, while M235A gave a statistically significant ($p < 0.0001$, 2-way ANOVA) but smaller (2.4-fold) decrease in EC₅₀. Both of these mutants had slightly lower affinity for the radioligand than WT (Table 3.6), indicating that the lower EC₅₀s is likely not due to improved ligand binding. In addition to this, C290A receptors also had a significantly lower Hill coefficient (n_H , slope of the calculated concentration-response curve at the EC₅₀ concentration of ligand) than WT (Figure 3.8).

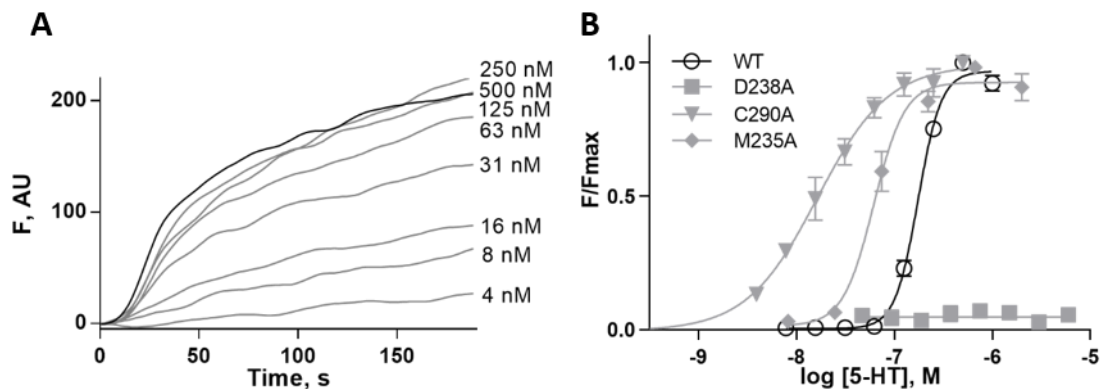


Figure 3.8: Responses of 5-HT_{3A} receptors with Y441-adjacent mutations. A) Fluorescent responses (F in arbitrary units, AU) of C290A mutant receptors on addition of 5-HT at 20 s. B) Concentration-response curves from data as in A. Data are mean \pm SEM, $n \geq 3$

Neither F242A nor S297A had any notable effect on receptor function, indicating that they do not play major roles in function, and neither is likely to be a key interaction partner for Y4.7.

3.2.3 Molecular dynamics and mechanism of action of Y4.7

To further explore the specific effect and mechanism of action of Y4.7, I started collaborating with Alessandro Crnjar, a molecular dynamics modeller in Carla Molteni's laboratory at King's College, London. All computational work in this section was performed by Alessandro Crnjar, while all experimental work in this section is mine. The hypotheses and ideas arose in discussions between us over the course of our collaboration.

3.2.3.1 Background

We defined two main possibilities for the mechanism of action of Y4.7 (Figure 3.9). The first was a 'vertical' mechanism, where residue 4.7 would affect receptor function by its effect propagating up along the M4 and affecting the interaction of the tip of M4 with the ECD, especially the pivotal Cys-loop. The second possibility was a 'horizontal' mechanism, where

residue 4.7 would affect receptor function by its effect propagating through M1/M3 to affect the channel pore-lining helix M2.

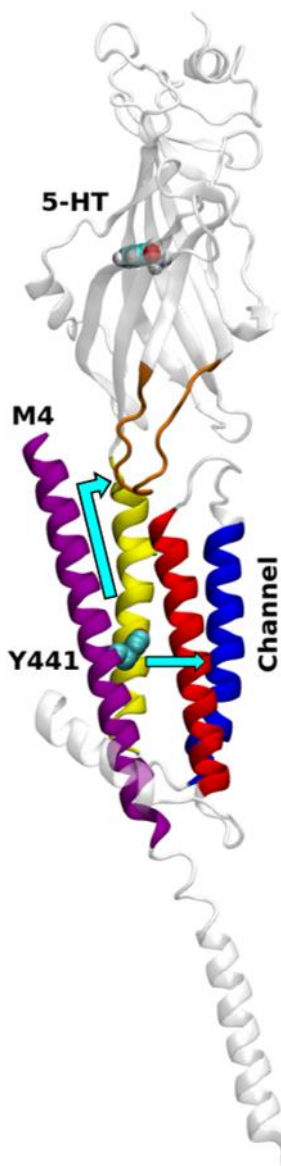


Figure 3.9: Two proposed mechanisms of action for Y4.7.

A single subunit of the 5-HT_{3A} receptor showing the proposed vertical and horizontal paths in cyan. The ligand and residue Y441 are shown as spheres, transmembrane helices M1 in yellow, M2 in blue, M3 in red, M4 in purple, and the Cys-loop in orange. (Figure adapted from Crnjar, A., Mesoy, S., Lummis, S. C. R., & Molteni, C. (2021) under a Creative Commons Attribution License (CC BY). Copyright 2021 Crnjar, Mesoy, Lummis and Molteni.)

3.2.3.1.A Proposed vertical mechanism of M4 action

The interaction between the M4 tip and the ECD was first proposed to be crucial to channel opening on ligand binding by DaCosta and Baenziger (DaCosta and Baenziger, 2009). They

describe an ‘uncoupled’ conformation of the *Torpedo* nicotinic acetylcholine receptor, where ligand binding does not cause channel opening, and proposed that the M4-ECD interaction is required to allow the channel opening signal to propagate from the ECD into the TMD and to the pore. This suggested mechanism is intuitively appealing and has plausible underpinnings in the structural data we have, and is also supported by Alcaino et al. (2017), which shows that allosteric modulation can propagate from the M4 tip to loop C in the ECD of the $\alpha 4\beta 2$ receptor. DaCosta and Baenziger also suggested an appealing mechanism for a lipid-dependent this M4-ECD interaction, shown in Figure 3.10.

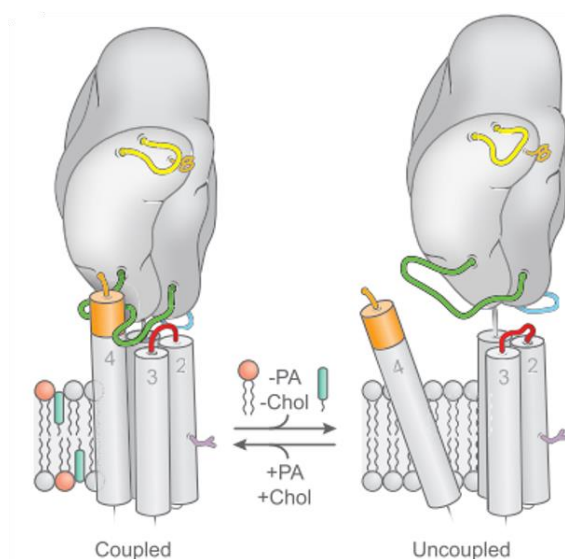


Figure 3.10: Suggested lipid-dependent structural rearrangements of M4 affecting ECD-TMD interactions, particularly with the Cys-loop (in green). (Figure used under the Creative Commons Attribution License (CC BY) from DaCosta, C. & Baenziger, J., (2009). Copyright 2009 American Society for Biochemistry and Molecular Biology.)

A plausible extension of these hypotheses is that Y4.7 might be able to ‘pin’ the M4 to the rest of the TMD, perhaps by interacting with D238. This would parallel the proposal in DaCosta et al. (2013) that a thicker or more hydrophobic bilayer can push M4 close enough to interact with the ECD and allow ‘coupling’ of ligand binding to channel opening. In our case, we proposed that the Y4.7A and D238A mutations could be weakening the interaction of the M4 with the rest of the TMD, allowing it to remain at a distance and preventing signal transduction from the ligand binding site to the channel pore.

If Y4.7 acts through this vertical mechanism, we would expect to observe changes in the tip of M4, or even the Cys-loop itself when comparing the WT and Y4.7A receptors.

3.2.3.1.B Proposed horizontal mechanism of M4 action

M4 could also affect channel opening by affecting the neighbouring helices M1 and/or M3, and through them the pore-lining M2. Domville and Baenziger (2018) shows that the naturally occurring M4 mutation C418W in the *Torpedo* nAChR, which alters channel function, does not affect M4-loop C interactions, but is energetically coupled to two residues on M1 (S226 and T229) (Domville and Baenziger, 2018).

If Y4.7 acts through M1/M3 rather than through the M4 tip, then we should be able to observe changes in M1/M3 when comparing the WT and Y4.7A receptors.

3.2.3.2 Molecular dynamics simulation of Y4.7A receptors

My collaborator built two 5-HT_{3A} receptor models, one WT and one with Y4.7A mutations in all subunits, based on the 6DG8 structure. He ran two simulations of each in a randomly distributed 6:7:7 cholesterol:POPC:POPE (phosphatidylethanolamine) lipid bilayer, equilibrated for 150 ns before each was simulated for 250 ns. The majority of the simulation analysis was performed on the 50-250 ns time window of these four simulations. The specific details of this work and the computational results are described in Crnjar et al. (2021), and recapitulated here for context. The computational results in sections 3.2.3.2.A and 3.2.3.2.B below are not my own work, but the work of Alessandro Crnjar, though we collaborated tightly for the duration of this work, and shared discussions of data analysis and the directing the investigations.

3.2.3.2.A Investigation of vertical effects of Y4.7A on M4 and the ECD

To test the ‘vertical mechanism’ hypothesis, we first sought to determine what effects (if any) Y4.7A had on M4 itself (especially the tip), and its interaction with the ECD. We evaluated the difference between the WT and mutant M4 by three metrics: the root mean square fluctuation (RMSF) of M4 residues, the time-averaged dynamical correlation between residue 4.7 and other M4 residues, and intramolecular interactions (H-bonds and π-π interactions) (Figure 3.11).

To explore whether Y4.7A was affecting the flexibility or mobility of M4 (especially the tip), we calculated the RMSF with respect to the post-equilibration position of each residue (averaged over the five subunits of a simulation) (Figure 3.11A). Residue 425 was restrained in the models, so we discounted the small RMSFs of residues near 425. Y4.7A had no significant effect on the RMSF of M4 residues either below, at, or above the level of residue 4.7, indicating that it does not measurably increase M4 mobility or flexibility. We observed that the RMSF of individual residues increased towards the tip of M4, and propose that the M4 tip extending beyond the lipid bilayer may explain part of that increase.

To more specifically explore the effect of Y4.7A on M4 above the 4.7 position, we next calculated the time-averaged dynamical correlation (C_{ij}) of key individual M4 residues with residue 4.7 (Figure 3.11B). For this we chose Y4.14 (Y448) and W4.25 (W459), which are both structurally important residues, with one at the tip of M4. A C_{ij} value of 0 indicates no correlation between the movements of two residues, whereas 1 indicates that two residues consistently move in the same direction at the same time, acting like a single rigid body. While the C_{ij} values varied between subunits and replications, we saw no consistent change in correlation with residue 4.7 between the WT and mutant simulations. The movement of residue 4.7 correlated with that of Y4.14, as expected from their proximity on the M4 helix. However, the movement of W4.25 was not notably correlated to the movement of residue 4.7 in either WT or mutant simulations, again not supporting the proposed ‘vertical’ mechanism.

Finally we investigated some intramolecular interactions (H-bonds and π - π interactions) of selected residues (Figure 3.11C, D). We found no significant differences between the WT and mutant simulations, other than the expected changes at residue 4.7 itself.

In sum, none of the factors we explored supported the ‘vertical mechanism’ proposal that Y4.7A could be affecting the M4-ECD interaction. We next turned to explore the ‘horizontal’ mechanism.

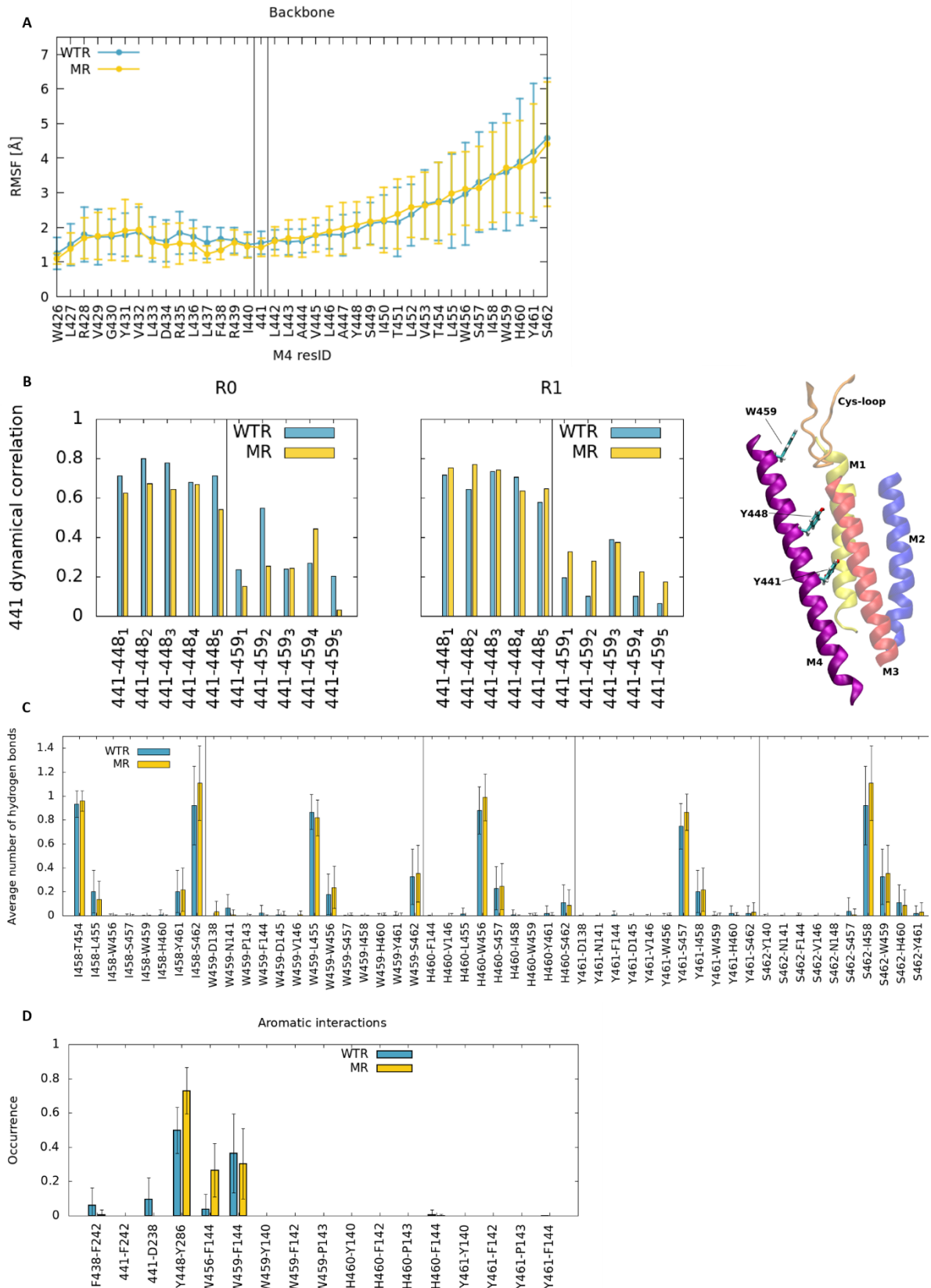


Figure 3.11: M4 characteristics in molecular dynamics simulations. Characteristics of the WT (blue) and Y4.7A (Y441A, yellow) 5-HT_{3A} simulations: A) RMSF of M4 amino acid backbone atoms. B) Average dynamic correlation of residue 4.7 (441) backbone atoms with those of residue 448 and 459. Subscripts denote the five different subunits in the modelled receptor, and a snapshot of the TMD of one subunit shows the positioning of the selected residues. R0 and R1 are two separate simulations of the same receptors from the same starting conditions. C) H-bonds of residues at the tip of M4. D) π - π interactions and an anion- π interaction involving M4 residues. (Figures taken with slight modifications under the Creative Commons Attribution License (CC BY) from Crnjar, A., Mesoy, S., Lummis, S. C. R., & Molteni, C. (2021). Copyright 2021 Crnjar, Mesoy, Lummis and Molteni.)

3.2.3.2.B Investigation of horizontal effects of Y4.7A on M1, M3, and M2

To explore whether Y4.7A could be affecting the rest of the transmembrane domain ‘horizontally’, potentially through residue D238 (where alanine mutation has the same effect as Y4.7A), we calculated the average hydrogen bonds formed by Y4.7 and D238 in the two simulations (Figure 3.12A and B). Aside from the expected difference that residue 4.7 cannot form side chain hydrogen bonds or aromatic interactions in the Y4.7A mutant receptor, the two models had similar hydrogen bonding patterns. However, the analysis did indicate a slight hydrogen bond propensity between D238 and residue K255 (K4') of M2, which is situated less than two helical turns from the main restriction of the channel pore (L9', which is L260) (Figure 3.12). These two residues have previously been predicted to form a salt bridge (Maricq et al., 1991) To explore whether this might realistically affect channel function, we further investigated the D238-K255 distance in the WT and mutant simulation (Figure 3.12C). Here we saw the Y4.7A simulations displaying firstly a marked reduction in occupancy of the state where the D238-K255 distance was less than 4Å, and concomitantly a higher occupancy of >7Å distances between the two residues.

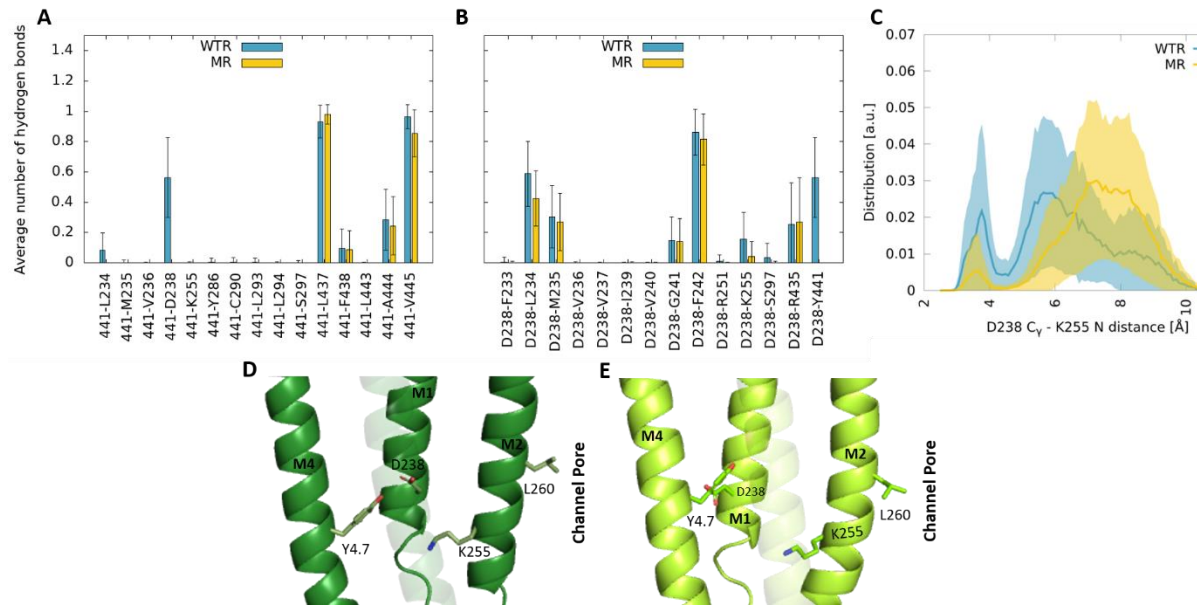


Figure 3.12: Horizontal effects of Y4.7A. A, B) Hydrogen bonds in molecular dynamics simulations of WT (blue) and Y4.7A (Y441A, yellow) of A) residue 4.7 and B) D238 with accessible residues. C) Plot of the distance between the C_γ of D238 and the terminal nitrogen of K255. D, E) 5-HT_{3A} TMD showing the positions of key residues. Closed (6be1) in dark green, serotonin-bound (6dg8) in light green, with M3 transparent for clarity in both. (Figures A-C adapted from Crnjar, A., Mesoy, S., Lummis, S. C. R., & Molteni, C. (2021) under the Creative Commons Attribution License (CC BY). Copyright 2021 Crnjar, Mesoy, Lummis and Molteni.)

Individual traces of the D238-K255 distance over time in each subunit of the simulations are shown in Figure 3.13, exhibiting both transient and longer-term occupancies of the $<4\text{\AA}$ distance. These traces confirm that while both the WT and mutant receptor are both able to reach this state, the WT receptor spends longer time there overall. This was the first measurable difference we had found between the WT and mutant simulations, and highlighted K255 as a potential candidate for transmitting the effect of Y4.7A.

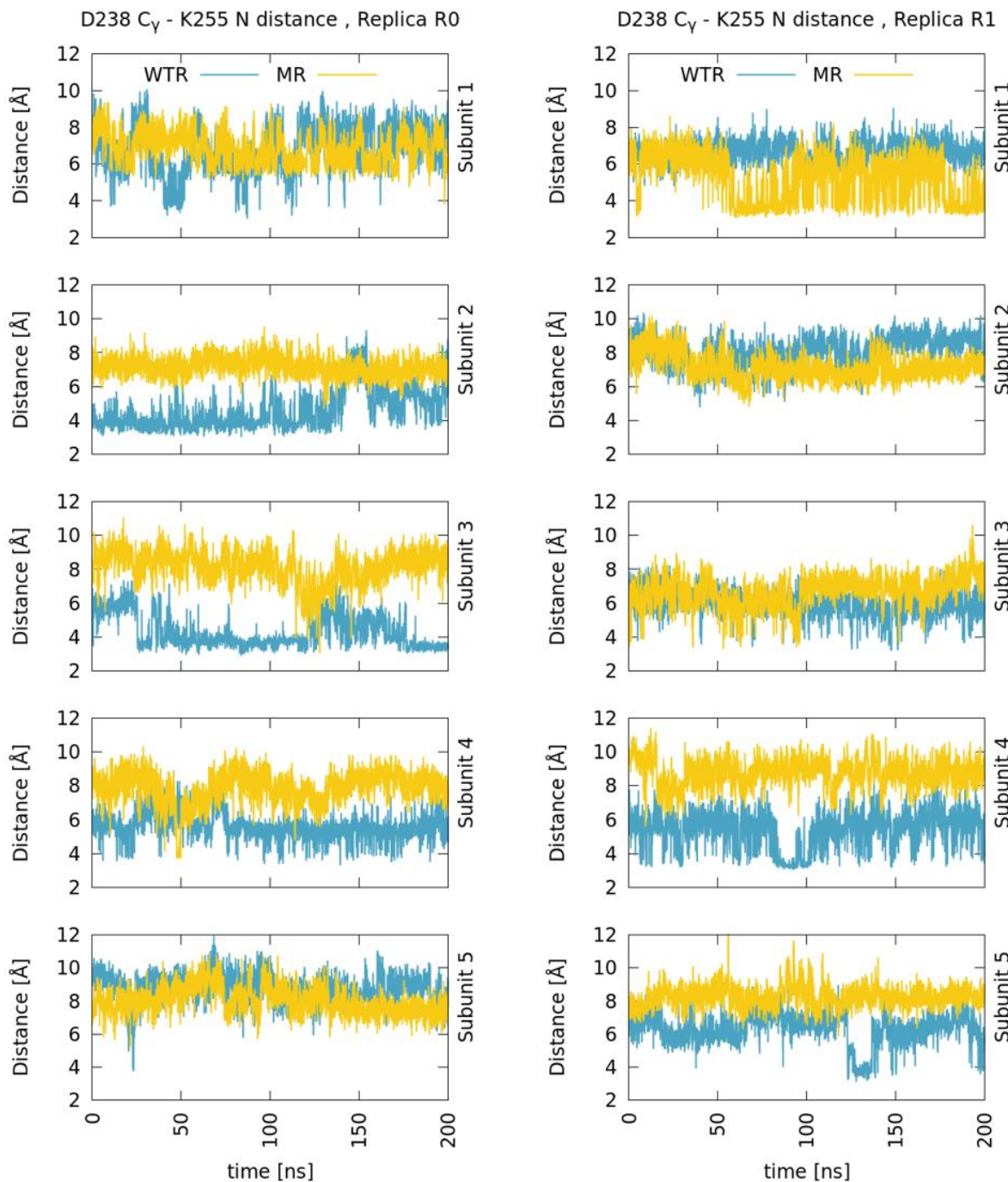


Figure 3.13: D238 C_γ-K255 terminal nitrogen distance over time in each subunit in each replica. WT receptor in blue and Y4.7A in yellow. (Figure taken with slight modifications under the Creative Commons Attribution License (CC BY) from Crnjar, A., Mesoy, S., Lummis, S. C. R., & Molteni, C. (2021). Copyright 2021 Crnjar, Mesoy, Lummis and Molteni.)

3.2.3.3 K255 as a potential interaction partner for D238

To investigate the role of K255 in channel function, I substituted in a range of residues at this position (Table 3.7). The K255A mutant receptor was WT-like, as were the K255Q, E and C mutant receptors. However, the K255L mutant receptor was non-responsive in the functional assay, yet showed WT-like ligand binding, recapitulating the phenotypes of Y4.7A and D238A.

Table 3.7: Parameters of 5-HT_{3A} receptors with substitutions of K255

Mutant	pEC ₅₀ (M)	EC ₅₀ (μM)	n _H	MRF	K _d	B _{max} (pmol/mg protein)
WT	6.76 ± 0.01	0.17	3.7 ± 0.3	273 ± 16	0.28 ± 0.05	1.9 ± 0.1
K255A	6.29 ± 0.02	0.52	2.6 ± 0.1	438 ± 12		
K255L+	NF				0.17 ± 0.02	0.4 ± 0.2
K255Q	6.95 ± 0.02	0.11	1.9 ± 0.2	1066 ± 5		
K255E	6.59 ± 0.02	0.26	4.4 ± 1.4	184 ± 10		
K255C	6.52 ± 0.03	0.30	2.3 ± 0.6	519 ± 117		

Data are mean ± SEM, n≥3. + indicates coexpression with chaperone RIC-3, MRF is maximum recorded fluorescence, NF = non-functional at concentrations up to 1 mM 5-HT. Typical MRF values for NF receptors were between 0 and 20. No pEC₅₀ or n_H values were significantly different from WT/WT+ and ≥5-fold change, p < 0.05, 2-way ANOVA. n≥3 technical replicates for the fluorescence assay, n≥3 biological replicates for the radioligand binding.

3.3 Discussion

The aim of this work was to characterise the role and function of the M4 helix in a cation-selective pLGIC, the 5-HT_{3A} receptor. This helix had previously been investigated in the bacterial homologs ELIC and GLIC (Hénault et al., 2015) and the anionic GABA_A (Cory-Wright et al., 2017) and Glycine α 1 (Haeger et al., 2010) receptors, and from these data it was predicted that alanine mutations in cation-selective mammalian M4 helices (like the 5-HT_{3AR} M4) would have small effects on receptor function, and mostly cause slight decreases in EC₅₀ (Therien and Baenziger, 2017). Contrary to these predictions, I found that three mutations in the 5-HT_{3AR} M4 helix completely abolished receptor function (D4.0A, Y4.7A and W4.25A). Of these, two (D4.0A and W4.25A) showed no measurable radioligand binding and the third (Y4.7A) showed WT-like ligand binding (Figure 3.2, Figure 3.5).

3.3.1 Role of D4.0 in 5-HT_{3A}R function

D4.0 has been shown to be important for both cation-selective and anion-selective pLGIC expression, with an alanine mutation here abolishing cell surface expression in several receptors (da Costa Couto et al. 2020; Lo et al. 2008; Mesoy and Lummis 2021). It is therefore unsurprising that D4.0A abolished ligand binding in the 5-HT_{3A} receptor. Maturation analysis in Lo et al. (2008) shows that the D4.0A mutation in the GABA_A receptor decreases levels of the mutant receptor at the cell surface without affecting forward trafficking or endocytosis, and the authors suggest that mutant subunits are trapped in the ER due to impaired receptor assembly. Two of the D4.0 substitutions in the 5-HT_{3A} receptor (D4.0E and D4.0N) reduced or abolished receptor function here, but that could be overcome by coexpression with the chaperone RIC-3 (Table 3.3), strengthening the hypothesis that mutations at this position are affecting receptor folding, assembly, and/or export to the plasma membrane.

A possible explanation for the importance of D4.0 is that it could be interacting with a nearby residue, and that that interaction is important for receptor expression. R251 initially seemed a promising candidate for interacting with D4.0 in its role in receptor expression, as R251A had

the same effect as D4.0A (Table 3.4). All other substitutions tested at position 251 also abolished receptor function, even the fairly conservative R251K substitution.

R251 has been thoroughly investigated over the years, as part of the pore-lining M2 helix. In the 5-HT_{3A} receptor, an R251C mutant has previously been shown to be functional (R278C in Reeves et al. (2001)) in *Xenopus* oocytes. The same R251C (R278C) substitution was performed in Panicker et al. (2002), where the mutant was found to be WT-like by two-electrode voltage clamp in *Xenopus* oocytes. Interestingly, I found the R251K mutant non-responsive even when assayed it in oocytes as in Reeves et al. (2001). This was surprising, as R251K appears to be a more conservative mutation than R251C. This might indicate that while removing the charge at position 251 is tolerated in the 5-HT_{3A} receptor, changing its position is not. The next two paragraphs review substitutions of this lysine residue in different pLGICs: every lysine in these paragraphs is at the equivalent position to R251 in the 5-HT_{3A} receptor.

In the acetylcholine receptors, results of substitutions at the equivalent position are also variable: in the *Torpedo* $\alpha 2\beta\gamma\delta$ receptor expressed in oocytes, α K242E and α K242Q both abolish receptor function, while β K248E, γ K251E and δ K256E all have no measurable effect on receptor function (Imoto et al., 1988). Similarly, α K242C abolishes receptor function in the muscle-type AChR in oocytes (Akabas et al., 1994). In HEK293 cells, in contrast, α K242C has minimal effects on receptor function (Wilson and Karlin, 1998). Interestingly, in the recent $\alpha 7$ nAChR structures, a D445-K238 salt bridge (equivalent to D434-R251 here) is present in all the receptor states (resting, open, desensitized), and is hypothesised to functionally contribute to channel opening (Noviello et al., 2021).

Finally, in the GABA_A $\alpha 1$ receptor expressed in oocytes, an R255C substitution reduces but does not abolish ligand-induced currents, and shows no accessibility to sulphydryl reagents (Xu and Akabas, 1996).

Altogether this shows a variable role for this lysine residue in receptor function, though frequently substitutions here do abolish receptor function, as in the 5-HT_{3A} receptor in this work. While the exact role of R251 could not be determined, I did exclude E300 and F242

from being candidates for main interaction partners for D4.0 in its role in allowing ligand binding, as substitutions of both were well tolerated.

3.3.2 Role of W4.25 and aromatic residues in M4 in 5-HT_{3A}R function

The W4.25A mutation also abolished radioligand binding at the cell surface. A C-terminal Trp (W475) is also crucial to function in the GABA ρ 1 receptor (Reyes-Ruiz et al., 2010), at least in part through a key interaction with L207 in the Cys-loop (Estrada-Mondragón et al., 2010). In the α 4 β 2 nACh receptor, the post-M4 segment has been shown to be functionally connected to the ECD, though this interaction mainly involves other residues than the post-M4 Trp (Alcaino et al., 2017). Together, these data indicate that a Trp at the tip of the M4 helix can be important to both receptor function and folding/assembly/export.

As for the other aromatic residues in the 5-HT_{3A} M4 helix, two (Y4.14 and W4.22) appeared to play some role in receptor folding/assembly/export, as Y4.14A and W4.22A required coexpression with RIC-3 for function. The Y4.14A/W4.22A double mutant was also WT-like when coexpressed with RIC-3. This is in contrast to ELIC, where mutating M4 aromatic residues to alanine generally decreases EC₅₀ (Hénault et al. 2015).

In the same vein, aliphatic-to-aromatic mutations at the ELIC M4-M1/M3 interface have been shown to decrease EC₅₀ (Carswell et al., 2015). However, none of the aliphatic-to-aromatic mutations in the 5-HT_{3A} M4 had this effect, indicating that the 5-HT_{3A} M4 plays a very different role in receptor function to the ELIC M4 helix.

3.3.3 Role of Y4.7 in 5-HT_{3A}R function

Mutating Y4.7 to Ala abolished receptor function but not ligand binding at the cell surface in not only the m5-HT_{3A} receptor but also in h5-HT_{3A}-AE receptors. This demonstrates that ligand binding is insufficient to allow correct channel opening in these mutant receptors. Some plausible explanations for these data are:

- 1) The Y4.7A mutation might cause the receptor to enter the desensitized state, where the ligand binds but the channel does not open in response.

- 2) The Y4.7A mutant receptor could be in the ‘uncoupled’ state previously described in nAChRs, where neither the channel pore nor the ligand binding sites are in the desensitized conformation, yet ligand binding does not cause channel opening, or even affect the conformation of the channel pore, as the ligand binding sites are allosterically uncoupled from the channel pore (DaCosta and Baenziger, 2009).
- 3) The Y4.7A mutation might affect the structure of the TMD, perhaps collapsing the channel or rendering channel opening more energetically costly than normal ligand binding can overcome.

To investigate the mechanism of action of Y4.7 in the m5-HT_{3A} receptor, I examined nearby residues in search of potential interaction partners.

3.3.3.1 Residues near Y4.7 in the 5-HT_{3A} receptor

D238A is the only Ala mutation of residues near Y4.7 that had the same effect as Y4.7A: abolishing receptor function but not ligand binding (Table 3.6), indicating that the two could be functionally connected. D238 is highly conserved in the 5-HT_{3A}R family, but not beyond, though some anion-selective pLGICs also have a polar residue at this position (Figure 3.14A).

Based on the closed 5-HT_{3A}R structure 6be1 (Figure 3.7, dark green), D238 is in a position to potentially form a hydrogen bond to the hydroxyl group of Y4.7. However, the WT functionality of the Y4.7F mutant receptor showed that the hydroxyl group of Y4.7 was not crucial to its role in receptor function. A more recent open structure of the 5-HT_{3A}R (Figure 3.7, light green) shows D238 could form a hydrogen bond with the aromatic ring of Y4.7, which would be an excellent candidate for the functional link between these two residues, and explain the requirement for the aromatic ring.

This might suggest that a polar substitution of Y4.7 should also suffice for function. However, the only polar substitution I tested, Y4.7S, would be too short to achieve this hydrogen bond (the minimum distance between the hydroxyl groups of D238 and S4.7 would be 4.8 Å).

Mutation of the equivalent residue to D238 in the GABA_A α1 subunit to leucine (S240L) results in a ~4-fold increase in EC₅₀ on expression in HEK293 cells (Akk et al., 2008), while mutation to cysteine (S241C) has no measurable effect on receptors expressed in *Xenopus* oocytes (Stewart et al., 2013). This indicates that this residue is far less crucial to receptor function in the GABA receptor than in the 5-HT_{3A} receptor, which might reflect a broader pattern between anion-selective and cation-selective pLGICs.

Most other mutations near Y4.7 had little or no measurable effect on receptor function. C290A had the largest effect, showing an almost ten-fold decrease in EC₅₀, as well as a markedly shallower Hill slope than WT. This cysteine is conserved across the 5-HT₃ receptor subunits and present in many anionic pLGICs, but not in nAChRs (Figure 3.14C). While the role of C290 is not clear from the structure and this functional data alone, it could be acting as a redox sensor, a role for cysteine under increasing scrutiny (Held, 2020). Intriguingly, the terminal sulphur of C290 is 3.7 Å from the terminal carbon of M235 (in the closed structure 6be1, Figure 3.7), which is sufficient for a CH-S interaction that could confer some specific interaction (as shown in e.g. Reddi et al. (2016)). As C290A and M235A both cause some decrease in EC₅₀, this might indicate that the two interact to promote receptor function in the WT receptor.

The other residues that I investigated by alanine substitution here have various degrees of sequence conservation across pLGICs (Figure 3.14): S297 is fairly conserved across cation-selective pLGICs, but not in anionic pLGICs, where this position in fact often contains an Ala. This fits well with an Ala mutation here having little impact on receptor function. Though I uncovered no functional role for F242 in 5-HT_{3A} receptor function, it is almost entirely conserved across pLGICs, perhaps indicating it does have a yet undiscovered specific role in pLGIC function. Finally, M235 is not highly conserved, and indeed is Ile or Val in 5-HT_{3C}, D and E subunits.

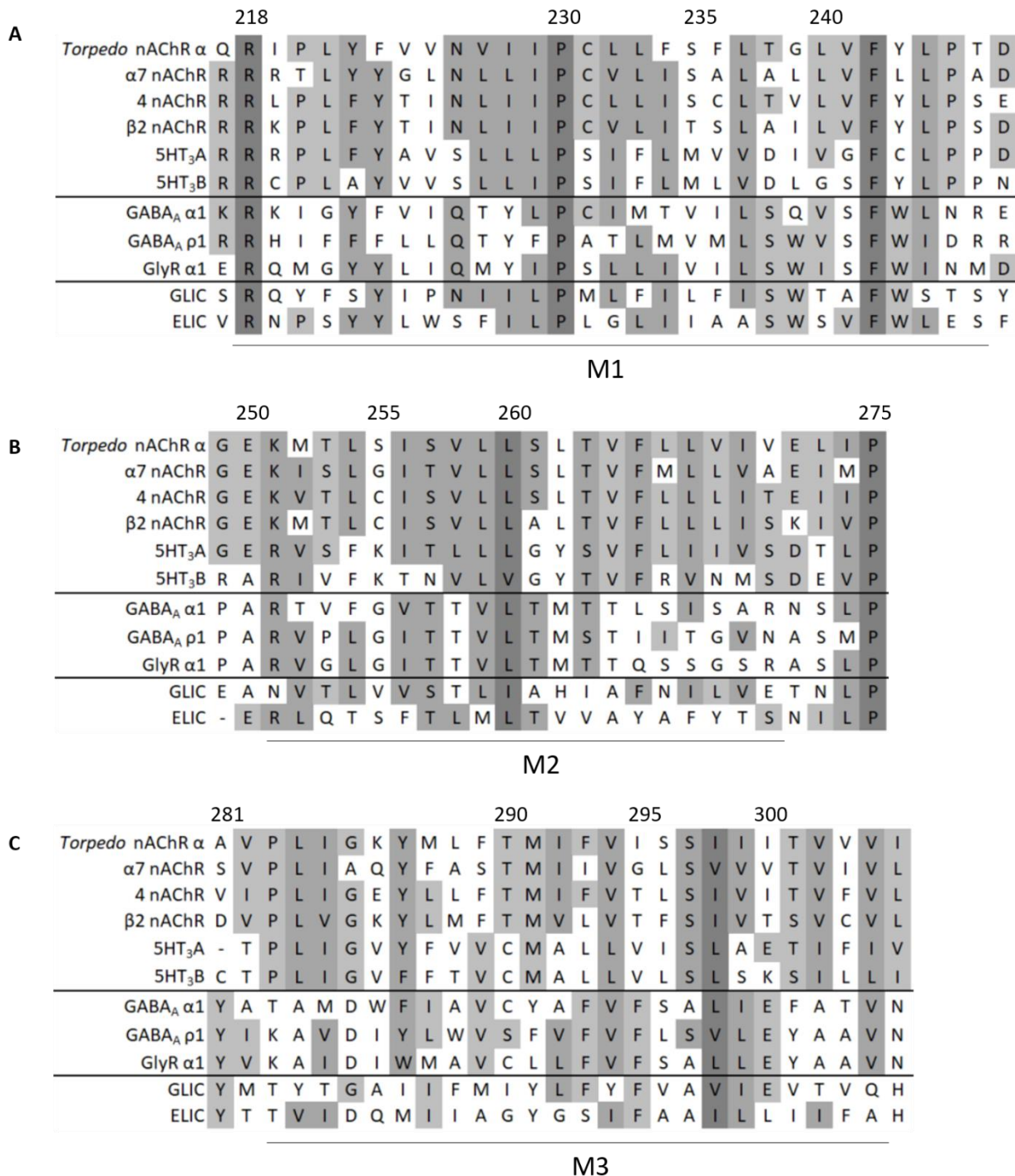


Figure 3.14: Sequence alignment of selected pLGIC M1, M2 and M3 helices. Uniprot numbers are in order: P02710, P36544, P09483, P12390, P23979, Q9JHJ5, P62813, P24046, P23415, Q7NDN8, P0C7B7. Residues coloured by conservation of sidechain properties. m5-HT_{3A} numbering is shown.

3.3.3.2 Molecular dynamics simulations to explore the mechanism of action of Y4.7

Molecular dynamics simulations revealed no effect of Y4.7A on the tip of M4 or its interactions with the ECD (Section 3.2.3.2.A). Initial analysis showed little effect of Y4.7A on M4-M1/M3 interactions, though a small difference in the average distance between D238 and K255 was observed (Figure 3.12B).

This small difference in average D238-K255 distance between the WT and mutant simulations is likely the result of a difference in their potential for interaction in the two simulations (Figure 3.12C). Firstly the D238-K255 distance is sub-4Å for longer in the WT simulation than in the mutant simulation. Secondly, of the >4Å D238-K255 distances, both the average distance and most often occupied distances are higher (i.e. further apart) in the mutant simulation than the WT simulation. Plots of the D238-K255 distances in each simulation (Figure 3.13) further show the consistency with which the WT simulations occupy a ~4Å distance, while the mutant simulations, even when reaching ~4Å distances, show much greater variation in distance occupied in those periods.

Altogether, this indicates that Y4.7 promotes favourable D238-K255 interactions, and that the Y4.7A mutation is detrimental to this interaction. Thus there is a potential pathway of interaction leading all the way from Y4.7 to K255, which itself is less than two helical turns from L260 (L9'), which forms the main restriction in the closed channel pore. This led me to explore the role of K255 in 5-HT_{3AR} function, and indeed a K255L mutation abolished receptor function without ablating ligand binding (Table 3.7). This indicates that position 255 in the receptor is involved in, or can affect, the mechanism that allows channel opening on ligand binding.

However, a lysine at this position is not itself crucial to 5-HT_{3A} receptor function in the same way as Y4.7 and D238 are, as evidenced by the fact that K255A had WT-like function (Table 3.7). In addition, this position tolerated substitutions with properties between those of Lys and Ala: K255Q (which is shorter than Lys and uncharged, but still polar), K255E (which is shorter and oppositely charged, but still charged) and K255C (which is shorter and uncharged but still polar) were all functional substitutions. K255 is highly conserved across 5-HT_{3A} receptors, although not otherwise in pLGICs (Figure 3.14), supporting an important role for this residue in the 5-HT_{3A} receptor.

The tolerance of the 5-HT_{3A} receptor for various substitutions at position 255 is well-documented. Substitutions of K255 with R, Q, S and G all cause small (<2-fold) decreases in EC₅₀ in 5-HT_{3A} receptors expressed in HEK293 cells (Gunthorpe et al., 2000), and a K255C substitution (K282C) is WT-like in 5-HT_{3A} receptors expressed in *Xenopus* oocytes (Panicker et al. 2002; Reeves et al. 2001). This tolerance extends to other pLGICs; in the muscle AChR, where the equivalent residue to K255 is S246, an S246C mutation causes a ~10-fold decrease in EC₅₀ (Akabas et al., 1992) in receptors expressed in oocytes. In the GABA_A receptor, the equivalent residue to K255 is G259, and a G259C mutation reduces maximum recorded current from oocytes, but is otherwise well tolerated (Xu and Akabas, 1996).

3.3.3.3 Proposed mechanism for the role of Y4.7 in 5-HT_{3A}R function

Y4.7A, D238A and K255L all prevented channel function but not ligand binding. Either the channel-opening signal sent by ligand binding is not reaching the channel, or the channel is rendered unable to open in response to the signal in these mutant receptors. I suggest that all three of these residues (Y4.7, D238 and K255) may be connected: Y4.7 and D238 are well positioned for interaction in the open structure (Figure 3.7), and the lack of Y4.7 causes an increased D238-K255 distance in the molecular dynamics simulations of the Y4.7A mutant (Figure 3.12 and Figure 3.13). These connections could form a link from the outer M4 helix to the pore-lining M2 helix which appears to be important for channel opening to occur in response to ligand binding.

An energetic coupling between residues on M4 and M1 has already been shown to be able to alter the stability of the receptor open state in the *Torpedo* muscle-type nAChR (Domville and Baenziger, 2018), demonstrating that a mutation in M4 can alter the orientation of M1 and affect receptor function. The residues in question here (Y4.7, D238 and K255) are all ‘below’ the level of the main channel restriction (L260), and analysis of the molecular dynamics simulations showed no effect of Y4.7 upwards along the M4, in the ECD, or above the level of L260 in any of the transmembrane helices (Figure 3.11), which leads me to suggest that the channel opening signal is likely not prevented from reaching the channel pore, or at least quite far into the transmembrane domain, in any of the relevant mutant receptors (with Y4.7A, D238A, or K255L mutations). Therefore I suggest it is likely that Y4.7A, D238A and K255L are all rendering the channel unable to open in response to ligand binding, rather than cutting the channel off from signals from the ECD, though this work does not uncover the specific mechanism by which they might be doing this.

To explore the mechanism of action of these residues (Y4.7, D238 and K255), we must understand which protein movements are required for channel opening. Comparing the closed and open states of receptors can show some of the movement that occurs on channel opening, though of course comparing two static states will miss intermediate movements, and some of the changes may happen after channel opening, rather than being prerequisites for it.

Comparing closed (6be1) and open (6dg8) 5-HT₃R structures (Basak, Gicheru, Rao, et al., 2018; Basak, Gicheru, Samanta, et al., 2018) (see also section 1.1.2), it is clear that on moving from the closed to the open state (pink to yellow in Figure 3.15), M1 and M4 both move ‘outwards’ (from the channel pore), while M4 and M3 both ‘straighten’ (relative to the plasma membrane). The movement of M2 is relatively small compared to these, but it does also move outwards and straighten somewhat. Polovinkin et al. (2018) shows the same outward movement of M2 accompanied by a twisting motion that moves L260 (L9') out of the channel pore. The morph video in the supplementary material (Polovinkin et al., 2018) also shows M1 and M4 moving outward on channel opening, and M4 moving upwards.

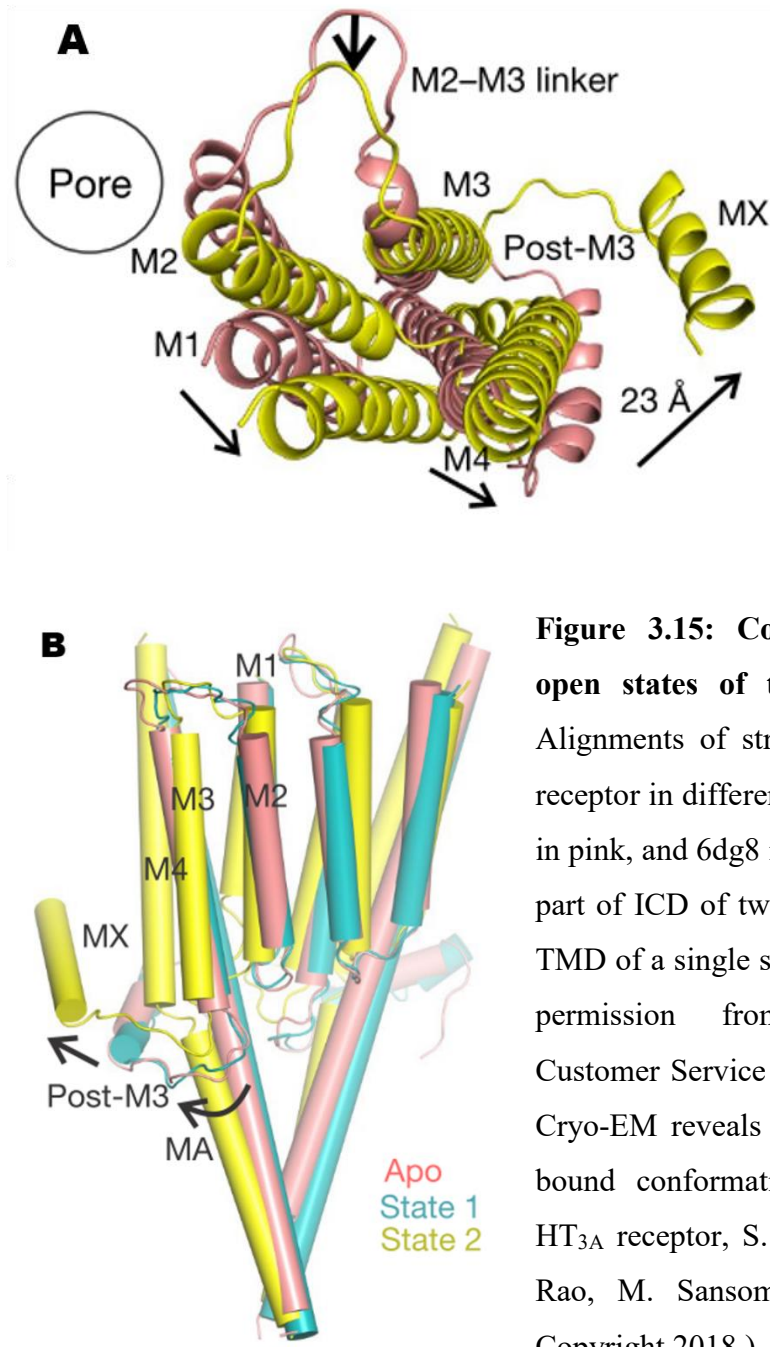


Figure 3.15: Comparing closed and open states of the 5-HT_{3A} receptor. Alignments of structures of the 5-HT_{3A} receptor in different states. 6be1 is shown in pink, and 6dg8 in yellow. A) TMD and part of ICD of two adjacent subunits. B) TMD of a single subunit. (Reprinted with permission from Springer Nature Customer Service Centre GmbH, Nature, Cryo-EM reveals two distinct serotonin-bound conformations of full-length 5-HT_{3A} receptor, S. Basak, Y. Gicheru, S. Rao, M. Sansom and S. Chakrapani, Copyright 2018.)

Many of these rearrangements involve one or more of Y4.7, D238, and K255. Determining which of these movements are required for channel opening, and which are dependent on each other, will be key to understanding the channel opening mechanism of 5-HT_{3A} receptors. It is also important to consider that the similar effects of these mutations could be due to effects other than specific residue-residue interactions involving Y4.7, D238 and K255 alone: there is a range of possible alternatives for the roles of these residues in receptor function, including possible interactions with other sidechains and/or main chain moieties, for example contributing to packing of the transmembrane helical bundle or stabilisation of certain conformational states. Based on my work in this chapter, I propose that Y4.7 and D238 are crucial to, and K255 is involved in, the mechanism of channel opening in response to ligand binding, and that understanding how they act will lead to a fuller understanding of 5-HT_{3A} receptor function.

3.4 Conclusions

In this chapter I have shown that two of the three non-functional M4 alanine mutations disrupt receptor expression (D4.0A and W4.25A), and one prevents receptor function but not ligand binding at the plasma membrane (Y4.7A). I then determined that residue D238 on M1 is a possible interaction partner for Y4.7, as D238A gave the same non-functional phenotype as Y4.7A. Finally, with the aid of molecular dynamics, in collaboration with Alessandro Crnjar, I identified K255 on M2 as a possible interaction partner of D238, extending the chain all the way to the pore-lining helix. I suggest that Y4.7, D238 and K255 are all involved in allowing channel opening in response to ligand binding, and that Y4.7 and D238 are required for this process.

Chapter 4 The role of the M4 helix in the $\alpha 4\beta 2$ receptor

4.1 Introduction

In Chapter 3 I showed that 27 out of 28 alanine mutations in the M4 helix of a cation-selective pLGIC (the 5-HT_{3A} receptor) either had negligible effect on receptor function, or ablated receptor folding/assembly/export. One alanine mutation, Y4.7A, prevented channel opening but not ligand binding. These results did not conform to our predictions for the effects of alanine mutations in the M4 helix of a cation-selective pLGIC, which was that they would generally cause slightly increased sensitivity to ligand and promote channel opening.

To determine whether this unexpected result in the 5-HT_{3A}R study was an outlier or part of a wider pattern in cation-selective pLGICs, I next explored the other major family of cation-selective pLGICs, nAChRs. The most prevalent nAChR in the human brain is the $\alpha 4\beta 2$ nAChreceptor (Lomazzo et al., 2010), which I chose as my next target for understanding the functional role of the M4 helix. As the most accessible and least conserved of the pLGIC transmembrane helices, the M4 is an attractive target for potential therapeutics, and determining whether its role or mechanism varies between pLGIC subunits could contribute to the search for new drugs.

To be able to compare my work in the $\alpha 4\beta 2$ nACh and the 5-HT_{3A} receptors, and find similarities and differences between cation-selective pLGIC M4s, I started my investigation with the equivalent experiments to those I had performed on the 5-HT_{3A} receptor: mutating each residue in the $\alpha 4\beta 2$ M4 to alanine, and assaying the resultant mutants after expression in HEK293 cells.

4.2 Results

4.2.1 Characterisation of $\alpha 4\beta 2$ nAChRs with M4 alanine substitutions

The $\alpha 4\beta 2$ nACh receptor is a heteropentamer consisting of $\alpha 4$ and $\beta 2$ subunits. To examine the role of the M4 helix in the $\alpha 4\beta 2$ receptor, I coexpressed the $\alpha 4$ and $\beta 2$ subunits with alanine mutations at equivalent positions together. For ease of comparison, I use the positional numbering system introduced in section 1.2 (Figure 1.6), which is based on the alignment of pLGIC sequences, and starts at the highly conserved aspartic acid residue near the intracellular end of M4. I refer to mutants containing the equivalent mutations in both $\alpha 4$ and $\beta 2$ as ‘double mutants’, and mutants containing a mutation in only one subunit type as ‘single mutants’. I expressed these mutants in HEK293 cells, and assayed receptor function with a fluorescence assay using a membrane-potential sensitive fluorescent dye, and receptor folding/assembly with radioligand binding.

4.2.1.1 Characterisation of WT $\alpha 4\beta 2$ nACh receptors

In this work I used an L9’A (L257A) mutation in the $\alpha 4$ subunit of the WT and all mutant receptors, hereafter referred to as ‘WT and by their other mutations. The L9’A mutation increases agonist sensitivity without affecting ion selectivity (Fonck et al., 2005; Tapper et al., 2004). The increased sensitivity allows better detection of receptor function, and more opportunity to detect changes in that function. I transfected the HEK293 cells with a 1:2 ratio of $\alpha 4$ to $\beta 2$ nAChR DNA to promote expression of the high-sensitivity 2($\alpha 4$):3($\beta 2$) receptor over the low sensitivity 3($\alpha 4$):2($\beta 2$) receptor (as in Fonck et al. (2005)), and promote a homogeneous population of receptors.

I first characterised the ‘WT receptor in HEK293 cells by incubating it with a membrane-potential sensitive dye and assaying the response to addition of nicotine (Figure 3.1). This gave an EC₅₀ of 19 nM (pEC₅₀ = 7.73 ± 0.06 M). This is lower than the EC₅₀ of 3.4 μM reported in Fitch et al. (2003) for rat $\alpha 4\beta 2$ nACh receptors using similar methods. This was as expected, firstly because the L9’A decreases EC₅₀ by ~40 fold (Fonck et al., 2005; Tapper et al., 2004), and secondly, the HEK293 cell used in Fitch et al. (2003) were stably transfected

with the $\alpha 4\beta 2$ nACh DNA, and likely expressed a heterogeneous mix of low sensitivity $3(\alpha 4):2(\beta 2)$ receptors and high sensitivity $2(\alpha 4):3(\beta 2)$ receptors.

I also coexpressed the ‘WT with chaperones RIC-3 and NACHO, which mediate nAChR assembly (Matta et al., 2017). For any nAChR mutants discussed in this thesis, I compare the characteristics of mutants coexpressed with chaperones with the characteristics of ‘WT coexpressed with chaperones, and the characteristics of mutants expressed on their own with the characteristics of ‘WT expressed on its own. Coexpression with the two chaperones is denoted by a + (e.g. ‘WT+).

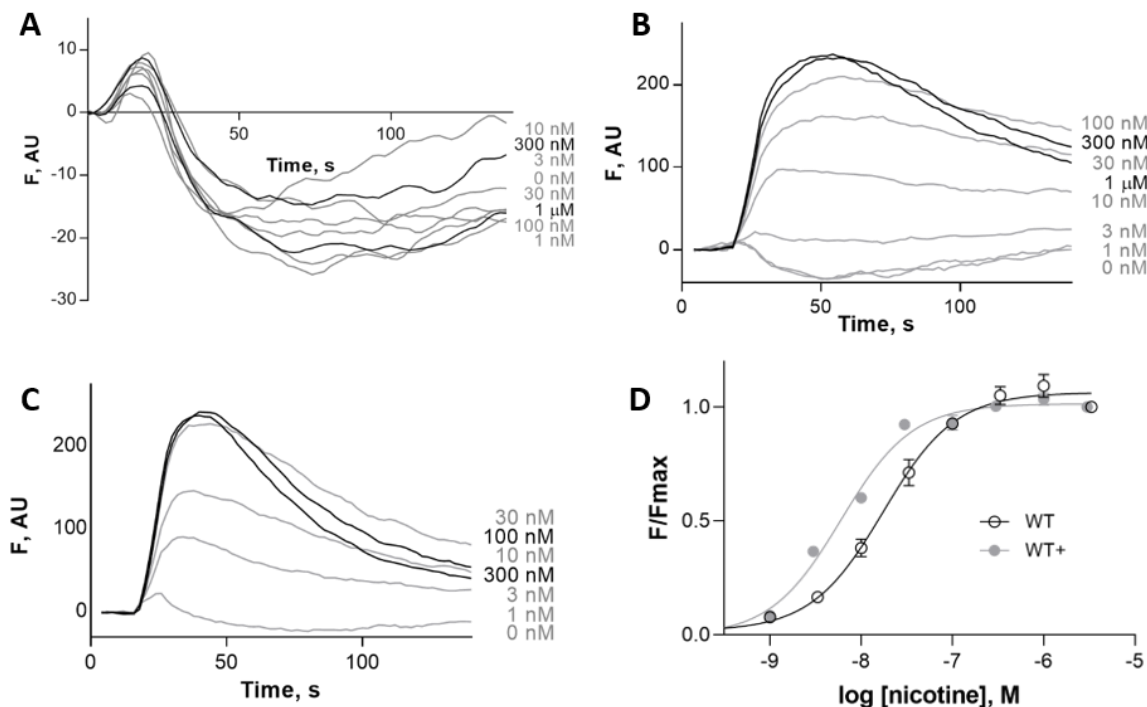


Figure 4.1: Typical responses of $\alpha 4\beta 2$ nACh receptors in HEK293 cells. Fluorescent responses (F in arbitrary units AU) on addition of nicotine at 20 s in A) mock transfected cells, B) cells expressing ‘WT $\alpha 4\beta 2$ nAChR, C) cells expressing ‘WT $\alpha 4\beta 2$ nAChR and chaperones RIC-3 and NACHO (‘WT+). D) Concentration-response curve of ‘WT with and without chaperones. Data are mean \pm SEM, $n \geq 3$. B-D (Adapted with permission from Mesoy and Lummis 2020. Copyright 2020 American Chemical Society.)

4.2.1.2 9 out of 28 $\alpha 4\beta 2$ nACh M4 alanine mutations abolished receptor function

In the initial fluorescence assay, 13 of the 28 double mutants showed ‘WT-like function, one showed a >5-fold increase in EC₅₀, and 14 were nonresponsive (Table 4.1). Of the 14 nonresponsive mutants, five showed ‘WT-like function when coexpressed with the two chaperones RIC-3 and NACHO. Altogether therefore, 18 double alanine mutants were ‘WT-like, one showed an increased EC₅₀, and 9 showed no function, even when coexpressed with chaperones.

Table 4.1: Parameters of $\alpha 4\beta 2$ nACh receptors with M4 alanine substitutions (next page)

Position (α4/β2)	Mutant	pEC ₅₀ (M)	EC ₅₀ (nM)	n _H	MRF	n
	UT	NF				3
	UT+	NF				3
	'WT	7.73 ± 0.06	19	2.5 ± 0.3	131 ± 15	3
	'WT+	8.22 ± 0.04	6	1.1 ± 0.1	255 ± 22	3
D358/D350	D4.0A+	NF				6
R359/R351	R4.1A+	NF				3
I360/L352	I/L4.2A	7.70 ± 0.16	20	1.5 ± 0.8	70 ± 5	3
F361/F353	F4.3A+	NF				3
L362/L354	L4.4A+	NF				3
W363/W355	W4.5A	7.97 ± 0.09	11	1.2 ± 0.3	148 ± 20	3
M364/I356	M/4.6A	7.59 ± 0.06	26	0.9 ± 0.1	74 ± 8	3
F365/F357	F4.7A+	NF				3
I366/V358	I/V4.8A+	8.27 ± 0.08	5	1.5 ± 0.4	155 ± 23	3
I367/F359	I/F4.9A	7.89 ± 0.09	13	1.2 ± 0.3	195 ± 2	3
V368A/V360	V4.10A	7.51 ± 0.10	31	2.2 ± 1.3	65 ± 11	3
C369/C361	C4.11A+	8.06 ± 0.19	9	0.4 ± 0.1	79 ± 10	3
L370/V362	L/V4.12A+	8.25 ± 0.03	6	1.0 ± 0.1	188 ± 5	3
L371/F363	L/F4.13A	8.21 ± 0.09	6	1.5 ± 0.4	249 ± 16	3
G372/G364	G4.14A	6.95 ± 0.08*	112	1.2 ± 0.2	85 ± 2	5
T373/T365	T4.15A+	NF				3
V374/V366	V4.16A	7.45 ± 0.09	36	0.9 ± 0.2	140 ± 21	4
G375/G367	G4.17A	8.03 ± 0.10	9	0.9 ± 0.2	117 ± 13	3
L376/M368	L/M4.18A+	7.31 ± 0.1	49	1.1 ± 0.2	122 ± 6	3
F377/F369	F4.19A+	NF				3
L378/L370	L4.20A+	8.02 ± 0.07	10	1.5 ± 0.2	316 ± 13	3
P379/Q371	P/Q4.21A+	NF				3
P380/P372	P4.22A	7.50 ± 0.05	32	1.1 ± 0.1	69 ± 3	3
W381/L373	W/L4.23A	7.41 ± 0.15	39	0.8 ± 0.2	138 ± 13	3
L382/F374	L/F4.24A	7.44 ± 0.09	36	1.4 ± 0.4	174 ± 14	4
A383/Q375	'WT/Q4.25A	7.69 ± 0.05	20	1.6 ± 0.3	158 ± 7	3
A384/N376	'WT/N4.26A+	NF				3
C385/Y377	C/Y4.27A	7.68 ± 0.04	21	1.5 ± 0.2	132 ± 8	3

Data are mean ± SEM. NF = non-functional at concentrations up to 1 μM nicotine (n≥3). *nH significantly different from 'WT/'WT+ or pEC₅₀ significantly different from 'WT/'WT+ and ≥5-fold change, p < 0.05, 2-way ANOVA. MRF is maximum recorded fluorescence, typical MRF for NF receptors was between 0 and 25. n=3x indicates 3 technical replicates of x biological replicates, n=4 indicates two biological replicates. Column 1 is the standard

residue numbering, column 2 is my M4 comparative numbering starting at a highly conserved aspartate residue.

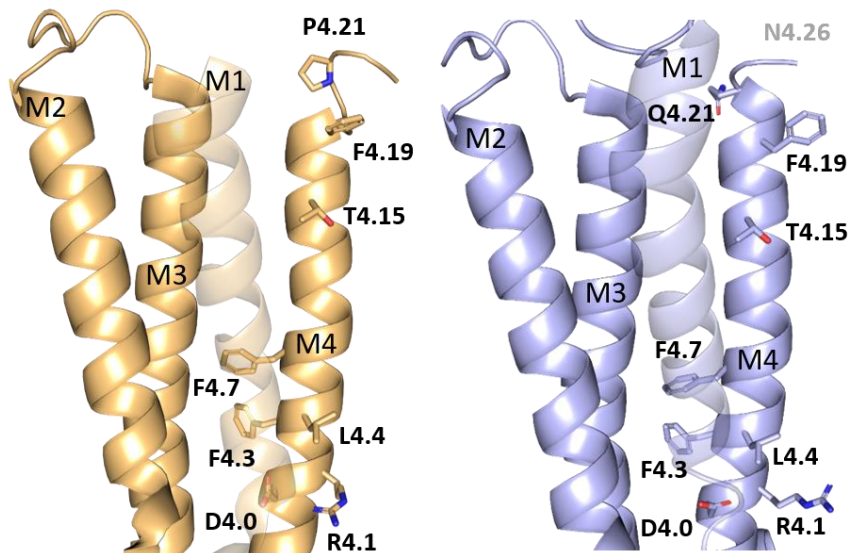


Figure 4.2: Key $\alpha 4\beta 2$ nAChR M4 residues. The TMD of single $\alpha 4$ (brown) and $\beta 2$ (blue) subunits from a human $\alpha 4\beta 2$ X-ray crystallography structure (5kxi) showing residues where alanine mutations abolish receptor function as sticks (except $\beta N4.26$, which is not present in the 5kxi structure). (Adapted with permission from Mesoy and Lummis 2020. Copyright 2020 American Chemical Society.)

4.2.1.3 6 out of 9 non-functional $\alpha 4\beta 2$ nAChR M4 double mutant receptors could be rescued by coexpression with a ‘WT’ subunit

To assess whether the $\alpha 4$ and $\beta 2$ M4 helices play equal roles in function, I assayed the function of every individual mutant in the 9 nonresponsive double mutants, i.e. coexpressing ‘WT $\alpha 4$ subunits with mutant $\beta 2$ subunits and vice versa (Table 4.2). Mutation of either subunit abolished function at positions 4.0, 4.1 and 4.21. All other single mutations in $\alpha 4$ were permissive to function. Three single mutations in $\beta 2$ were permissive to function, but $\beta T4.15A$ and $\beta F4.19A$ mutant receptors were non-functional. The apparent higher sensitivity

of the $\beta 2$ subunit to point mutations could be due to different roles between the $\alpha 4$ and $\beta 2$ M4 helices, but is more likely simply due to the 2:3 $\alpha 4:\beta 2$ subunit stoichiometry used in these experiments. I therefore turned my attention back to the double mutants, to further explore their lack of response in the functional assays.

Table 4.2: Parameters of $\alpha 4\beta 2$ nACh single M4 mutant receptors

Mutant	Mutant α (with L9'A mutation)				'WT α Mutant β				
	WT β	pEC₅₀ (M)	EC₅₀ (nM)	n_H	MRF	pEC₅₀ (M)	EC₅₀ (nM)	n_H	MRF
'WT+		8.22 ± 0.04	6	1.1 ± 0.1	255 ± 22	8.22 ± 0.04	6	1.1 ± 0.1	255 ± 22
D4.0A+	NF					NF			
R4.1A+	NF					NF			
F4.3A+	7.63 ± 0.12	24	0.6 ± 0.1	67 ± 10		8.13 ± 0.2	7	1.0 ± 0.4	133 ± 14
L4.4A+	8.74 ± 0.08	2	1.6 ± 0.4	93 ± 6		7.97 ± 0.36	10	0.8 ± 0.4	83 ± 12
F4.7A+	7.70 ± 0.05	20	1.3 ± 0.2	89 ± 7		8.57 ± 0.09	3	1.6 ± 0.7	48 ± 7
T4.15A+	7.45 ± 0.05*	35	1.8 ± 0.3	61 ± 15		NF			
F4.19A+	7.48 ± 0.03*	33	1.8 ± 0.2	57 ± 5		NF			
P/Q	NF					NF			
4.21A+									

Data are mean ± SEM, $n \geq 3$ technical replicates. NF = non-functional at concentrations up to 1 μ M nicotine. * n_H or pEC₅₀ significantly different from 'WT and c5-fold change, $p < 0.05$, 2-way ANOVA. MRF is maximum recorded fluorescence, typical MRF for NF receptors was between 0 and 25.

4.2.1.4 Radioligand binding showed 8 out of 9 non-responsive mutant receptors were capable of ligand binding

To determine whether the 9 nonresponsive double mutant receptors were able to bind ligand, I assayed the levels of binding of [³H]epibatidine. Epibatidine is a membrane-permeable nAChR agonist, so cannot distinguish between receptors trapped in the cell and those at the plasma membrane.

8 of the 9 non-functional double mutants showed epibatidine binding at levels comparable to ‘WT (Figure 4.3). As the ‘WT showed receptor function when expressed without chaperones, we know that this level of expression was sufficient for measurable responses in the functional assay. However, if protein production levels are the same in mutant and ‘WT receptors, but the mutant receptors do not reach the plasma membrane, that would explain the lack of responses in the functional assay.

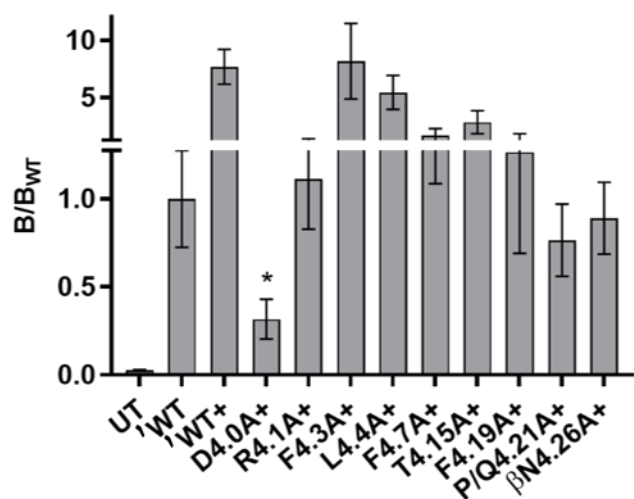


Figure 4.3: Single-point radioligand binding relative to ‘WT of non-responsive M4 mutants. B is specific binding of [3 H]epibatidine to transfected cell membranes. Data are mean \pm SEM, n=3-5, + indicates coexpression with chaperones RIC-3 and NACHO. *not significantly different from UT (untransfected cells), p<0.05, 2-way ANOVA. (Reprinted with permission from Mesoy and Lummis (2020). Copyright 2020 American Chemical Society.)

To distinguish between intracellularly expressed subunits and whole receptors at the plasma membrane, I attempted to use carbamylcholine as well as nicotine as the competitive ligands in this assay. Carbamylcholine is not membrane-permeable, and so measuring the level of [3 H]epibatidine binding with and without an excess of carbamylcholine should show how much of the ligand-binding capacity sits at the plasma membrane. However, these experiments failed to consistently show measurable binding of radioligand to ‘WT receptors at the plasma membrane. The ‘WT level of expression at the plasma membrane is sufficient for robust receptor responses in the functional assay, so this shows that these experiments cannot distinguish between receptors trapped inside the cell and receptors expressed to the

plasma membrane at a level sufficient to allow detection of their responses in the functional assay. Therefore I did not continue with this assay.

4.2.2 Characterisation of $\alpha 4\beta 2$ nAChRs with M4 non-alanine substitutions

To further explore each of the nine positions where alanine mutations abolished receptor plasma membrane expression and/or function, I mutated each residue to a series of similar residues, altering the residue charge, size, hydrophobicity, aromaticity and/or polarity compared to the original residue (Table 4.3). Figure 4.6 shows the position of these residues, and suggested potential interaction partners.

At four of the nine positions, all attempted substitutions abolished receptor function (D4.0, R4.1, T4.15, P/Q4.21). At two of the positions, all the substitutions were tolerated (F4.19, β N4.26), and the last three positions showed some selectivity in which substitutions were accepted (F4.3, L4.4, F4.7).

The β N4.26L mutant receptor showed concentration-dependent responses, indicating that this mutation did not completely abolish expression of the receptor to the plasma membrane, however the responses were too small to obtain reasonable parameters for the receptor. On co-expression with chaperones, the mutant receptor gave larger responses, and a ‘WT-like EC_{50} .

As D4.0A+ was the only receptor to not show measurable ligand binding so far, I also assayed the radioligand binding of D4.0E+, which was not significantly different from ‘WT (data not shown), indicating that D4.0 is important not only to receptor expression/assembly, but also to function. F4.3Y+ and L4.4V+ also showed ‘WT-like ligand binding, though that is less surprising as alanine substitutions at these positions had not abolished ligand binding (Figure 4.3).

Table 4.3: Parameters of $\alpha 4\beta 2$ nACh receptors with non-alanine substitutions of key M4 residues

Mutant	pEC ₅₀ (M)	EC ₅₀ (nM)	n _H	MRF	n
'WT	7.74 ± 0.05	18	1.6 ± 0.2	131 ± 15	3
'WT+	8.22 ± 0.04	6	1.1 ± 0.1	255 ± 22	3
D4.0E+	NF				
D4.0N+	NF				
D4.0R+	NF				
D4.0L+	NF				
R4.1K+	NF				
R4.1E+	NF				
R4.1S+	NF				
R4.1Q+	NF				
R4.1C+	NF				
R4.1L+	NF				
R4.1H+	NF				
F4.3L	7.49 ± 0.09	32	1.5 ± 0.4	221 ± 7	3
F4.3Y+	NF				
L4.4F+	7.96 ± 0.09	11	1.0 ± 0.2	278 ± 7	3
L4.4V+	NF				
F3.7Y+	7.85 ± 0.06	14	1.3 ± 0.2	308 ± 18	3
F3.7L+	NF				
T4.15D+	NF				
T4.15S+	NF				
T4.15C+	NF				
T4.15V+	NF				
F4.19Y	7.38 ± 0.07	42	1.2 ± 0.2	106 ± 6	3
F4.19L	7.54 ± 0.09	29	1.3 ± 0.3	64 ± 3	3
P/Q4.21F+	NF				
'WT/N4.26D	7.59 ± 0.08	26	1.8 ± 0.6	88 ± 4	3
'WT/N4.26K+	7.30 ± 0.06*	50	1.5 ± 0.3	96 ± 3	3
'WT/N4.26C+	8.22 ± 0.4	6	0.9 ± 0.6	102 ± 17	3
'WT/N4.26L	7.43 ± 0.1	37	3.6 ± 3	37 ± 2	3
'WT/N4.26L+	7.59 ± 0.05	26	1.4 ± 0.2	102 ± 3	3

Data are mean ± SEM. NF = non-functional at concentrations up to 1 μ M nicotine ($n \geq 3$). *nH significantly different from 'WT or pEC₅₀ significantly different from 'WT and ≥ 5 -fold change, $p < 0.05$, 2-way ANOVA. MRF is maximum recorded

fluorescence, typical MRF for NF receptors was between 0 and 25. n=3x indicates 3 technical replicates of x biological replicates, n=4 indicates two biological replicates.

4.2.3 Potential interaction partners of key M4 residues

To further explore the roles of the key M4 residues, I identified four residues on M1 and M3 (F239/231, Y240/Y232, Y283/Y275 and S294/286, Figure 4.6) as possible interaction partners for five of the eight residues where alanine mutation abolished channel responses but not ligand binding (R4.1, F4.3, L4.4, F4.7, T4.15). F4.19 had no suggested specific interaction partner in the $\alpha 4\beta 2$ structure (5kxi), and the potential interaction partners of P/Q4.21 and $\beta N4.26$ are in the extracellular domain.

S294/286 (on M3) was the only non-aromatic residue I identified as a potential interaction partner for F4.7, and is positioned in a way that might let it play a similar role to D238 on M1 in the 5-HT_{3A} receptor, i.e. linking residue 4.7 on the M4 helix to the M2 helix (Figure 3.12, Figure 4.4). Specifically, S294/286 is in a position to interact with both F4.7 on M4 and C252/C244 on M2. C252/244 is the equivalent residue to K255 in the 5-HT_{3A} receptor (Figure 3.14), and the spatial arrangement of F4.7-S294/286-C252/244 resembles that of Y4.7-D238-K255 in the 5-HT_{3A} receptor (Figure 3.12). I assayed the effect of substituting both an alanine and a leucine at this position in the $\alpha 4\beta 2$ receptor, as the K255A mutation has little effect in the 5-HT_{3A} receptor, but the K255L mutation gave insight into 5-HT_{3A} receptor function.

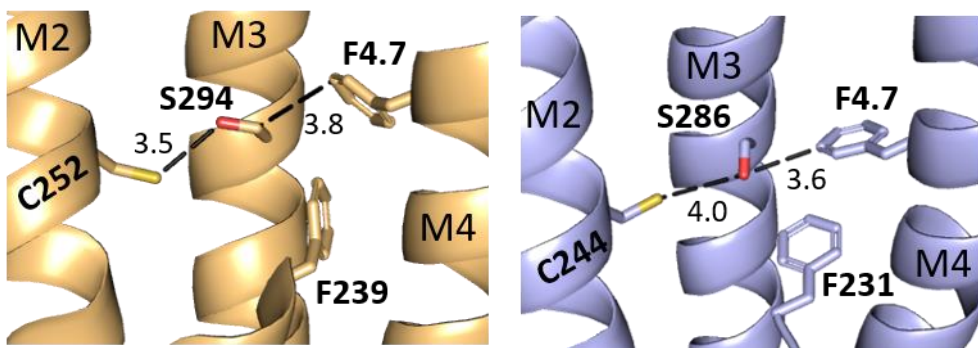


Figure 4.4: Potential M4-M3-M2 link in the $\alpha 4\beta 2$ receptor. 5kxi $\alpha 4$ (brown) and $\beta 2$ (blue) nAChR subunits showing sections of transmembrane helices M2. Distances in Å marked by dashed lines

Mutating these potential interaction partners to alanine showed that while Y240/232A was ‘WT-like’, the other alanine mutations all abolished function (Table 4.4). At positions 239/231 and 283/275, single alanine mutations in either subunit alone were also sufficient to abolish receptor function.

Radioligand binding revealed that the C252/244A mutant receptor showed ‘WT-like’ ligand binding levels (Figure 4.5), even though it was non-responsive in the functional assay. In contrast, both the non-functional aromatic mutants bound ligand at levels not significantly differentiable from untransfected cells (Figure 4.5).

Table 4.4: Parameters of $\alpha 4\beta 2$ nACh receptors with alanine substitutions in M1, M2, or M3

Mutant	pEC ₅₀ (M)	EC ₅₀ (nM)	n _H	MRF	n
'WT+	8.22 ± 0.04	6	1.1 ± 0.1	255 ± 22	3
F239A/F231A+	NF				
α F239A/ β WT+	NF				
α' WT/ β F231A+	NF				
Y240A/Y232A+	7.84 ± 0.08	14	0.9 ± 0.1	248 ± 9	3
Y283A/Y275A+	NF				
α Y283A/ β WT+	NF				
α' WT/ β Y275A+	NF				
S294/S286A+	NF				
C252/C244A+	NF				
C252/C244L+	NF				

Data are mean ± SEM. NF = non-functional at concentrations up to 1 mM nicotine ($n \geq 3$). No pEC₅₀ or n_H values were significantly different from 'WT+' and ≥5-fold change, $p < 0.05$, 2-way ANOVA. MRF is maximum recorded fluorescence, typical MRF for NF receptors was between 0 and 25. n=3x indicates 3 technical replicates of x biological replicates, n=4 indicates two biological replicates.

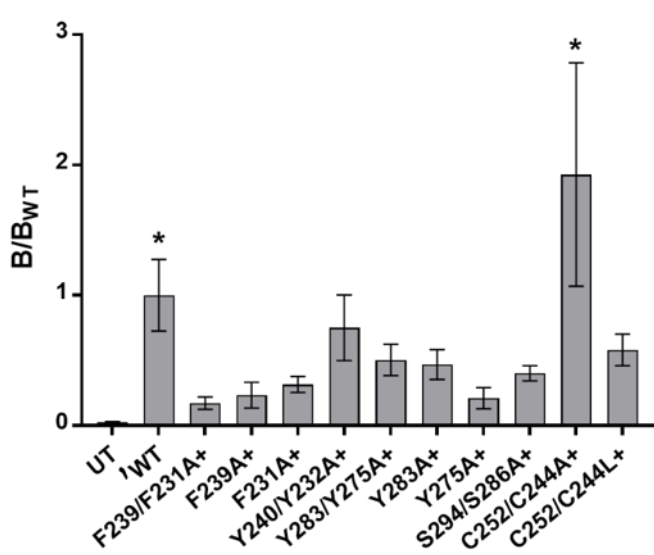


Figure 4.5: Single-point radioligand binding relative to 'WT of M1/M3 mutants. B is specific binding of [³H]epibatidine to transfected cell membranes. Data are mean ± SEM, n=3-10, *binding significantly different to UT, $p < 0.01$, 2-way ANOVA. + indicates coexpression with chaperones RIC-3 and NACHO, UT is untransfected cells.

4.3 Discussion

The aim of this work was to characterise the role and function of the M4 helix in a nAChR, to compare it to the already characterised M4 helices of ELIC, GLIC, and the GABA ρ 1R, GlyR α 1 and 5-HT_{3A} receptors (Cory-Wright et al. 2017; Haeger et al. 2010; Hénault et al. 2015; Mesoy and Lummis 2019). The initial prediction, based on the ELIC and GLIC data, was that Ala mutations in cation-selective pLGIC M4s would have only small effects on receptor function, and those would be mostly decreases in EC₅₀ (Therien and Baenziger, 2017). In Chapter 3 I found that, contrary to these predictions, three Ala mutations in the 5-HT_{3A} M4 abolished receptor function (D4.0A, Y4.7A, and W4.25A). Here, I extended that study to the $\alpha 4\beta 2$ nACh receptor, where nine Ala mutations in the M4 (D4.0A, R4.1A, F4.3A, L4.4A, F4.7A, T4.15A, F4.19A, P/Q4.21A and β N4.26A) completely abolished receptor function, establishing the M4 helix as crucial to $\alpha 4\beta 2$ nAChR function in particular, and cation-selective pLGIC function in general across both the nACh and 5-HT₃ receptor families.

4.3.1 Expression of non-responsive mutant receptors

Of the nine non-responsive $\alpha 4\beta 2$ nAChR M4 alanine mutants, one (D4.0A) showed no measurable radioligand binding, indicating that it was not detectably assembled into dimers able to bind ligand, and may not have been correctly folded. The other eight showed ‘WT-like’ ligand binding levels (Figure 4.3). However, the radioligand used here ([³H]epibatidine) is membrane-permeable, so this only shows that the ligand-binding receptors are folded and at least partially assembled (as ligand binding occurs between two subunits), and does not distinguish between receptors that have reached the plasma membrane and those that are folded and assembled but trapped inside the cell.

If all eight of the non-functional receptors that bound ligand at ‘WT-like’ levels are trapped inside the cell, that would show that the $\alpha 4\beta 2$ nAChR M4 is more crucial to receptor export than any other M4 studied so far. The closest would be the glycine receptor, where six out of 21 M4 alanine mutations abolish or severely diminish receptor cell-surface expression (Haeger et al., 2010).

Conversely, if these eight ligand-binding but non-responsive receptors are reaching the plasma membrane, but unable to open in response to ligand binding, that would match the phenotype both of the 5-HT_{3A} Y4.7A M4 mutant receptor, and one GABA_A receptor mutant (Y467A (Cory-Wright et al., 2017)), and indicate an extensive role for inwards-pointing residues along the length of the $\alpha 4\beta 2$ nAChR M4 in allowing channel opening in response to ligand binding.

Determining the cellular locations of these eight ligand-binding, non-responsive mutants is key to deducing the role of M4 in the $\alpha 4\beta 2$ nACh receptor, and how much the role of the M4 varies between different cation-selective pLGICs.

4.3.2 Potential roles of key M4 residues

To further explore the roles of the nine key M4 residues in the $\alpha 4\beta 2$ nACh receptor, I assayed the effects of substituting in different amino acids at each position (Table 4.3), and combined that information with the effect of alanine mutation at each position and the effects of mutations at the equivalent positions in other pLGIC M4 helices. An overview of the effects of alanine mutations in pLGIC M4 helices can be found in section 1.2.3 (Table 1.1).

D4.0A abolished both receptor function and detectable ligand binding, as it does in the 5-HT_{3A}, $\alpha 7$ nACh, and GABA_A receptors (da Costa Couto et al. 2020; Lo et al. 2008; Mesoy and Lummis 2021). The $\alpha 4\beta 2$ nACh receptor tolerated no other change at this position, either to a positively charged residue (D4.0R), to a polar residue (D4.0N), to a hydrophobic residue (D4.0L) or even an alternate negatively charged residue (D4.0E), indicating that the exact size, charge, and position of D4.0 are all important to its role in the receptor. The equivalent residue in the 5-HT_{3A} receptor tolerates mutation to both glutamic acid and asparagine (Table 3.3), indicating that this position is more sensitive in the $\alpha 4\beta 2$ nACh receptor.

R4.1 also tolerated no substitutions, either to an alternate positively charged residue (R4.1K), a negatively charged residue (R4.1E), a hydrophobic residue (R4.1L) or to various polar residues (R4.1S, Q, C, H). This might indicate that the length of R4.1 is important to its role, as the putative interactions in Figure 4.6D could not be attained by a shorter residue, even if it had the requisite charge/polarity for the interaction itself.

F4.3 surprisingly tolerated mutation to an aliphatic residue (F4.3L) but not to another aromatic residue (F4.3Y), indicating that the aromatic nature of F4.3 is not key to its function. Conversely, L4.4 tolerated mutation to an aromatic residue (L4.4F) but not to another aliphatic residue (L4.4V). This might indicate that the size of L4.4 is important, perhaps to fill a hydrophobic cavity (Figure 4.6D). More expectedly, F4.7 (Figure 4.6C) tolerated mutation to another aromatic residue (F4.7Y), but not to an aliphatic residue (F4.7L). F4.7 is the equivalent residue to Y4.7 in the 5-HT_{3A} receptor, which can also tolerate an aromatic substitution, but no other (Table 3.5).

All substitutions of T4.15 abolished receptor function, whether to a negative charge (T4.15D), a different polar group (T4.15S, C) or an aliphatic group (T4.15V). This was surprising, as the position of T4.15 in the structure (Figure 4.6B) showed no particularly plausible strong intramolecular interactions. However as the data indicate that T4.15 plays a specific role in M4, I suggest it could be interacting with lipids not visible in the structures currently available. Mutation of the equivalent residue (which is often a threonine across pLGICs) to alanine has no effect in the 5-HT_{3A} receptor (Mesoy et al. 2019), causes a small decrease in EC₅₀ in the $\alpha 7$ nAChR, ELIC, and GLIC (da Costa Couto et al. 2020; Hénault et al. 2015), but an increase in EC₅₀ in the *Torpedo* α subunit M4 (Roccamo et al. 1998; Thompson et al. 2020), where a T422W mutation also increases EC₅₀ (Tamamizu et al., 2000), indicating that the role of this conserved residue varies between pLGICs. In the muscle nAChR, T4.15 has specifically been shown to affect gating kinetics through a hydrogen bond (Bouzat et al. 2000).

F4.19 tolerated changes either to add a hydroxyl group (F4.19Y) or to be replaced with an aliphatic group (F4.19L), indicating a broad role, fairly non-specific beyond requiring a residue larger than an alanine at this position. This is consistent with it having no identifiable plausible intramolecular interactions that would require a specific characteristic at position 4.19 (Figure 4.6B). This position also frequently contains an aromatic residue across pLGICs, and an alanine mutation here increases EC₅₀ in the $\alpha 7$ nAChR, the GABA_A receptor, the glycine receptor and GLIC (Cory-Wright et al. 2017; da Costa Couto et al. 2020; Haeger et al. 2010; Hénault et al. 2015), though it decreases EC₅₀ in the α subunit of the *Torpedo* AChR and in ELIC (Hénault et al. 2015; Thompson et al. 2020), and has no effect in the 5-HT_{3A}

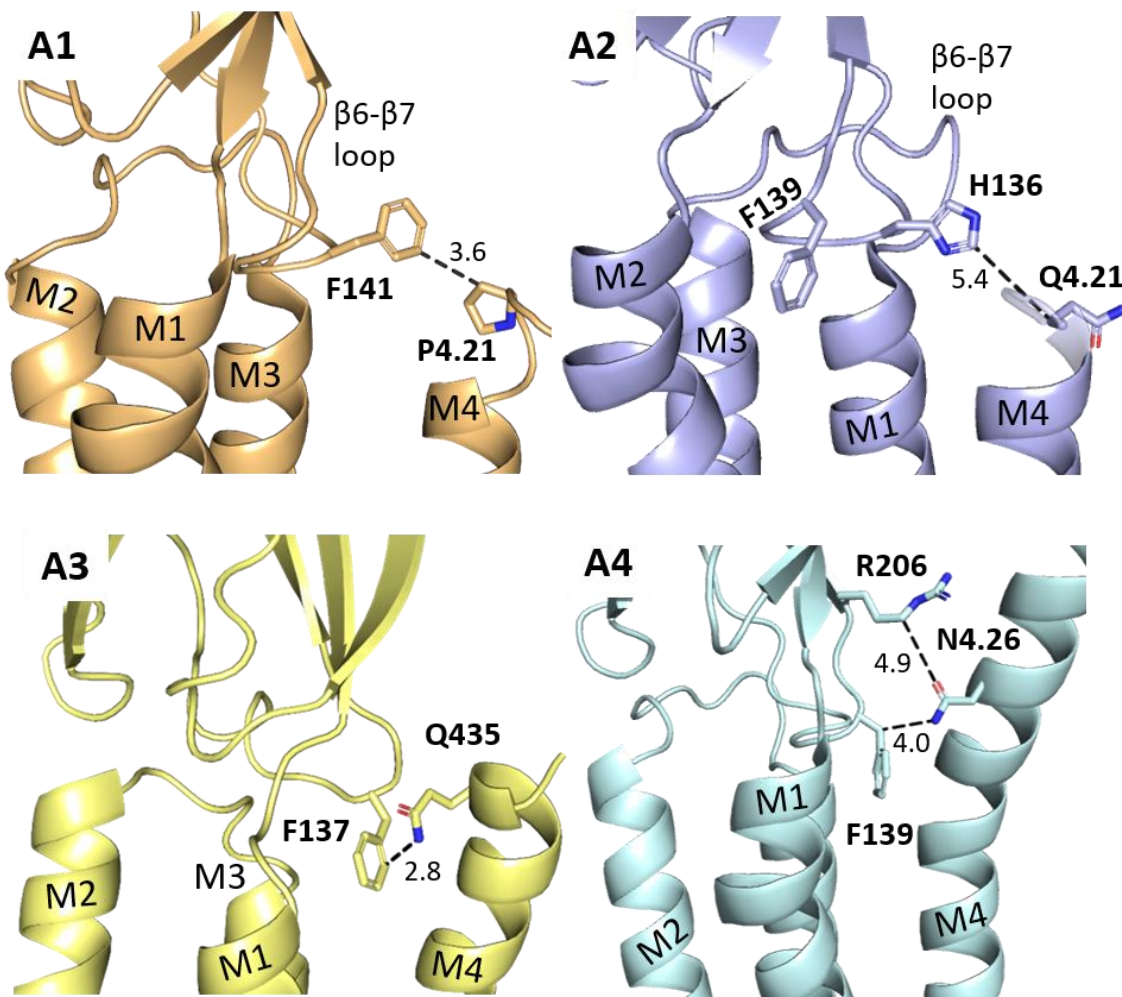
receptor (Mesoy et al. 2019). This might indicate a different role for this residue between mammalian and non-mammalian cation-selective pLGICs.

I selected to substitute phenylalanine at the P/Q4.21 position based on structural data. P4.21 in the $\alpha 4$ subunit is in a good position to interact with the crucial F141 in the Cys-loop (Figure 4.6A). Q4.21 in the $\beta 2$ subunit could also be able to interact with the equivalent residue (F137). It is at the wrong angle for interaction with F137 in the $\alpha 4\beta 2$ nAChR structure (5kxi), however that is an X-ray crystal structure of the receptor in detergent, and the tip of the M4 may not be in a physiologically relevant conformation. The equivalent residue to Q4.21 in the *Torpedo* nAChR (Q435) is only 2.8 \AA away from F137 in the structure 2BG9 (Figure 4.6A, yellow). W4.25 in the 5-HT_{3A} receptor is similarly positioned to P/Q4.21 in the $\alpha 4\beta 2$ receptor, and alanine mutation there also abolishes receptor function (section 3.2.1.3), indicating that an aromatic residue here might be sufficient for function. However, the P/Q4.21F mutation abolished receptor function, so was not sufficient to recapitulate the roles of P/Q4.21 in M4.

An alanine mutation at position 4.21 causes an increase of EC₅₀ in the *Torpedo* α subunit, the GABA ρ receptor, the glycine receptor and in GLIC (Cory-Wright et al. 2017; Haeger et al. 2010; Hénault et al. 2015; Thompson et al. 2020), a decrease in EC₅₀ in ELIC (Hénault et al. 2015), has no effect in the $\alpha 7$ nAChR (da Costa Couto et al., 2020), and abolishes receptor cell-surface expression in the 5-HT_{3A} receptor (Mesoy et al. 2019). This indicates a fairly consistent role for this residue across the non-mammalian and anionic pLGICs, and a range of roles (important for function, irrelevant to function, important to expression) across cation-selective pLGICs.

Finally, N4.26 tolerated all non-alanine substitutions tested, indicating that while an alanine here abolishes receptor function, a larger residue with a negative charge (N4.26D), a positive charge (N4.26K), a polar residue (N4.26C) or a hydrophobic residue (N4.26L) are all sufficient for receptor function (though the latter three require coexpression with chaperones to show receptor function). Intriguingly, in the AlphaFold predicted structure of the rat $\beta 2$ subunit (Jumper et al., 2021), this residue is less than 5 \AA from several ECD residues that it

could plausibly interact with (Figure 4.6A4), including F139 which is the equivalent of F144 in the $\alpha 4$ subunit.



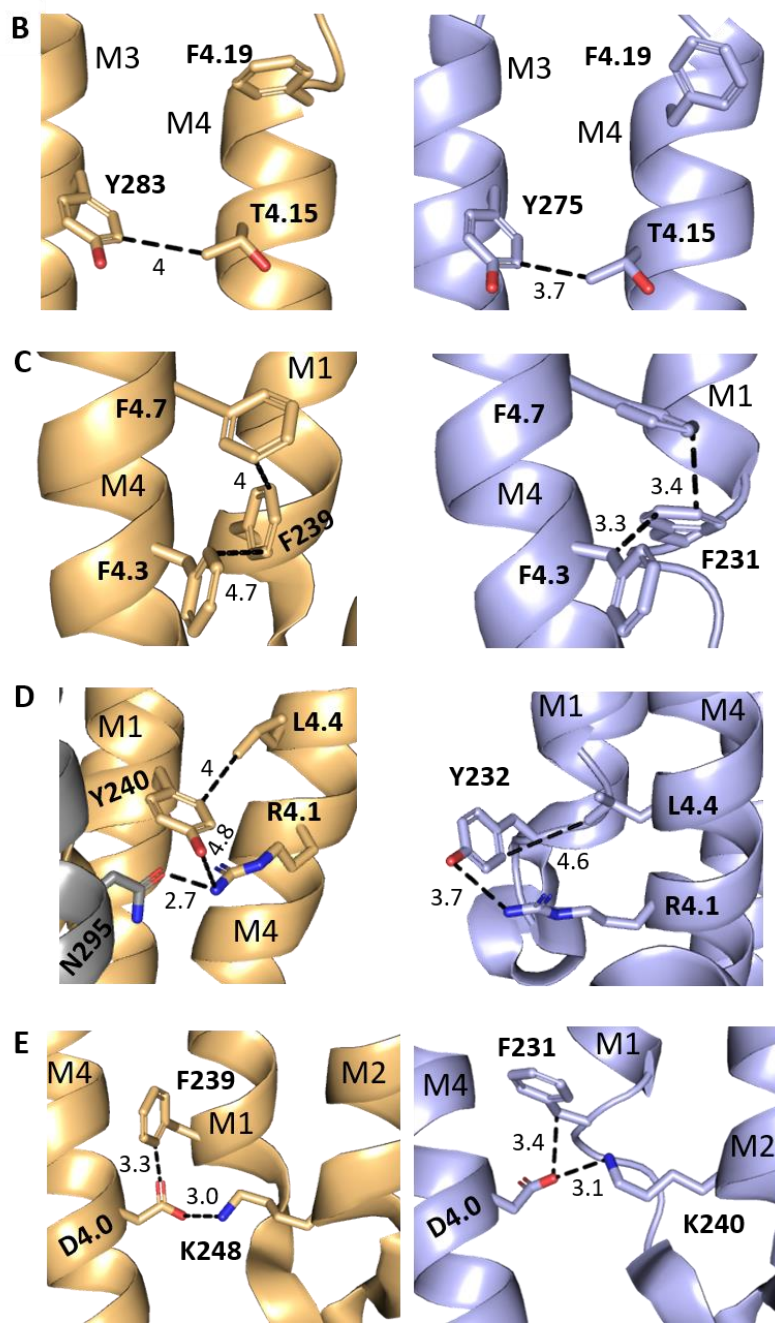


Figure 4.6: Potential interaction partners of key M4 residues. 5kxi $\alpha 4$ (brown) and $\beta 2$ (blue) nAChR subunits, *Torpedo* subunit (yellow) and Alphafold predicted structure of rat $\beta 2$ subunit (light blue, Uniprot P12390), showing key M4 residues and their local environment. Note 180° rotation of viewpoint in C and E compared to A, B and D. D) adjacent subunit shown in grey. Distances in Å marked by dashed lines.
(Adapted with permission from Mesoy and Lummis (2020). Copyright 2020 American Chemical Society.)

4.3.3 Potential interaction partners of key M4 residues

I identified four residues on M1 and M3 as potential interactions partners for key M4 residues. Close inspection of one of these potential interaction partners (S294/286) showed that it might play an equivalent role to D238 in the 5-HT_{3A} receptor. While S294/286 is on the M3 helix, and D238 is on M1, they both appear to be able to connect the same residue in M4 (F4.7 and Y4.7, respectively) to the same residue in M2 (C252/244 and K255) (Figure 4.4, Figure 3.12). In the 5-HT_{3A} receptor this appeared to be a functional link, and mutations at these three positions had the same effect: ablating receptor function without affecting ligand binding (Chapter 3).

While the data from the $\alpha 4\beta 2$ nACh receptor are less conclusive, they do support the suggestion that the $\alpha 4\beta 2$ nACh receptor may have an M4-M1/M3-M2 link functionally similar to the 5-HT_{3A} receptor. The loss of receptor function caused by C252/244A is different from the effect of the K255A mutation in the 5-HT_{3A} receptor, but the resultant non-functional $\alpha 4\beta 2$ nACh receptor does still bind ligand. This indicates that it, like F4.7 on M4 and Y4.7, D238 and K255 in the 5-HT_{3A}R, is likely involved in the same function as these residues: promoting channel opening in response to ligand binding.

All the M1/M3 alanine mutations of aromatic residues that abolished function also reduced detectable ligand binding to the receptors, indicating that the lack of function of these mutants is likely due to poor receptor expression, folding, or assembly. These results are fairly inconclusive: they could be indicating that these residues are not part of the same functional mechanism as the eight M4 residues in question (as those were all expressed, folded, and at least partially assembled), or alternatively that while these residues are part of the same functional mechanism as the M4 residues, they additionally play pivotal roles in protein expression/folding/assembly, and therefore cannot be used as tools to probe the mechanism of action. Regardless of why, the only specific conclusion that can be drawn here is that these aromatic residues (Table 4.4, Figure 4.5, Figure 4.6 B-E) must be important for the structural integrity of the $\alpha 4\beta 2$ nACh receptor. Interestingly, Y2783/Y275 has been shown elsewhere to be involved in energetic coupling to the Cys-loop (Alcaino et al., 2017),

indicating a mechanism through which it could be transmitting effects of M4 mutations to alterations in receptor function.

4.4 Conclusions

In this chapter I have shown that residues in the M4 helices of the $\alpha 4\beta 2$ nACh receptor are extensively involved in receptor expression, folding, assembly, and/or function. Of 28 double alanine mutants, one showed an altered EC₅₀ and nine were non-functional. These nine positions were spread along the length of M4, mostly facing towards M1/M3, and consisted of a range of amino acids, including charged, polar, aromatic, and large hydrophobic groups, as well as a proline. Three of these alanine mutations (D4.0A, R4.1A and P/Q4.21A) ablated function from either subunit alone. Mutations to similar amino acids were tolerated at five of these nine positions, but at the remaining four positions (D4.0, R4.1, T4.15, P/Q4.21) I found no amino acid that could be substituted in without abolishing receptor function. Altogether this shows that the M4 helix of the $\alpha 4\beta 2$ nACh receptor is crucial to its function, and that changes in the M4 can affect receptor function.

Chapter 5 The role of the M4 helix in cation-selective pLGICs depends on the environment

5.1 Introduction

In Chapters 3 and 4 I showed that the M4 helix is integral to the function of 5-HT_{3A} and $\alpha 4\beta 2$ nACh receptors, and a single M4 mutation can abolish function in either receptor. In the 5-HT_{3A} receptor I found that one M4 mutation (Y4.7A) prevents channel opening without ablating ligand binding. In the $\alpha 4\beta 2$ nACh receptor I showed that eight alanine mutations along M4, of residues of varied sizes and polarities, prevented receptor function without diminishing receptor expression, folding, or at least partial assembly. However, I was unable to disambiguate mutations that affected full assembly or receptor export to the plasma membrane from mutations that prevented receptor function in response to ligand application.

I next expressed key M4 mutants from Chapters 3 and 4 in *Xenopus laevis* oocytes and assayed receptor function by two-electrode voltage clamp, for two reasons. Firstly, *Xenopus* oocytes can be more permissive to receptor expression than HEK cells (Denning et al., 1992), and secondly, single-cell two-electrode voltage clamp is a more informative technique than the comparatively slow, population-averaged fluorescent dye methods used for the initial screen. The aim was to perform more fine-grained analysis of any changes in receptor action and potentially give insight into which part of receptor function any given mutation was affecting.

5.2 Results

5.2.1 Single-cell assays of 5-HT_{3A} receptors

5.2.1.1 Characterisation of WT 5-HT_{3A} receptors in *Xenopus* oocytes

Examination of the WT 5-HT_{3A} receptor expressed in *Xenopus* oocytes with two-electrode voltage clamp (Figure 5.1, Table 5.1) yielded an EC₅₀ of 1.7 µM (pEC₅₀ = 5.76 ± 0.05 M), consistent with previous work (Price et al. 2017). The curve shows rapid activation on ligand addition, desensitisation on continued exposure, and deactivation on removal of ligand.

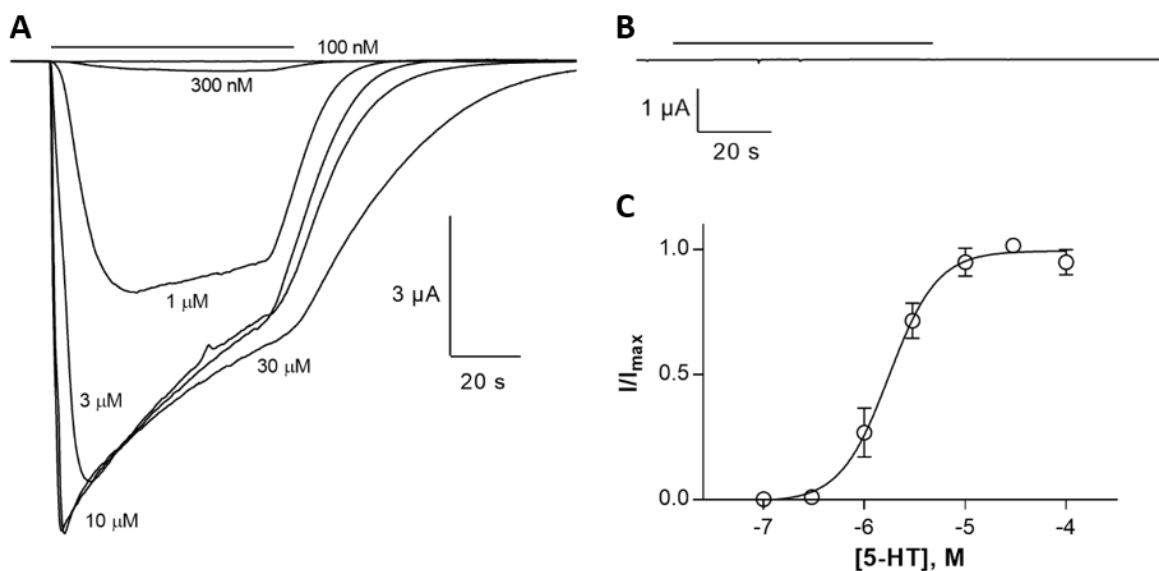


Figure 5.1: Typical responses of 5-HT_{3A} receptors in *Xenopus* oocytes. Current recordings on addition of 5-HT as indicated by black bar. A) Oocytes injected with 5-HT_{3AR} RNA, B) mock injected oocytes C) Concentration-response curve from WT data. Data are mean ± SEM, n=4. (5.1C adapted from Crnjar, A., Mesoy, S., Lummis, S. C. R., & Molteni, C. (2021) under a Creative Commons Attribution License (CC BY). Copyright 2021 Crnjar, Mesoy, Lummis and Molteni.)

5.2.1.2 Characterisation of a 5-HT_{3A}R M4 mutant receptor in *Xenopus* oocytes

I first assayed the Y4.7A mutant receptor in oocytes, which in HEK293 cells was capable of ligand binding but not of measurable function (sections 3.2.1.3 and 3.2.1.4). Unexpectedly, when expressed in *Xenopus* oocytes, the Y4.7A mutant gave WT-like responses (Table 5.1, Figure 5.2). At this point I repeated sequencing of the full WT and Y4.7A mutant genes that had been used for expression in HEK293 cells and here, ascertaining that each had the correct mutation and no off-target mutations.

Table 5.1: Parameters of 5-HT_{3A} receptors in *Xenopus* oocytes

Mutant	pEC ₅₀ (M)	EC ₅₀ (μM)	n _H	I _{max} (nA)	n
WT	5.76 ± 0.05	1.7	1.8 ± 0.3	8790 ± 3460	4
Y4.7A	5.98 ± 0.10	1.0	1.0 ± 0.1	7110 ± 1590	4

Data are mean ± SEM. No values were significantly different from WT, p<0.05, 2-way ANOVA.

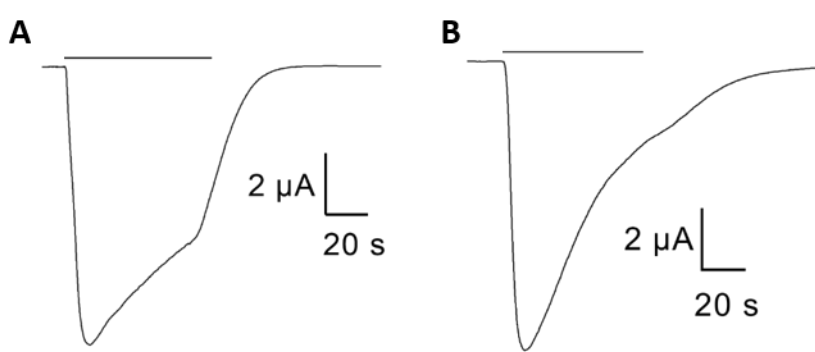


Figure 5.2: Typical current recordings of 5-HT_{3A} receptors on addition of 3 μM 5-HT. A) WT and B) Y4.7A receptor responses to ligand addition (indicated by black bar).

This difference between the Y4.7A receptor being inactive in HEK293 cells and WT-like in *Xenopus* oocytes cannot be due to a change in receptor expression, folding, assembly or

export to the plasma membrane. I had already determined that the Y4.7A receptor was well expressed in HEK293 cells and capable of binding ligand at the plasma membrane (section 3.2.1.4). Thus there must be some other difference between the Y4.7A receptor in HEK293 cells and *Xenopus* oocytes, and this difference must cause the disconnect between ligand binding and channel opening in HEK293 cells but not in *Xenopus* oocytes.

5.2.1.3 Characterisation of 5-HT_{3A}R M1, M2, and M3 mutant receptors in *Xenopus* oocytes

I next examined the two mutants I had identified in Chapter 3 as having the same effects on receptor function as Y4.7A (abolishing response in the functional assay but not ligand binding): D238A and K255L. The effects of these mutants on receptor function in HEK293 cells indicated that they were likely functionally connected to Y4.7, and might form a chain of interactions from M4 to the pore-lining helix M2 (Figure 3.12). When expressed in oocytes and assayed with by two-electrode voltage clamp, the K255L mutant receptor showed WT-like function, while the D238A mutant receptor was non-responsive (Table 5.2).

I additionally characterised the K255A and K255Q mutant receptors in oocytes, to further explore the requirements at position 255 (based on the K255A mutant receptor not disrupting receptor function in HEK293 cells). Both the K255A and K255Q mutant receptors were WT-like in oocytes.

Table 5.2: Parameters of 5-HT_{3A} receptors with alanine substitutions in M1-M3 in *Xenopus* oocytes

Mutant	EC ₅₀ (μM) HEK†	pEC ₅₀ (M)	EC ₅₀ (μM)	n _H	I _{max} (nA)	n
WT	0.17	5.76 ± 0.05	1.7	1.8 ± 0.3	8790 ± 3460	4
D238A	NF	NF				16
K255A	0.52	5.48 ± 0.06	3.3	1.9 ± 0.5	10580 ± 3570	3
K255L+	NF	5.74 ± 0.05	1.8	1.4 ± 0.2	982 ± 242	3
K255Q	0.11	5.93 ± 0.04	1.2	2.1 ± 0.4	7350 ± 4120	3
M235A	0.07	4.69 ± 0.05*	20	1.2 ± 0.1	3560 ± 1220	3
F242A	0.28	5.92 ± 0.05	1.2	2.0 ± 0.3	2750 ± 500	12
C290A	0.02	5.40 ± 0.15*	4.0	0.5 ± 0.1*	9940 ± 4840	9

Data are mean ± SEM. NF = non-functional at concentrations up to 30 μM.

Typical I_{max} values for NF receptors were between 5 and 50 nA. *significantly different from WT, p < 0.05, 2-way ANOVA. †Values from Table 3.6 and Table 3.7.

I also further assessed three of the mutations near Y4.7 in the 5-HT_{3A} receptor: M235A, F242A, and C290A (Figure 3.7). The C290A mutant receptor gave the same EC₅₀ as WT in oocytes, where in HEK cells it had given a lowered EC₅₀ (Table 3.6). However the change in n_H compared to WT was the same here as in HEK cells: a statistically significant reduction (Table 5.2, Figure 5.3). The M235A mutant receptor had a ~10-fold increased EC₅₀ compared to WT in oocytes, where in HEK cells there was a smaller decrease in EC₅₀ (Table 3.6). Finally, F242A was WT-like.

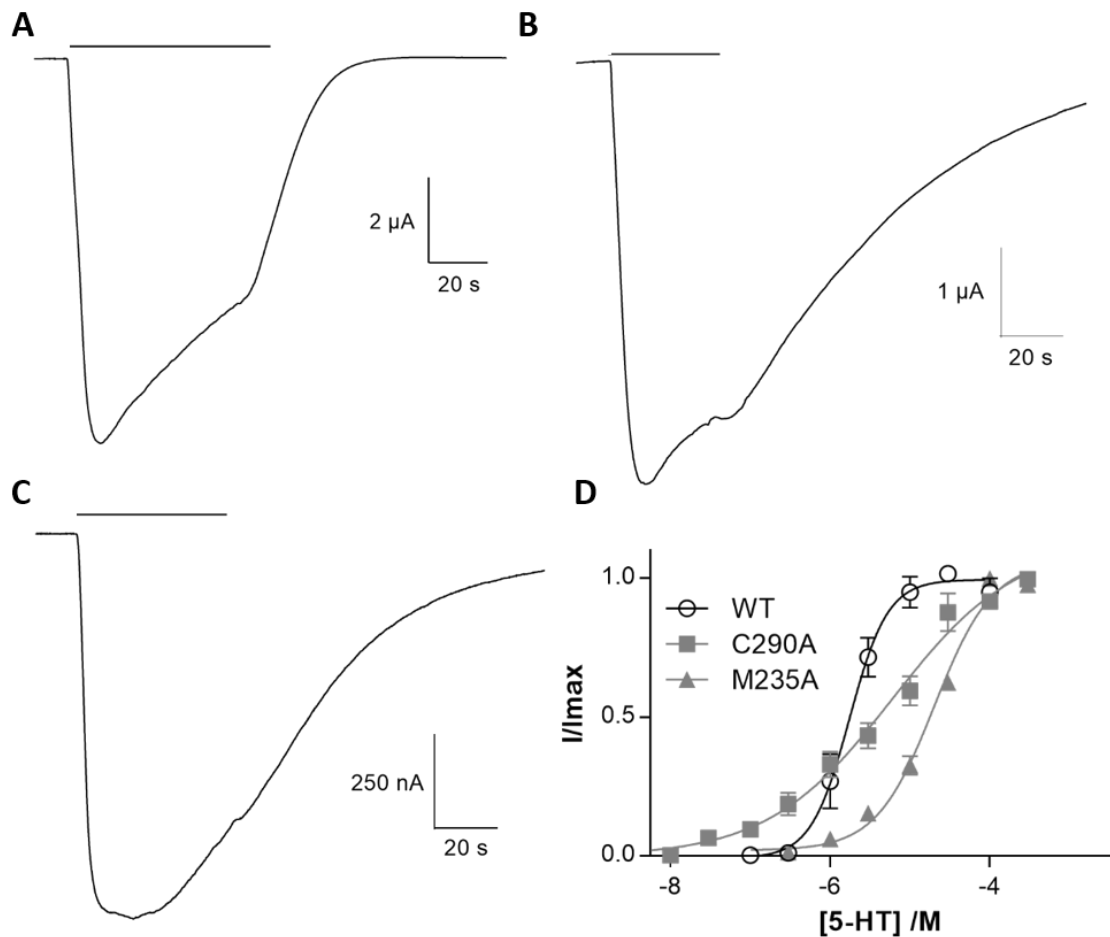


Figure 5.3: WT and mutant 5-HT_{3A}R responses to 3 μM 5-HT in *Xenopus* oocytes.

Current recording on addition of ligand (as indicated by the black bar) to A) WT, B) C290A and C) M235A 5-HT_{3A} receptors. D) Concentration-response curves from data as in A-C. Data are mean ± SEM, $n \geq 3$.

5.2.1.4 Characterisation of 5-HT_{3A} receptors in HEK293 cells with a single-cell assay

The experiments in sections 3.2.1.3 and 3.2.3.3 in Chapter 3 and sections, 5.2.1.2 and 5.2.1.3 here showed starkly different results of two mutations (Y4.7A and K255L) in the two different expression systems used (HEK293 cells and *Xenopus* oocytes). However, these experiments used different functional assays: the receptors in HEK293 cells were assayed in

a population of cells using the indirect measurement of fluorescence change in a dye moving in and out of the membrane on changes in membrane potential, and the receptors in oocytes were assayed in single cells, directly measuring the current across the membrane. To determine whether it was the assay or the expression system that was causing these differences in receptor function, I assayed the WT and one mutant (Y4.7A) receptor with single-cell patch-clamp in HEK293 cells. The cells were cotransfected with EGFP in a separate vector to select for cells that were successfully transfected, and Y4.7A cells were also cotransfected with RIC-3 to promote receptor expression/folding/export.

I performed current recordings on ten WT 5-HT_{3A} cells that showed EGFP expression on five separate days. Nine of these showed robust responses to ligand (average peak current was 1287 ± 324 pA) (Figure 5.4), and one showed an ambiguous response to ligand.

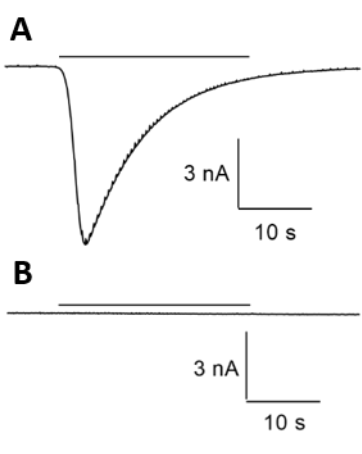


Figure 5.4: Typical responses of 5-HT_{3A} receptors in HEK293 cells with single-cell patch clamp. Current recordings on addition of 10 μ M 5-HT as indicated by black bar in single cells transfected with A) WT 5-HT_{3A}R DNA and B) Y4.7A 5-HT_{3A}R DNA.

I performed current recordings on ten EGFP-expressing Y4.7A cells on two different days. None of the ten cells showed any response to ligand (average peak recorded current after ligand addition was 36 ± 58 pA). The chance of getting a robust ligand response from a WT cell was 90%, so these data indicate that the Y4.7A receptor was non-functional when expressed in HEK293 cells and assayed by single-cell patch clamp ($p < 0.000001$, binomial probability). Therefore the change in observed functionality of Y4.7A between HEK293 cells and oocytes was likely to have been caused not by the different assay techniques, but an actual difference in receptor function in these two cellular environments.

5.2.2 Single-cell assays of $\alpha 4\beta 2$ nACh receptors

Having shown that expression in oocytes could allow previously non-responsive 5-HT_{3AR} M4 mutants to function, I next assayed all the non-functional $\alpha 4\beta 2$ nAChR M4 mutants identified in section 4.2.1.2 in oocytes, as well as the mutant that had shown a >5-fold shift in EC₅₀ (G4.14A) and two mutants that had caused altered EC₅₀s, though the change was <5-fold (L/F4.13A and L/M4.18A).

5.2.2.1 Characterisation of ‘WT $\alpha 4\beta 2$ nACh receptors in *Xenopus* oocytes

Two electrode voltage clamp of transfected oocytes showed rapid activation and desensitisation of receptors, and deactivation on removal of ligand (Figure 5.5). I measured an EC₅₀ of 165 nM ($pEC_{50} = 6.84 \pm 0.05$) for nicotine, similar to previous values for $\alpha 4\beta 2$ nAChRs containing an L9'A mutation in the $\alpha 4$ subunit (Fonck et al., 2005; Xiu et al., 2009).

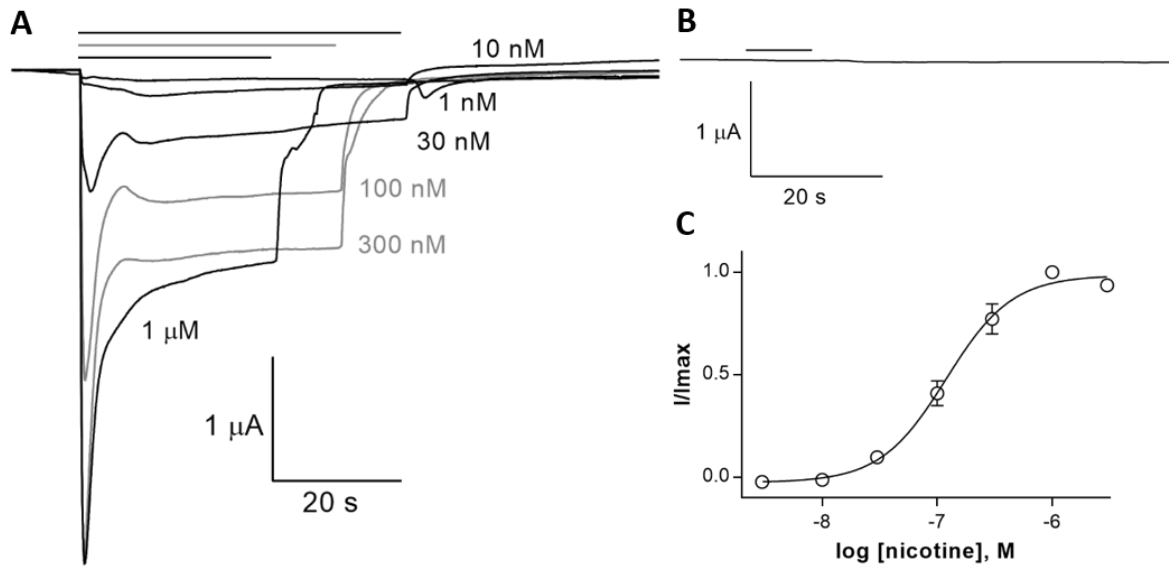


Figure 5.5: Typical responses of $\alpha 4\beta 2$ nACh receptors in *Xenopus* oocytes. Current recordings on addition of nicotine as indicated by black bar. A) Oocytes expressing 'WT $\alpha 4\beta 2$ nAChR, B) mock injected oocytes C) Concentration-response curve from 'WT data. Data are mean \pm SEM, $n=4$.

5.2.2.2 Characterisation of $\alpha 4\beta 2$ nACh receptors with key M4 mutations in *Xenopus* oocytes

I assayed the eight double mutants that were expressed and bound ligand but showed no channel activity in HEK293 cells, as well as the one that was poorly expressed/assembled and non-responsive in HEK293 cells (D4.0A) (Table 4.1, Figure 4.3).

Strikingly, seven of the eight mutant receptors that could bind ligand but showed no channel action in HEK293 cells showed robust responses to ligand when assayed with two-electrode voltage clamp in *Xenopus* oocytes (Table 5.3), and all of these seven showed a decreased EC₅₀ compared to 'WT. The only mutant receptor that could bind ligand but showed no channel activity in HEK293 cells and also non-functional in *Xenopus* oocytes was F4.7A.

D4.0A showed no receptor function in oocytes, consistent with the effect of the equivalent mutation in all pLGICs tested so far (da Costa Couto et al., 2020; Lo et al., 2008) except in

the *Torpedo* muscle-type nicotinic α subunit (Thompson et al. 2020), though in the latter case the D4.0A mutation was present in only 2 of 5 subunits in the receptor.

Table 5.3: Parameters of $\alpha 4\beta 2$ nACh receptors with M4 alanine substitutions

Mutant	EC ₅₀ (nM) HEK†	EC ₅₀ (nM) Oocyte	pEC ₅₀ (M)	n _H	I _{max} (nA)	n
'WT	19	165	6.84 ± 0.05	1.4 ± 0.2	2300 ± 764	3
D4.0A	NF	NF				4
R4.1A	NF	88	7.06 ± 0.10*	1.2 ± 0.3	152 ± 30	6
F4.3A	NF	42	7.37 ± 0.08*	1.7 ± 0.5	1090 ± 500	3
L4.4A	NF	50	7.30 ± 0.06*	1.9 ± 0.4	1380 ± 830	4
F4.7A	NF	NF				4
T4.15A	NF	52	7.28 ± 0.10*	1.2 ± 0.3	190 ± 130	3
F4.19A	NF	38	7.43 ± 0.05*	1.6 ± 0.3	7900 ± 1940	4
P/Q4.21A	NF	54	7.28 ± 0.06*	1.4 ± 0.2	1430 ± 610	6
'WT/N4.26A	NF	77	7.11 ± 0.04*	1.5 ± 0.2	1800 ± 460	8

Data are mean ± SEM. NF = non-functional at concentrations up to 1 μ M nicotine.

Typical I_{max} values for NF receptors were between -5 and 15 nA.*significantly different from 'WT, p < 0.001, 2-way ANOVA. †Values from Table 4.1

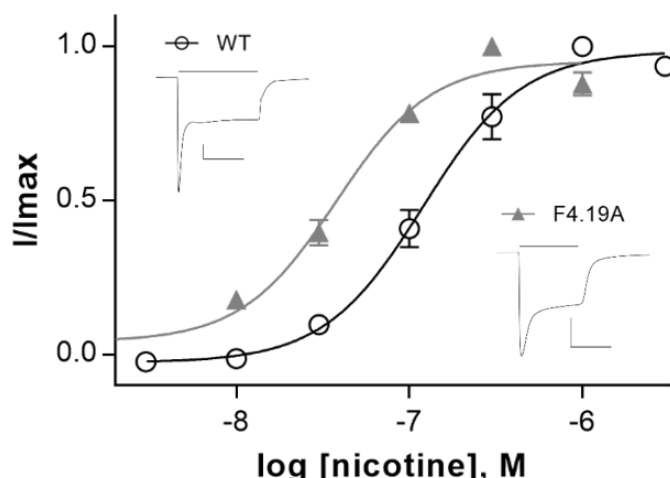


Figure 5.6: 'WT and mutant $\alpha 4\beta 2$ receptors in *Xenopus* oocytes. Concentration-response curves of 'WT and F4.19A $\alpha 4\beta 2$ nAChRs. Insets: Current recordings at 300 nM, with nicotine addition indicated by black bar. Scale bars are 500 nA and 20 s.

5.2.2.3 Characterisation of additional $\alpha 4\beta 2$ nACh mutant receptors in *Xenopus* oocytes

The M4 mutant nACh receptor that showed a >5-fold increase in EC₅₀ when assayed in HEK293 cells (G4.14A), and two other mutant nACh receptors (L/F4.13A and L/M4.18A) that had shown a statistically significant, but smaller than 5-fold, change in EC₅₀ in HEK cells (section 4.2.1.2), all showed decreased EC₅₀s compared to ‘WT when expressed in oocytes (Table 5.4).

Table 5.4: Parameters of additional $\alpha 4\beta 2$ nACh receptors with M4 alanine substitutions

Mutant	EC ₅₀ (nM) HEK	EC ₅₀ (nM) Oocyte	pEC ₅₀ (M)	n _H	I _{max} (nA)	n
‘WT	19	165	6.84 ± 0.05	1.4 ± 0.2	2300 ± 760	3
L/F4.13A	6	92	7.04 ± 0.04*	1.2 ± 0.1	1470 ± 160	4
G4.14A	101	109	6.96 ± 0.05*	2.1 ± 0.5	390 ± 130	4
L/M4.18A	5	95	7.02 ± 0.07*	1.5 ± 0.4	3100 ± 1090	3

Data are mean ± SEM. *significantly different from ‘WT, p < 0.001, 2-way

ANOVA.

5.3 Discussion

The aim of this work was to characterise the 5-HT₃AR and $\alpha 4\beta 2$ nAChR M4 mutants of interest identified in HEK293 cells in Chapters 3 and 4 in another expression system, *Xenopus* oocytes. Surprisingly, nine out of the eleven mutants that were non-responsive but showed WT/WT-like ligand binding in HEK293 cells, were functional when expressed in *Xenopus* oocytes. That these residues are key to receptor function in one expression system but incidental in another, points to the cellular environment of a receptor as a strong modulator of receptor function, and indicates that the M4 helix might play different functional roles in receptors expressed in the two different systems.

5.3.1 Most mutations that abolish 5-HT_{3A} or $\alpha 4\beta 2$ receptor function in HEK293 cells have little effect in *Xenopus* oocytes

Y4.7A, D238A and K255L mutant 5-HT_{3A} receptors were all non-responsive in HEK cells (section 3.2). Two of these three (Y4.7A and K255L) showed WT-like function in oocytes, while the D238A mutant receptor remained non-functional (Table 5.1, Table 5.2). Similarly, of the eight $\alpha 4\beta 2$ nACh M4 alanine mutant receptors that were non-functional in HEK cells (section 4.2.1.2), all but one (F4.7A) were functional (and even showed a small gain of function) in oocytes (Table 5.3).

While this was initially surprising, it does fit with previous work in this area, which also shows inconsistencies between effects of similar mutations in cation-selective pLGICs. The results of previous studies generally fit the same pattern of mutations in cation-selective pLGIC M4 helices having no measurable effect or causing small gains of function in *Xenopus* oocytes, but being detrimental to function in HEK293 cells. The $\alpha 7$ nAChR M4 mutation P468A has no effect on receptor function when assayed in oocytes (da Costa Couto et al., 2020), yet completely abolishes function (but not expression to the cell surface or ligand binding) when assayed in HEK cells (Noviello et al., 2021). More broadly, studies showing that deletion of the C-terminal end of the M4 helix has no effect on function in ELIC (Hénault et al. 2015) or the *Torpedo* nAChR (Tobimatsu et al., 1987) were both performed using receptors expressed in *Xenopus* oocytes, while studies showing that the C-terminus of M4 is required for function in the 5-HT_{3A} receptor (Butler et al., 2009; Pons et al., 2004) assayed receptors expressed in HEK293 cells. Add to this my work showing that M4 alanine mutations can completely abolish receptor function in the 5-HT_{3A} and $\alpha 4\beta 2$ nACh receptors when expressed in HEK cells (Mesoy et al. 2019; Mesoy and Lummis 2021), yet almost exclusively have no effect or cause small gains of function in these receptors expressed in *Xenopus* oocytes (Crnjar et al. (2021), Table 5.1, and Table 5.3), and a strong pattern emerges of the role of the M4 helix in cation-selective pLGICs varying between the HEK cell and the oocyte cellular environment. The only exception to this pattern I have found so far is that alanine mutations in the α subunit of the *Torpedo* muscle nAChR expressed in oocytes cause both increased and decreased EC₅₀s. I note that these mutations are only present in two of the

five subunits of these heteropentamers, and what effect an M4 mutation in all subunits would have is as yet unknown. Thus it appears that the effects of individual mutations, and therefore the roles of individual residues, as well as the roles of entire segments (like the C-terminal end of M4) and possibly the roles or existence of residue-residue interactions, depend on the expression system of the receptor.

This sort of context-dependent effect of M4 mutations has not been found in anion-selective or bacterial pLGICs. Indeed, alanine mutations in anion-selective pLGIC M4 helices (especially of aromatic residues) are generally detrimental to receptor function in both HEK cells (Cory-Wright et al., 2017) and oocytes (Haeger et al., 2010; Tang and Lummis, 2018).

Taken together, these data indicate that the M4 helix of cation-selective, but not anion-selective, pLGICs is crucial to receptor function in HEK293 cells (where small mutations in M4 can completely abolish receptor function), but poorly optimised for function in *Xenopus* oocytes (where M4 mutations generally promote receptor function).

5.3.1.1 How cellular context might be affecting cation-selective pLGIC function and mechanism

The major differences between HEK cells and oocytes that might explain the different effects of M4 mutations on cation-selective pLGIC function are 1) protein expression levels, 2) post-translational modifications (PTMs), 3) intracellular factors, and 4) the composition and characteristics of the plasma membrane itself.

In the 5-HT_{3A} and α7 nACh receptors, the relevant M4 mutants that are functional in oocytes but not in HEK cells (Y4.7A and P468A, respectively) have been shown to be expressed and able to bind ligand at the cell surface in HEK cells (Mesoy et al. 2019; Noviello et al. 2021), which precludes factor 1 (protein expression levels) as a possible explanation for the inconsistency in function between the two expression systems. In the α4β2 nACh receptor, eight of the nine non-functional M4 mutant receptors are well enough folded and assembled to bind ligand in HEK cells (Figure 4.3), though whether this binding is extracellular or intracellular is not yet determined.

PTMs and intracellular factors cannot access most M4 residues, including almost all the positions where mutation has different effects in HEK cells and oocytes, rendering them less likely candidates for altering the role of M4. Therefore the composition of the plasma membrane is the strongest candidate for causing this switch in role of M4 and effects of M4 mutations in the 5-HT_{3A} and nACh receptors.

5.3.1.2 How membrane composition can modulate pLGIC function

It is well known that lipids can modulate pLGIC activity, both through specific binding and through modulating the properties of the plasma membrane as a whole (section 1.3.3.1, well reviewed in Thompson and Baenziger (2020)). Many drugs act on transmembrane proteins not only through specific ligand-protein interactions, but also by altering bulk lipid bilayer properties (Kapoor et al., 2019). Structural studies and photolinking have also shown various lipids bound to, and in some cases affecting the function of, the GABA_{AR}, GlyR, GluCl and GLIC (Althoff et al., 2014; Budelier et al., 2019; Cheng et al., 2018; Hamouda et al., 2005; Hibbs and Gouaux, 2011; Huang et al., 2017; Laverty et al., 2019; Tong et al., 2019).

The M4 helix has repeatedly been shown to act as a lipid sensor, translating changes in lipid bilayer composition into effects on pLGIC function, especially in cation-selective pLGICs (Baenziger et al. 2000; Carswell et al. 2015; DaCosta and Baenziger 2009; Fong and McNamee 1986; Nievas et al. 2008; Rankin et al. 1997; Roccamo et al. 1998; Santiago et al. 2001). Of particular relevance, it has been shown that lipid composition can cause the *Torpedo* nAChR to enter an uncoupled state (where the receptor can bind ligand without it causing channel opening, even though the receptor is not in a desensitized state) (DaCosta et al., 2009; DaCosta and Baenziger, 2009), which is very similar to the state of the Y4.7A 5-HT_{3A} and P468A α 7 nACh mutant receptors (and potentially some α 4 β 2 nAChR M4 mutants) in HEK293 cells (but not in oocytes).

I suggest that some difference in lipid composition between HEK cells and oocytes (section 1.3.3) may be causing the receptors to function differently in the two contexts. Exactly which lipid might be causing this functional difference, or whether it causes the difference through specific binding or through altering the bulk properties of the plasma membrane, is unclear.

One possible specific suggestion is that the higher cholesterol levels in oocytes than in HEK cells (see discussion in section 1.3.3) could be causing the functional difference. Cholesterol is well known to be important for nAChR function, it is proposed to bind both to the $\alpha 4\beta 2$ nACh and the 5-HT_{3A} receptors (Guros et al. 2020; Walsh et al. 2018), molecular dynamics studies have shown it is able to intercalate into the M4-M1/M3 interface in the open but not the closed state of the glycine receptor (Dämgen and Biggin, 2021), and it can alter bulk membrane properties. However, the cause of this functional difference in pLGICs could also be the presence or absence of a different lipid, or indeed a combination of lipids.

5.3.1.2.A Potential effects of specific lipid binding

Y4.7 in the 5-HT_{3A} M4 helix has been predicted to form a H-bond with cholesterol as an essential part of channel gating (Guros et al. 2020). My collaborator Alessandro Crnjar also found several potential H-bonds between lipids and Y4.7 and D238 in both the WT and Y4.7A mutant simulations of the 5-HT_{3A} receptor (Figure 5.7). This suggests that there is much potential for a lipid-protein interaction here that might occur in one but not the other of HEK cells and oocytes, and could cause differences in the contribution of the M4 helix in 5-HT_{3A} function in the two different environments.

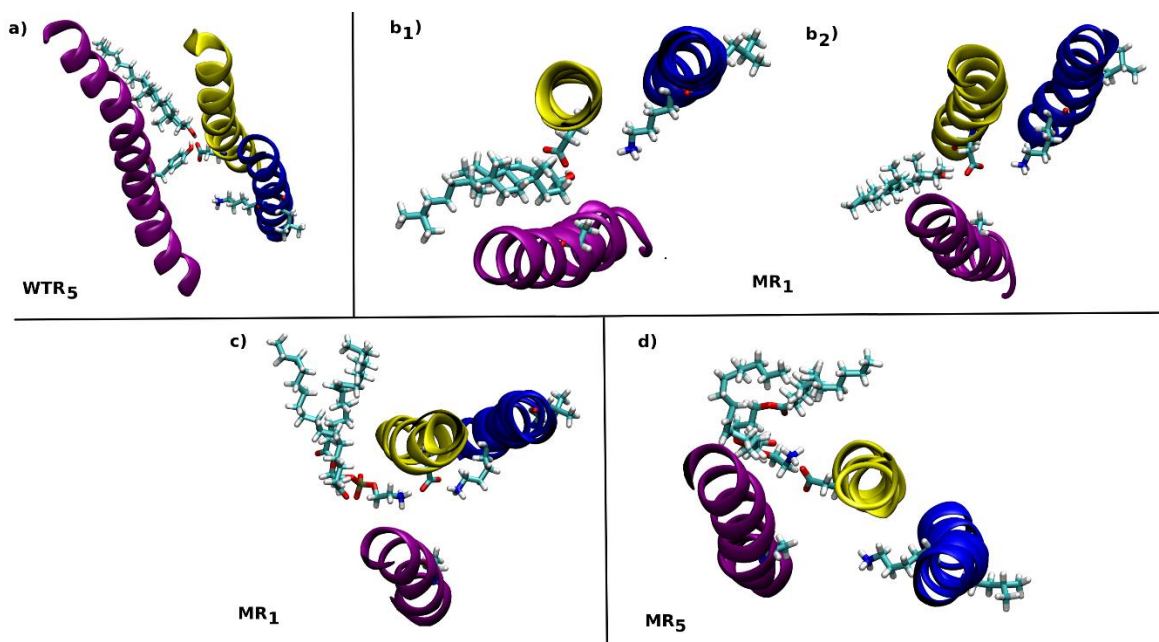


Figure 5.7: Snapshots from MD simulations of the 5-HT_{3A} receptor. M4 in purple with Y4.7 in sticks, M1 in yellow with D238 in sticks, and M2 in blue with K255 and L260 in sticks. Lipids are A, C, D) POPE, B) cholesterol. (Figure adapted from Crnjar, A., Mesoy, S., Lummis, S. C. R., & Molteni, C. (2021) under a Creative Commons Attribution License (CC BY). Copyright 2021 Crnjar, Mesoy, Lummis and Molteni.)

Several of the key M4 residues in the $\alpha 4\beta 2$ nACh receptor are also well placed to interact with membrane lipids. The 6cnj cryo-EM structure of the human $\alpha 4\beta 2$ nACh receptor shows 10 cholestryl hemisuccinate moieties (modelled as cholesterol), which bind between M1/M4 and between M3/M4. R4.1 is near the M1/M4 cholesterol, with the β R4.1 terminal nitrogen 3.1 Å from the hydroxyl group of the cholesterol (Figure 5.8), giving the potential for an H-bond here. The R4.1A mutation abolished receptor function when present in only $\alpha 4$ or only $\beta 2$ subunits (Table 4.2), indicating that its role is essential in both subunits. Intriguingly, none of the substitutions tested were tolerated at this position (Table 4.3), indicating that its exact size, shape and charge are all important to its role in receptor function.

F4.3 and β L4.4 both form part of the hydrophobic pocket where cholesterol binds (Figure 5.8), and alterations at these positions could affect the binding of cholesterol and other lipids.

This is supported by the fact that the receptor tolerates an F4.3L substitution but not F4.3Y, demonstrating the importance of an aliphatic group at this position.

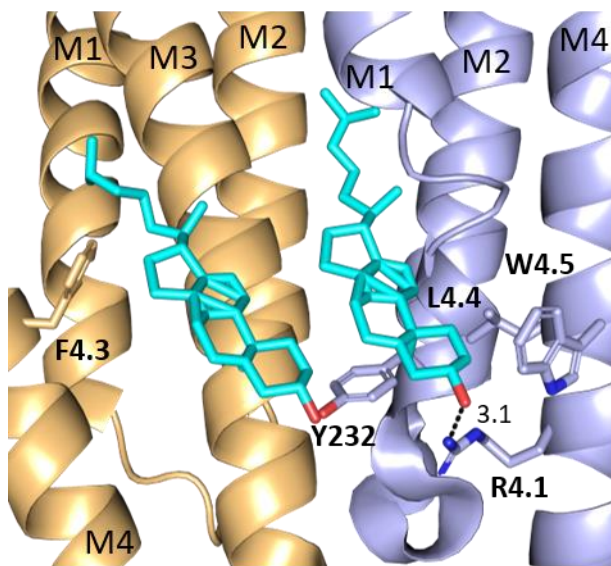


Figure 5.8: Cholesterol moieties in a human $\alpha_4\beta_2$ nAChR cryo-EM structure (6cnj). α_4 in gold and β_2 in blue, with relevant residues shown as sticks, cholesterol in cyan. Distance in Å marked by dashed lines.

F4.7 faces into the transmembrane domain, and is less exposed than some of the other key M4 residues. However, it is the equivalent to Y4.7 in the 5-HT_{3A} receptor, discussed above, where modelling shows several potential modes of interactions with lipids. F4.7 may even form a similar chain of interactions in towards M2 as Y4.7 does in the 5-HT_{3A} receptor (section 3.3.3.3, section 4.2.3).

T4.15 and F4.19 both lack likely intra-subunit interaction partners, indicating that they might bind lipids instead. A molecular dynamics simulation of the glycine receptor shows that cholesterol can intercalate between the M4 and M1/M3 helices here in the open but not the closed state of the receptor (Figure 5.9, M4 not shown) (Dämgen and Biggin, 2021).

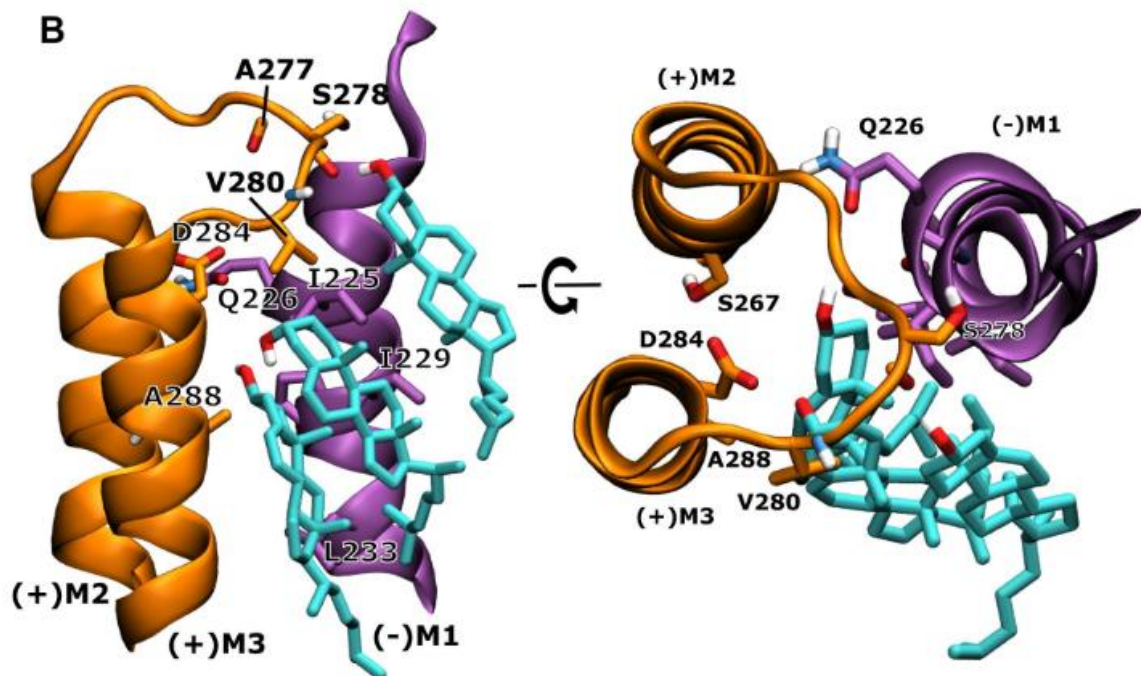


Figure 5.9: Representative snapshot of cholesterol binding representing examples of cholesterol observed in coarse-grained MD simulations. Primary subunit in orange and M1 of complementary subunit in purple, cholesterol in cyan, M4 not shown. Selected residues shown in stick representation. (Figure taken from Dämgen and Biggin (2021) under a Creative Commons Attribution License (CC BY). Copyright 2021 Dämgen and Biggin.)

Finally, P/Q4.21 and β N4.26 are both well-positioned to interact with the ECD (Figure 4.6), but their putative interactions with the ECD depend on the positioning of the M4, which could be affected by lipids binding. Additionally, a molecular dynamics simulation of the glycine receptor shows all outer-leaflet lipids in the simulation (POPC, POPE, cholesterol, and sphingomyelin) interact with the receptor at the ECD-TMD interface, and have more interactions with the ECD in the inactive state of the receptor than in the active state (Dämgen and Biggin, 2021).

5.3.1.2.B Potential effects of bulk membrane properties

The question of whether lipids affect pLGIC function by specific binding or by altering bulk membrane properties has been the subject of much debate, with interesting evidence on both sides that is well reviewed in Levitan (2017). Changes in bulk membrane properties could alter the angle or mobility of M4, as well as its interactions with both the M1/M3 interface and the ECD.

5.3.2 Most M4 mutations that alter 5-HT_{3A} or $\alpha 4\beta 2$ receptor function in HEK cells have different effects in *Xenopus* oocytes

The 5-HT_{3A} and $\alpha 4\beta 2$ nACh receptor mutants with altered function in HEK cells did not consistently show the same changes in receptor function when expressed in *Xenopus* oocytes (Figure 5.10). In the $\alpha 4\beta 2$ nACh receptor, the three M4 mutations that altered function in different directions in HEK cells all caused small decreases of EC₅₀ in oocytes. This supports the data from the mutants that were non-functional in HEK cells, and indicates that while specific residue of M4 are critical to its role in receptor function in HEK cells, in oocytes its role is less dependent on its exact sequence, and most mutations in M4 promote receptor function.

In the 5-HT_{3A} receptor, the pattern of changes was less consistent (Figure 5.10). One mutation (K255A) had the same effect in both systems, but three mutations had different effects: M235A caused a decreased EC₅₀ in HEK cells but an increased EC₅₀ in oocytes, F242A caused an increased EC₅₀ in HEK cells but no statistically significant effects in oocytes, and C290A caused a decreased EC₅₀ in HEK cells but an increased EC₅₀ in oocytes (though in both cases C290A displayed a lower Hill slope than the WT receptor). While these data are harder to interpret, they still support the supposition that certain transmembrane residues play very different roles in receptor function in the two expression systems.

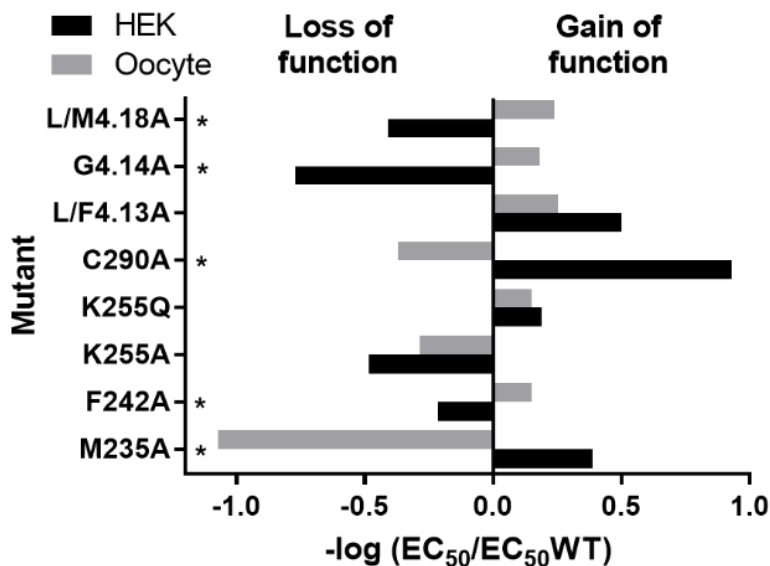


Figure 5.10: Changes in EC₅₀ of $\alpha 4\beta 2$ nACh (top) and 5-HT_{3A} (bottom) receptor mutants in HEK cells and oocytes. *change in pEC₅₀ significantly different between the two systems, $p < 0.05$, 2-way ANOVA.

5.4 Conclusion

In this chapter I have shown that many of the 5-HT_{3A} and $\alpha 4\beta 2$ nACh mutant receptors that were assembled and capable of ligand binding, but non-responsive in the functional assay in HEK293 cells, were functional when assayed in *Xenopus* oocytes (2 out of 3 5-HT_{3A} receptor mutants and 7 out of 8 $\alpha 4\beta 2$ nACh receptor mutants). For some of these mutants I showed that this cannot be due to lack of expression, folding, assembly, or export to the cell surface, as both the Y4.7A and K255L 5-HT_{3A} receptor mutants (which were non-responsive in HEK cells) were expressed and capable of binding ligand at the cell surface at WT-like levels. I also showed that this difference in function was not due to the different assays used to measure receptor function in the two expression systems, as the 5-HT_{3A} receptor mutant Y4.7A was non-responsive when assayed by whole-cell patch-clamp in HEK cells. Finally I

determined that M4 mutations that altered receptor function in either of these receptors in HEK cells often had different effects on receptor function in oocytes.

Altogether these data indicate that the M4 plays different roles in receptor function in these two expression systems, implying that receptor function is dependent on the cellular context. In HEK cells the M4 is crucial to the function of these cation-selective receptors, and most changes here that have any effect are detrimental to receptor function. Conversely, in oocytes the M4 helix is not ‘well’ optimised for receptor function, and most changes here have no effect or improve receptor function.

Finally, having excluded most of the factors that might differ between HEK cells and oocytes (expression levels, PTMs, and intracellular factors), I suggest that the difference in lipid composition and properties of the lipid bilayer between HEK cells and oocytes cause this difference in M4 role between the two expression systems.

Chapter 6 The N-terminal helix of the 5-HT_{3A} receptor

6.1 Introduction

The aim of this work was to investigate the role of the N-terminal helix in 5-HT_{3A}R function, as evidence from the GlyR indicates that it could form part of a small molecule-binding site of interest for receptor modulation.

6.1.1 Ligand binding near the N-terminal helix

The N-terminal helix (NTH) sits above the pLGIC ligand binding site (Figure 6.1). Recent work has found that the N-terminal helix of the GlyR forms part of a small molecule-binding site (Figure 6.2) where ligand binding modulates the GlyR affinity for glycine (Huang et al., 2017). The NTH also contributes to a small molecule-binding site in the acetylcholine binding protein (AChBP), a soluble protein from molluscs homologous to the pLGIC ECD (Spurny et al., 2015).

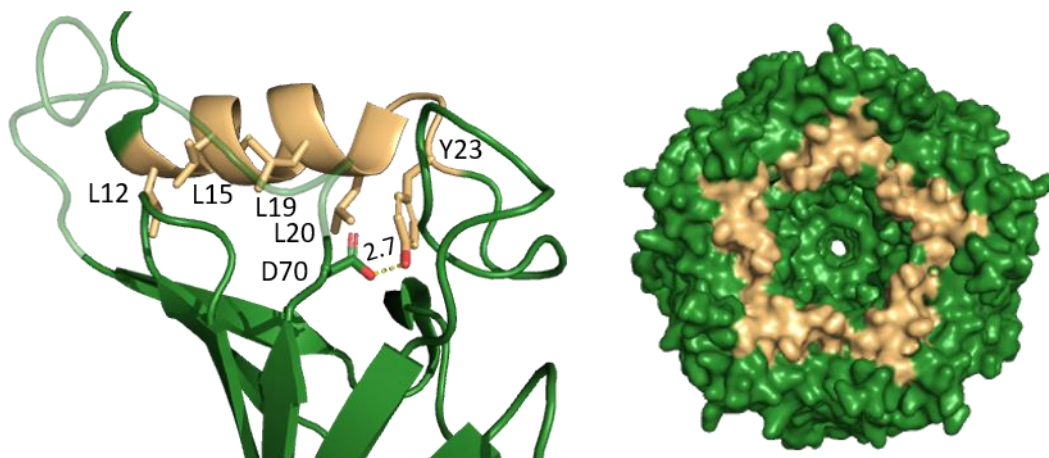


Figure 6.1: N-terminal helix of the 5-HT_{3A} receptor. Closed 5-HT_{3A}R in green showing the NTH in beige. Selected residues shown as sticks on the left, with distance in Å marked by dashes.

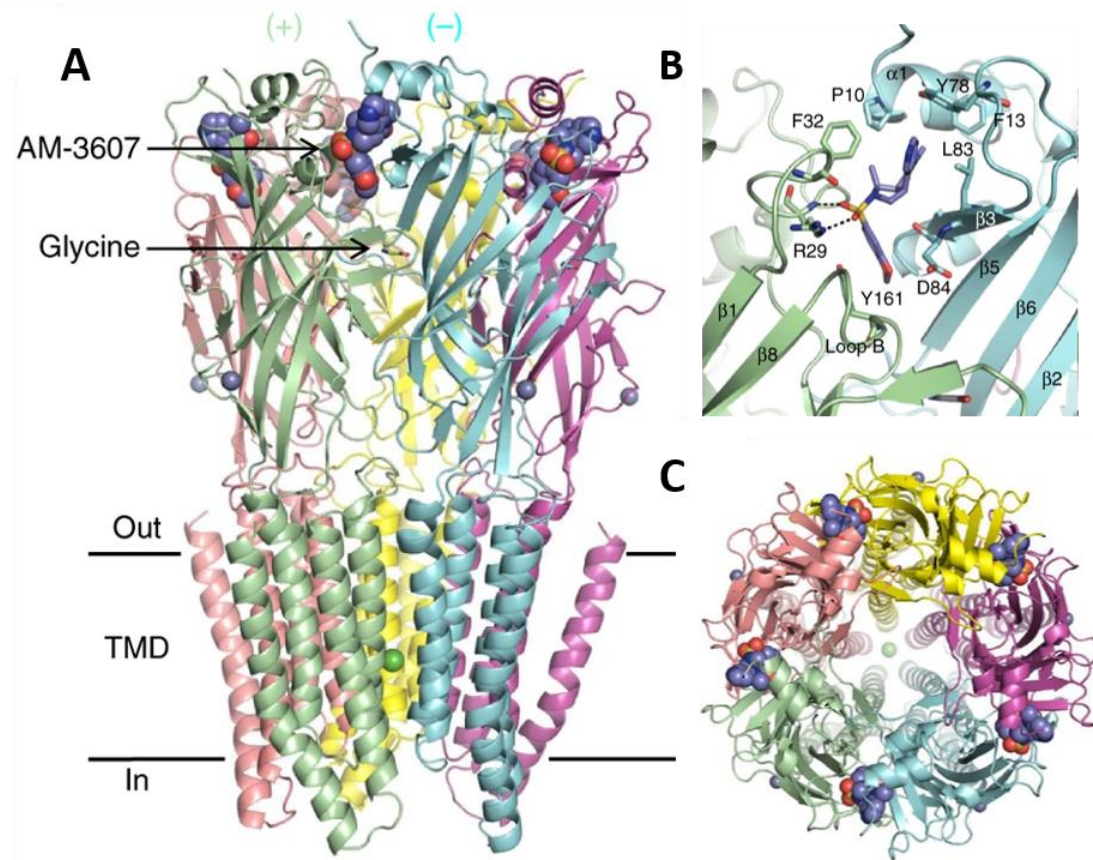


Figure 6.2: Small molecule binding near the NTH of the GlyR. A) GlyR α 3 in complex with AM-3607 (blue spheres) and glycine (grey sticks). Zn²⁺ (grey spheres) and Cl⁻ (green sphere) also shown. B) Binding site occupied by AM-3607 (blue sticks), with glycine in orthosteric ligand binding site below (grey sticks). C) View of A) down the pore axis from above the extracellular domain. (Reprinted by permission from Springer Nature: Springer Nature, *Nature Structural & Molecular Biology*, Crystal structures of human glycine receptor α 3 bound to a novel class of analgesic potentiators, Huang, X; Shaffer, PL; Ayube, S; Bregman, H; Chen, H; Lehto, SG; Luther, JA; Matson, DJ; McDonough, SI; Michelsen, K; Plant, MH; Schneider, S; Simard, JR; Teffera, Y; Yi, S; Zhang, M; Dimauro, EF, Gingras, J, Copyright (2017).)

6.1.2 The N-terminal helix in other pLGICs

The N-terminal helix contains residues 12-23 of the 5-HT₃AR. Three residues in the NTH (L15, L19, and Y23) are highly conserved between anion-selective and cation-selective

pLGICs (Figure 6.3), indicating that these may be of particular importance. Other residues like R/K14 are conserved within a pLGIC subfamily but not beyond, indicating that this domain might be able to provide opportunities for receptor target selectivity.

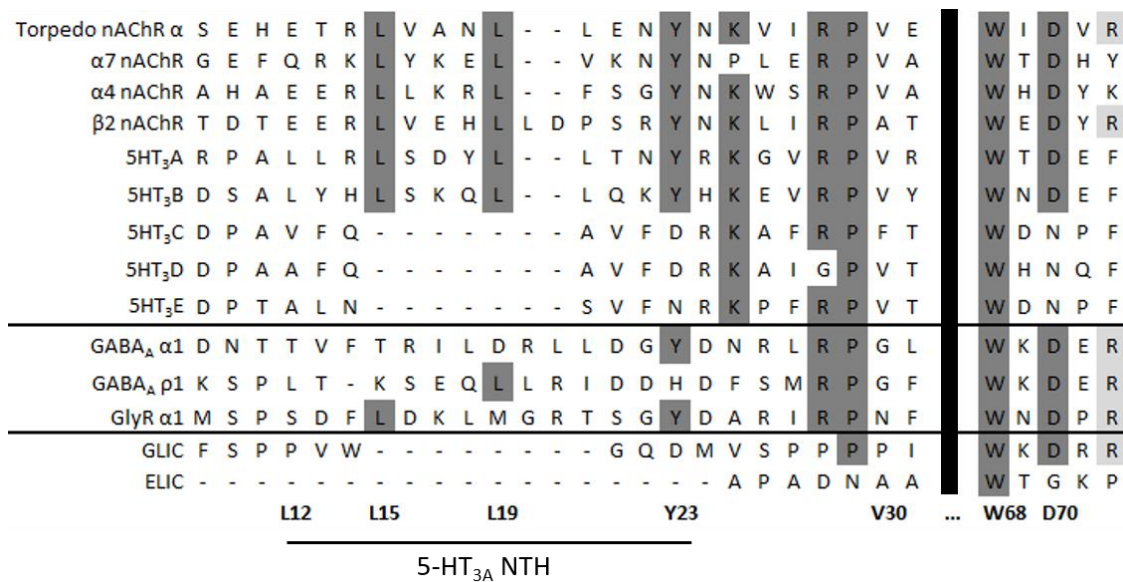


Figure 6.3: Sequence alignment of selected pLGICs around the 5-HT_{3A}R NTH.

Uniprot numbers are in order: P02710, P36544, P09483, P12390, P46098, O95264, Q8WXA8, Q70Z44, A5X5Y0, P62813, P24046, P23415, Q7NDN8, P0C7B7. Residues coloured by identity, 5-HT_{3A} numbering shown. Residues 32-67 by 5-HT_{3A} numbering excluded for simplicity.

Exchanging the NTH and nearby regions between the human α1 and α7 nAChRs indicates that the NTH affects nAChR function (Luo et al., 2009). The top of the nAChR ECD mainly consists of three regions: the NTH (residues 2-14), an unstructured loop (residues 15-32), and the main immunogenic region (MIR, residues 60-81). Switching in residues 2-14, 1-32 or 60-81 alone from the α1 nAChR to the α7 nAChR abolishes receptor expression as measured by antibody binding. However, switching in residues 2-14 and 60-81 together from α1 to α7 causes a 13-fold reduction in receptor sensitivity to acetylcholine (ACh), while switching in residues 1-32 and 60-81 together from α1 to α7 causes a 10-fold increase in receptor sensitivity to ACh. Conversely, substituting in residues 66-76 (the MIR) from fetal α7 to the

$\alpha 1$ nAChR caused a slight decrease in sensitivity to ACh, and increased the rate of desensitisation compared to the $\alpha 1$ WT receptor.

Mutation of NTH residues to alanine is detrimental to $\alpha 7$ nAChR expression as measured by α -bungarotoxin binding: 4 out of 12 NTH alanine mutants showed <60% of WT ligand binding. Proline substitutions in this region had larger effects: all 12 proline mutations in the NTH reduced ligand binding to <60% of WT levels, 5 of which abolished detectable binding. Individual proline mutations in the $\alpha 3\beta 4$ and $\alpha 4\beta 2$ nAChR NTHs also abolished or drastically reduced receptor expression (Castillo et al., 2009).

6.1.3 The N-terminal helix in the 5-HT_{3A} receptor

The 5-HT₃R NTH runs from L12-Y23 in the 5-HT_{3A} and 5-HT_{3B} subunits, but appears to be absent in the C-E subunits (Figure 6.3). Y23 has previously been shown to be critical for receptor formation, with Y23A, Y23S, and Y23F mutations abolishing both receptor function, ligand binding, and cell surface staining measured by immunofluorescence in HEK293 cells (Price and Lummis, 2004). When expressed in *Xenopus* oocytes, Y23A and Y23F mutant receptors remain non-functional, while Y23S mutant receptors show WT-like receptor function, indicating that mutations here are detrimental to receptor formation, but that this can be overcome in some cases by the more permissive expression conditions of *Xenopus* oocytes.

In this work I characterised receptors with alanine mutations at all positions of the NTH. Due to the high content of leucine residues in the NTH, I also assessed the effect of mutating each of these to aspartic acid (which has a sidechain of similar size to leucine, but with a negative charge).

6.2 Results

6.2.1 Characterisation of 5-HT_{3A}Rs with NTH alanine and aspartic acid substitutions

6.2.1.1 Characterisation of WT 5-HT_{3A} receptors

The WT 5-HT_{3A} receptor showed an EC₅₀ of 0.17 µM (pEC₅₀ = 6.76 ± 0.01 M) and a Hill slope of 3.7 ± 0.3 (Figure 3.1), consistent with previously published data (Lummis et al., 2011). Coexpression with RIC-3 had no statistically significant effect on the recorded parameters of WT receptor function in HEK293 cells.

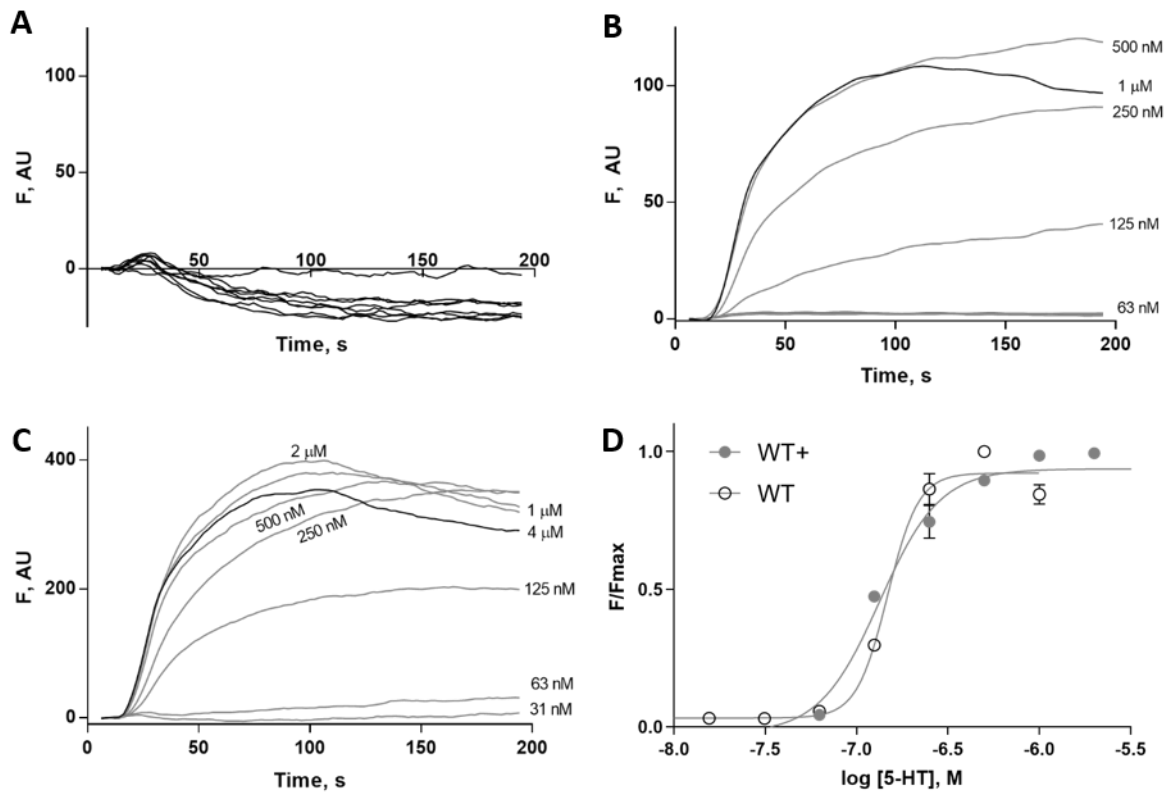


Figure 6.4 Typical responses of 5-HT_{3A} receptors in HEK293 cells. Fluorescent responses (F in arbitrary units, AU) on addition of 5-HT at 20 s in A) mock transfected cells, B) cells expressing WT 5-HT_{3AR}, C) cells expressing WT 5-HT_{3AR} and RIC-3. D) Concentration-response curve from WT data. Data are mean \pm SEM, $n \geq 3$. This figure is the same as Figure 3.1 in Chapter 3.

6.2.1.2 Characterisation of 5-HT_{3ARs} with NTH alanine substitutions

In the initial fluorescence assay, nine of the eleven alanine mutants showed function not significantly different from WT, and two were nonresponsive (Table 6.1).

Table 6.1: Parameters of 5-HT_{3A} receptors with NTH alanine substitutions

Mutant	pEC ₅₀ (M)	EC ₅₀ (μM)	n _H	MRF	B/B _{WT}	n
WT	6.76 ± 0.01	0.2	3.7 ± 0.3	273 ± 16	1.0 ± 0.5	3
WT+	6.89 ± 0.04	0.13	2.5 ± 0.4	349 ± 35		3
L12A	6.64 ± 0.03	0.2	2.4 ± 0.3	227 ± 30		3
L13A	6.64 ± 0.03	0.2	3.7 ± 0.9	288 ± 1		3
R14A	6.7 ± 0.02	0.2	3.0 ± 0.3	393 ± 5		3
L15A+	NF				0.0 ± 0.1	3
S16A	6.75 ± 0.02	0.2	3.0 ± 0.3	372 ± 6		3
D17A	6.32 ± 0.04	0.5	2.5 ± 0.4	243 ± 5		3
H18A	6.58 ± 0.02	0.3	4.2 ± 0.5	349 ± 14		3
L19A+	NF				0.0 ± 0.0	3
L20A	6.10 ± 0.1	0.8	5.5 ± 4.2	75 ± 7	0.8 ± 0.3	3
N21A	6.51 ± 0.02	0.3	3.5 ± 0.4	252 ± 7		3
Y23A+ [†]	6.88 ± 0.03	0.1	3.1 ± 0.6	152 ± 3		3

Data are mean ± SEM. + indicates coexpression with RIC-3, NF = non-functional at concentrations up to 1 mM 5-HT. MRF is maximum recorded fluorescence, typical MRF for NF receptors was between 0 and 20. No pEC₅₀ or n_H values were significantly different from WT/WT+ and ≥5-fold change, p < 0.05, 2-way ANOVA. n=3x indicates 3 technical replicates of x biological replicates, n=4 indicates two biological replicates. [†]4 out of 6 biological replicates showed response to ligand, the remaining 2 showed no response to ligand addition

I further assayed the non-responsive mutant receptors (L15A and L19A) and one functional mutant receptor (L20A) by radioligand binding, and found that neither the L15A nor the L19A mutant receptors showed ligand binding, unlike the L20A receptor (which showed ligand binding not significantly different from WT). As these mutations are all outside the ligand binding site, I interpreted this to mean that these mutations were likely interfering with receptor expression, folding, assembly or export, rather than ligand binding itself.

6.2.1.3 Characterisation of 5-HT_{3A}Rs with NTH aspartic acid substitutions

I next investigated the leucine residues of the NTH by mutating them individually to aspartic acid (Table 6.2). Only one of the aspartic acid mutants showed any response in the functional assay, and that required coexpression with the chaperone RIC-3 and had reduced maximal fluorescence, perhaps indicating that receptor expression, folding, assembly or export was impaired.

Table 6.2: Parameters of 5-HT_{3A} receptors with NTH aspartic acid substitutions

Mutant	pEC ₅₀ (M)	EC ₅₀ (μM)	n _H	MRF	B/B _{WT}	n
WT	6.76 ± 0.01	0.2	3.7 ± 0.3	273 ± 16	1 ± 0.5	3
WT+	6.89 ± 0.04	0.13	2.5 ± 0.4	349 ± 35		3
L12D+	NF				0.01 ± 0.0	3
L13D+	NF				0.01 ± 0.0	3
L15D+	NF				0.0 ± 0.01	3
L19D+	NF				0.01 ± 0.0	3
L20D+ [†]	6.71 ± 0.02	0.2	5.4 ± 0.7	98 ± 2	0.0 ± 0.0	6

Data are mean ± SEM. NF = non-functional at concentrations up to 1 mM 5-HT. MRF is maximum recorded fluorescence, typical MRF for NF receptors was between 0 and 20. No pEC₅₀ or n_H values were significantly different from WT/WT+ and ≥5-fold change, p < 0.05, 2-way ANOVA. n=3x indicates 3 technical replicates of x biological replicates, n=4 indicates two biological replicates for the fluorescence assay data, for the radioligand binding n indicates biological replicates. [†]3 out of 7 biological replicates showed response to ligand, the remaining 4 showed no response to ligand addition.

I performed radioligand binding on all the non-functional aspartic acid mutants, and found that none bound ligand (Table 6.2). Strikingly, even the L20D mutant showed no radioligand binding, even though it had shown responses to ligand in the functional assay.

6.2.1.4 Characterisation of other 5-HT_{3A} receptors with mutations in and near the NTH

To complement the systematic alanine and leucine mutation schemes, I also performed some individual mutations driven by sequence analysis and functional roles (

Table 6.3). I predicted that D70 was a potential interaction partner for Y23 (Figure 6.1), so tested the effects of mutating each of these, as well as assessing the double mutant Y23D/D70Y. I also assayed the H18Y mutant receptor, as this is the only difference between the mouse and human NTH sequences.

Table 6.3: Parameters of 5-HT_{3A} receptors with selected NTH substitutions

Mutant	pEC ₅₀ (M)	EC ₅₀ (μM)	n _H	MRF	B/B _{WT}	n
WT	6.76 ± 0.01	0.2	3.7 ± 0.3	273 ± 16	1 ± 0.5	3
WT+	6.89 ± 0.04	0.13	2.5 ± 0.4	349 ± 35		3
Y23D+				0.0 ± 0.0		3
Y23F+	NF			0.01 ± 0.01		3
D70A+	NF			0.0 ± 0.0		3
D70Y+				0.0 ± 0.0		3
Y23D/D70Y+				0.02 ± 0.0		3
H18Y	6.18 ± 0.08	0.7	2.2 ± 0.7	195 ± 3		3

Data are mean ± SEM. + indicates coexpression with RIC-3, NF = non-functional at concentrations up to 1 mM 5-HT. MRF is maximum recorded fluorescence, typical MRF for NF receptors was between 0 and 20. No pEC₅₀ or n_H values were significantly different from WT/WT+ and ≥5-fold change, p < 0.05, 2-way ANOVA. . n=3x indicates 3 technical replicates of x biological replicates, n=4 indicates two biological replicates for the fluorescence assay data, for the radioligand binding n indicates biological replicates.

The Y23A mutant receptor only responded in the fluorescence assay when coexpressed with RIC-3, indicating that this mutation is detrimental to protein folding. Interestingly, Y23F was non-responsive even on coexpression with RIC-3. To further explore this I measured the

specific binding of Y23A (coexpressed with RIC-3), which gave a K_d of 0.63 ± 0.20 nM, and a B_{max} of 504 ± 50 fmol/mg, which is not significantly different ($p < 0.05$, 2-way ANOVA) to the WT receptor values of 0.28 ± 0.05 nM and 1911 ± 112 fmol/mg.

6.2.2 Characterisation of NTH mutant 5-HT_{3A}Rs in *Xenopus* oocytes

I assayed the two most interesting mutants, L20D and Y23F, by two-electrode voltage clamp in *Xenopus* oocytes (Figure 6.5). Two-electrode voltage clamp allows more precise determination of channel properties than the fluorescence assay used above, which would allow me to further probe the L20D mutant. Additionally, *Xenopus* oocytes are known to generally be more permissive to pLGIC expression than HEK cells – in part perhaps due to the oocytes being kept at 16°C, allowing slower and more accurate protein folding (Denning et al., 1992). This might allow expression, folding, assembly and export of mutant receptors that were lacking in one or more of these in HEK cells.

Y23F mutant receptors showed no detectable function in oocytes ($n=10$). L20D mutant receptors gave similar results in oocytes as they did in HEK cells: of 10 oocytes injected with L20D mRNA, four gave no response to ligand, and the remaining five gave small currents (almost 100-fold smaller than the WT, a larger change than the approximately threefold reduction in MRF seen in the fluorescence assay (Table 6.2)). However, analyzing the L20D data revealed otherwise WT-like receptor function. This indicates that the level of expression to the plasma membrane is drastically reduced by the L20D mutation, but no change in receptor function itself could be detected.

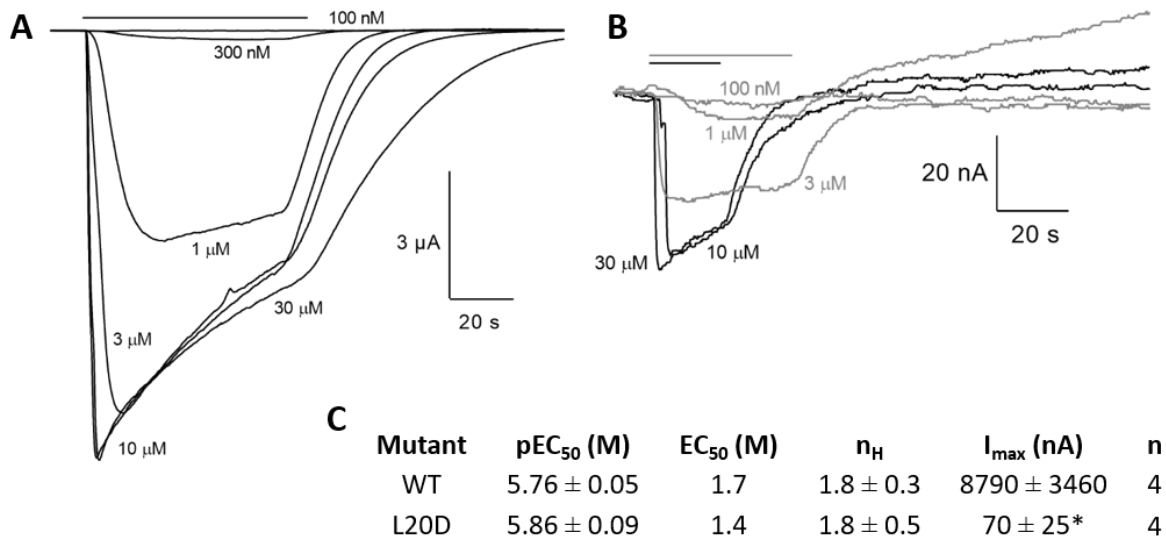


Figure 6.5: WT and mutant 5-HT_{3A}R responses in *Xenopus* oocytes. A, B) Current recordings on addition of ligand (as indicated by time bars) of A) WT and B) L20D mutant receptors. C) Characteristics of receptors (mean ± SEM) from data as in A and B.

*significantly different from WT, $p < 0.05$, 2-way ANOVA.

6.3 Discussion

The aim of this work was to characterise the role and function of the N-terminal helix in the 5-HT_{3A} receptor. I found, consistent with data from other pLGICs, that the NTH is crucial to correct receptor expression, folding, assembly and/or export. Furthermore, mutations here that did not affect receptor formation/export had little or no effect on receptor function, indicating that this is not a good site for receptor function modulation in the 5-HT_{3A}R.

6.3.1 N-terminal helix 5-HT_{3A} mutant receptors in HEK293 cells

Only three out of eleven alanine mutations measurably affected receptor function: one (Y23A) reduced detectable receptor levels, but this effect could be mitigated by coexpression with RIC-3. Two others (L15A and L19A) ablated receptor expression to the cell surface, and this effect could not be mitigated by coexpression with RIC-3. These latter two residues point

in towards the rest of the ECD from the NTH, and may be involved in hydrophobic interactions between the NTH and the ECD (Figure 6.1). Aspartic acid substitutions for the leucine residues of the NTH had more dramatic effects than the alanine mutations: four out of five of these (L12D, L13D, L15D, L19D) were non-functional in the functional assay, and the mutant receptors could not be detected by radioligand binding, even on co-expression with RIC-3 (Table 6.2). Altogether, this is consistent with previous work showing that mutations in pLGIC NTHs are detrimental to receptor expression, folding, assembly and/or export (Castillo et al., 2009).

Surprisingly, the only functional Leu-Asp mutant receptor (L20D) could not be detected in the radioligand binding assay. This might indicate that the fluorescent assay is more sensitive than the radioligand binding assay, and that the level of expression of the L20D receptor is sufficient for a response in the fluorescent assay but not for detection by radioligand binding. Even if the fluorescent assay is not in and of itself more sensitive than the radioligand binding assay, in the former the HEK cells can communicate with each other (as evidenced by electrophysiological recordings of HEK293 cells coupled to e.g. cardiomyocytes (McSpadden et al., 2012; Patel et al., 2014)). This could amplify the signal of receptors in one cell opening, which would add more sensitivity to the fluorescent assay. This helps explain the much larger difference in recorded I_{max} values between the WT and L20D receptors in oocytes (~100-fold) compared to the smaller (~3-fold) difference in maximum recorded fluorescence between the WT and L20D receptors in HEK cells as well.

This hypothesis is supported by the inconsistency of responses of the L20D receptor in the fluorescent assay: of seven biological replicates of the L20D receptor coexpressed with RIC-3 in the fluorescent assay (each of which had three technical repeats), three showed WT-like responses to ligand, and four showed no responses to ligand. To minimise variability between the assays, I performed the radioligand binding on cells harvested from the same transfection as ones that showed activity in the fluorescent assay, yet was still unable to detect the mutant receptors by radioligand binding. This might be indicating that the expression levels of the L20D mutant receptor are only just high enough to occasionally give responses in the fluorescent assay.

Finally, data on Y23 was consistent with previous work (Price and Lummis, 2004), showing that this residue is important for receptor expression. Interestingly, coexpression with RIC-3 could rescue Y23A expression but not Y23F expression, indicating that Y23 plays a very particular role in the receptor.

6.3.2 N-terminal helix 5-HT_{3A} mutant receptors in *Xenopus* oocytes

The responses of the mutant receptors in oocytes were consistent with their responses in HEK cells. The L20D mutant receptor showed extremely reduced I_{max} levels, indicating that expression/folding/assembly/export is much lower than of the WT receptor, as it was in HEK cells (though this has greater effect on measured I_{max} in oocytes than on the measured MRF in HEK cells, due to I_{max} being measured in single cells, and MRF across a communicating population of cells here). Likewise, the functional characteristics of the mutant receptor were otherwise WT-like (Figure 6.5). The Y23F receptor was non-functional here, consistent with its behaviour in HEK cells.

6.4 Conclusions

In this chapter I have shown that the N-terminal helix of the 5-HT_{3A} receptor is important for correct receptor expression, folding, assembly, and/or export, that mutations here to alanine can disrupt these aspects of receptor formation, and mutations of hydrophobic leucine residues to charged aspartic acid residues always disrupt receptor formation/export, and in most cases completely abolish it.

Chapter 7 Discussion

The aim of my PhD work was to explore the role in pLGICs of the outermost lipid-facing helix M4, and the peripheral N-terminal helix in the ECD. This work was done with the long-term view of aiming to better understand the mechanism of action of pLGICs.

In Chapters 3 and 4 I found that the M4 helix of the cation-selective 5-HT_{3A} and α4β2 nACh receptors is crucial to the function of these receptors when they are expressed in HEK293 cells. I also examined the mechanism of action of key M4 residues, particularly Y4.7 in the 5-HT_{3A} receptor. I found that Y4.7 likely interacts with D238 on the M1 helix, which in turn appears to be connected to K255 on the pore-lining M2 helix. In Chapter 5 I showed that the role of critical M4 residues in these receptors is strikingly different when they are expressed in *Xenopus* oocytes, where most of the M4 mutations either had no measurable effect or caused a slight increase in receptor sensitivity. Finally, I showed in Chapter 6 that the N-terminal helix of the 5-HT_{3A}R is crucial to receptor expression, folding, assembly and/or export.

7.1 Consequences

7.1.1 Determining the role of M4 in pLGICs

My work has shown that the M4 helix is crucial to cation-selective pLGIC function in HEK293 cells. This allows us to look further into the M4 as a potential site for modulating pLGIC activity in humans and animals. The M4 helix has several advantages over other mechanistically key parts of the receptor in this regard. Firstly, unlike helices further into the transmembrane domain, it is easily accessible, both at the C-terminal end which extends above the lipid bilayer, and to lipid soluble molecules within the lipid bilayer (as in e.g. Budelier et al. (2019); Tong et al. (2019)). Secondly, the M4 helix shows greater sequence diversity between pLGICs than highly conserved sites involved in pLGIC function like the

ligand binding site or channel pore, potentially allowing for higher subunit selectivity in small molecule binding. Even within cation-selective pLGICs the role of M4 varies, as evidenced by comparing the different effects of alanine mutations between the 5-HT_{3A} and α4β2 nACh receptors in HEK cells. Thirdly, while many of the M4 mutations studied here had large effects on receptor function, often ablating it, it is likely that smaller effects could be achieved by subtler alterations to the receptor, e.g. by drugs binding to the M4. This could achieve modulation of receptor function, which is in most cases more clinically useful than direct channel opening or channel blocking.

Beyond characterising the role of M4 as a whole, identifying the key residues in the M4 helices of the 5-HT_{3A} and α4β2 nACh receptors has allowed me to draw conclusions about the internal mechanisms of function of these receptors. In the 5-HT_{3A} receptor, I determined that the M4 helix is likely involved in receptor function through specific interactions with the M1 or M3 helix residues (depending on the particular subunit), and that this connection may reach in to the M2 helix, right below the main channel restriction. In the α4β2 nACh receptor, individual residues at eight positions across the length of the M4 helix proved to be crucial to receptor function in HEK cells. While I could not determine as much about the specific roles of each of these residues as I could about Y4.7 in the 5-HT_{3AR}, identifying the key residues has opened the path to understanding the function of the M4 helix in the α4β2 nAChR, and these data together with the 5-HT_{3A} M4 work together lay the groundwork for understanding the role and variations therein of M4 across different pLGICs.

7.1.2 Differences in pLGIC function between HEK cells and oocytes

The stark difference between the effects of M4 mutations on receptors expressed in HEK cells and receptors expressed in *Xenopus* oocytes was by far the most unexpected result in this work. While I did not have time to determine the exact cause of this difference between receptor function in HEK cells and oocytes, there is already much to be gained from the observation that there is a difference. This highlights the issue of choosing appropriate model systems for pLGIC (and any protein) expression. Beyond that, if the differences in function I observed between these systems are indeed due to differences in lipid composition of the plasma membrane between the two expression systems, it would open the door to a range of

questions about the lipid sensitivity of cation-selective pLGICs, with potential implications for drug targeting and receptor modulation *in vivo*.

7.2 Limitations and future work

A limitation of this work was my inability to determine whether non-responsive $\alpha 4\beta 2$ nACh mutant receptors were expressed to the cell surface, due to the radioligand used being membrane-permeable (unlike the radioligand used for assaying 5-HT₃AR expression, which was not). The next step I would propose here would be immunofluorescence, using an antibody to the $\alpha 4$ or $\beta 2$ subunit, or adding a tag to either subunit (the $\beta 2$ might be more appropriate as the post-M4 segment is longer here and should make a C-terminal tag very accessible) and using an antibody to that tag. This can distinguish between receptors at the plasma membrane and receptors inside the cell (as in e.g. Cooper and Millar (2002)).

Determining the cellular location of the non-responsive $\alpha 4\beta 2$ M4 mutant nACh receptors in HEK cells would be an important step in either cementing or refuting one of the main proposals of my thesis: that seven $\alpha 4\beta 2$ M4 mutant nACh receptors may be switched from active to inactive by changing their environment from oocytes to HEK cells.

Another limitation to this work is that I was unable to determine the exact causal element of the difference in activity between cation-selective M4 mutant receptors expressed in HEK cells and in oocytes. This is an important question opened up by my work, and the answers could have wide-ranging implications for our understanding of the human nervous system and our treatment of many neurological disorders. A range of experiments would be useful for answering this question: Firstly, a better understanding of the comparison between HEK cells and oocytes, and even the comparison of these to the native pLGIC environment, would give a better basis for asking this question than the current incomplete comparisons by different methods under different conditions of the composition of these environments (section 1.3.3). A top-down approach to determining the causal factor of the activation/inactivation I observed in some 5-HT₃AR and $\alpha 4\beta 2$ nAChR M4 mutants would be to assay the activity of these M4 mutants in a range of expression systems, both mammalian and non-mammalian, to determine whether there is a pattern to which environments are

permissive to their function and which are not. A bottom-up approach might start with increasing or decreasing the proportion of individual lipids in each expression system, to determine the effect of each of those changes, as in e.g. Li et al. (2016, 2019); Santiago et al. (2001).

If lipids or lipid composition do turn out to be as important to cation-selective pLGIC function as my work indicates they may be, then a host of experimental avenues will be opened up. Assessing the activity of various pLGICs (and mutants thereof) in purified lipid environments (e.g. as in DaCosta and Baenziger (2009); Hénault et al. (2019)) would allow determination of the roles and effects of specific lipid compositions on individual pLGICs. Using structural methods like native cryo-EM or native mass spectrometry, one could ask which lipids (if any) are natively bound to these pLGICs, and how strongly (Tong et al., 2019). This could be complemented with molecular dynamics simulations investigating the states of protein-lipid interactions over time. Across all of these avenues of inquiry, it would be fruitful to distinguish the effects of specific binding of lipids to pLGICs, from the effects of lipids acting through changing the bulk properties of the membrane, a question long discussed and with much contradictory evidence, well discussed in Levitan (2017).

Throughout the kinds of work discussed above, a running question must be how these effects vary between pLGIC families and specific subunits, and how that might be used to distinguish between specific pLGICs *in vivo*.

References

- Akbas, M. H., Kaufmann, C., Archdeacon, P., & Karlin, A. (1994). Identification of acetylcholine receptor channel-lining residues in the entire M2 segment of the α subunit. *Neuron*, 13(4), 919–927. [https://doi.org/10.1016/0896-6273\(94\)90257-7](https://doi.org/10.1016/0896-6273(94)90257-7)
- Akbas, M. H., Stauffer, D. A., Xu, M., & Karlin, A. (1992). Acetylcholine Receptor Channel Structure Probed in Cysteine-Substitution Mutants. *Science*, 258(5080), 307–310. <https://doi.org/10.1126/SCIENCE.1384130>
- Akk, G., Li, P., Bracamontes, J., Reichert, D. E., Covey, D. F., & Steinbach, J. H. (2008). Mutations of the GABA-A Receptor α 1 Subunit M1 Domain Reveal Unexpected Complexity for Modulation by Neuroactive Steroids. *Molecular Pharmacology*, 74(3), 614–627. <https://doi.org/10.1124/MOL.108.048520>
- Alcaino, C., Musgaard, M., Minguez, T., Mazzaferro, S., Faundez, M., Iturriaga-Vasquez, P., Biggin, P. C., & Bermudez, I. (2017). Role of the cys loop and transmembrane domain in the allosteric modulation of α 4 β 2 nicotinic acetylcholine receptors. *Journal of Biological Chemistry*, 292(2), 551–562. <https://doi.org/10.1074/jbc.M116.751206>
- Alexander, J. K., Sagher, D., Krivoshein, A. V., Criado, M., Jefford, G., & Green, W. N. (2010). *Ric-3 Promotes 7 Nicotinic Receptor Assembly and Trafficking through the ER Subcompartment of Dendrites*. <https://doi.org/10.1523/JNEUROSCI.6344-09.2010>
- Althoff, T., Hibbs, R. E., Banerjee, S., & Gouaux, E. (2014). X-ray structures of GluCl in apo states reveal a gating mechanism of Cys-loop receptors. *Nature* 2014 512:7514, 512(7514), 333–337. <https://doi.org/10.1038/nature13669>
- Baenziger, J. E., Hénault, C. M., Therien, J. P. D., & Sun, J. (2015). Nicotinic acetylcholine receptor-lipid interactions: Mechanistic insight and biological function. In *Biochimica et Biophysica Acta - Biomembranes* (Vol. 1848, Issue 9, pp. 1806–1817). <https://doi.org/10.1016/j.bbamem.2015.03.010>

- Baenziger, J. E., Morris, M. L., Darsaut, T. E., & Ryan, S. E. (2000). Effect of membrane lipid composition on the conformational equilibria of the nicotinic acetylcholine receptor. *Journal of Biological Chemistry*, 275(2), 777–784.
<https://doi.org/10.1074/jbc.275.2.777>
- Barman Balfour, J. A., Goa, K. L., & Perry, C. M. (2000). Alosetron. *Drugs*, 59(3), 511–518.
<https://doi.org/10.2165/00003495-200059030-00008>
- Barrantes, F. J. (2007). Cholesterol effects on nicotinic acetylcholine receptor. In *Journal of neurochemistry: Vol. 103 Suppl* (Issue s1, pp. 72–80). John Wiley & Sons, Ltd (10.1111). <https://doi.org/10.1111/j.1471-4159.2007.04719.x>
- Barrantes, F. J. (2015). Phylogenetic conservation of protein-lipid motifs in pentameric ligand-gated ion channels. *Biochimica et Biophysica Acta - Biomembranes*, 1848(9), 1796–1805. <https://doi.org/10.1016/j.bbamem.2015.03.028>
- Basak, S., Gicheru, Y., Rao, S., Sansom, M. S. P., & Chakrapani, S. (2018). Cryo-EM reveals two distinct serotonin-bound conformations of full-length 5-HT3A receptor. In *Nature* (Vol. 563, Issue 7730, pp. 270–274). Nature Publishing Group.
<https://doi.org/10.1038/s41586-018-0660-7>
- Basak, S., Gicheru, Y., Samanta, A., Molugu, S. K., Huang, W., Fuente, M. la de, Hughes, T., Taylor, D. J., Nieman, M. T., Moiseenkova-Bell, V., & Chakrapani, S. (2018). Cryo-EM structure of 5-HT3A receptor in its resting conformation. *Nature Communications*, 9(1), 514. <https://doi.org/10.1038/s41467-018-02997-4>
- Bhatnagar, S., Nowak, N., Babich, L., & Bok, L. (2004). Deletion of the 5-HT3 receptor differentially affects behavior of males and females in the Porsolt forced swim and defensive withdrawal tests. *Behavioural Brain Research*, 153(2), 527–535.
<https://doi.org/10.1016/J.BBR.2004.01.018>
- Bouzat, C., Barrantes, F., & Sine, S. (2000). Nicotinic receptor fourth transmembrane domain: Hydrogen bonding by conserved threonine contributes to channel gating kinetics. *Journal of General Physiology*, 115(5), 663–671.
<https://doi.org/10.1085/jgp.115.5.663>

- Budelier, M. M., Cheng, W. W. L., Chen, Z. W., Bracamontes, J. R., Sugasawa, Y., Krishnan, K., Mydock-McGrane, L., Covey, D. F., & Evers, A. S. (2019). Common binding sites for cholesterol and neurosteroids on a pentameric ligand-gated ion channel. *Biochimica et Biophysica Acta - Molecular and Cell Biology of Lipids*, 1864(2), 128–136. <https://doi.org/10.1016/j.bbalip.2018.11.005>
- Butler, A. S., Lindesay, S. A., Dover, T. J., Kennedy, M. D., Patchell, V. B., Levine, B. A., Hope, A. G., & Barnes, N. M. (2009). Importance of the C-terminus of the human 5-HT3A receptor subunit. *Neuropharmacology*, 56(1), 292–302. <https://doi.org/10.1016/j.neuropharm.2008.08.017>
- Cahill, K., Lindson-Hawley, N., Thomas, K. H., Fanshawe, T. R., & Lancaster, T. (2016). Nicotine receptor partial agonists for smoking cessation. *The Cochrane Database of Systematic Reviews*, 2016(5). <https://doi.org/10.1002/14651858.CD006103.PUB7>
- Carswell, C. L., Hénault, C. M., Murlidaran, S., Therien, J. P. D., Juranka, P. F., Surujballi, J. A., Brannigan, G., & Baenziger, J. E. (2015). Role of the Fourth Transmembrane α Helix in the Allosteric Modulation of Pentameric Ligand-Gated Ion Channels. *Structure*, 23(9), 1655–1664. <https://doi.org/10.1016/j.str.2015.06.020>
- Carswell, C. L., Sun, J., & Baenziger, J. E. (2015). Intramembrane aromatic interactions influence the lipid sensitivities of pentameric ligand-gated ion channels. *Journal of Biological Chemistry*, 290(4), 2496–2507. <https://doi.org/10.1074/jbc.M114.624395>
- Castillo, M., Mulet, J., Aldea, M., Gerber, S., Sala, S., Sala, F., & Criado, M. (2009). Role of the N-terminal alpha-helix in biogenesis of alpha7 nicotinic receptors. *Journal of Neurochemistry*, 108(6), 1399–1409. <https://doi.org/10.1111/j.1471-4159.2009.05924.x>
- Castillo, M., Mulet, J., Gutié Rrez, L. M., Ortiz, J. A., Castelá, F., Gerber, S., Sala, S., Sala, F., & Criado, M. (2005). Dual Role of the RIC-3 Protein in Trafficking of Serotonin and Nicotinic Acetylcholine Receptors*. *Journal of Biological Chemistry*, 280, 27062–27068. <https://doi.org/10.1074/jbc.M503746200>
- Changeux, J. P., & Edelstein, S. J. (2001). Allosteric mechanisms in normal and pathological nicotinic acetylcholine receptors. *Current Opinion in Neurobiology*, 11(3), 369–377.

[https://doi.org/10.1016/S0959-4388\(00\)00221-X](https://doi.org/10.1016/S0959-4388(00)00221-X)

Chen, X., Webb, T. I., & Lynch, J. W. (2009). The M4 transmembrane segment contributes to agonist efficacy differences between α 1 and α 3 glycine receptors. *Molecular Membrane Biology*, 26(5–7), 321–332. <https://doi.org/10.1080/09687680903120319>

Cheng, A., McDonald, N. A., & Connolly, C. N. (2005a). Cell surface expression of 5-hydroxytryptamine type 3 receptors is promoted by RIC-3. *The Journal of Biological Chemistry*, 280(23), 22502–22507. <https://doi.org/10.1074/jbc.M414341200>

Cheng, A., McDonald, N. A., & Connolly, C. N. (2005b). Cell surface expression of 5-hydroxytryptamine type 3 receptors is promoted by RIC-3. *Journal of Biological Chemistry*, 280(23), 22502–22507. <https://doi.org/10.1074/jbc.M414341200>

Cheng, W. W. L., Chen, Z. W., Bracamontes, J. R., Budelier, M. M., Krishnan, K., Shin, D. J., Wang, C., Jiang, X., Covey, D. F., Akk, G., & Evers, A. S. (2018). Mapping two neurosteroid-modulatory sites in the prototypic pentameric ligand-gated ion channel GLIC. *Journal of Biological Chemistry*, 293(8), 3013–3027.
<https://doi.org/10.1074/jbc.RA117.000359>

Coe, J. W., Brooks, P. R., Vetelino, M. G., Wirtz, M. C., Arnold, E. P., Huang, J., Sands, S. B., Davis, T. I., Lebel, L. A., Fox, C. B., Shrikhande, A., Heym, J. H., Schaeffer, E., Rollema, H., Lu, Y., Mansbach, R. S., Chambers, L. K., Rovetti, C. C., Schulz, D. W., ... O'Neill, B. T. (2005). Varenicline: An $\alpha_4\beta_2$ nicotinic receptor partial agonist for smoking cessation. *Journal of Medicinal Chemistry*, 48(10), 3474–3477.
https://doi.org/10.1021/JM050069N/SUPPL_FILE/JM050069NSI20050419_042121.PDF

Colman, A., Bhamra, S., & Valle, G. (1984). Post-translational modification of exogenous proteins in *Xenopus laevis* oocytes. *Biochemical Society Transactions*, 12(6), 932–937.
<https://doi.org/10.1042/BST0120932>

Colombo, S. F., Mazzo, F., Pistillo, F., & Gotti, C. (2013). Biogenesis, trafficking and up-regulation of nicotinic ACh receptors. *Biochemical Pharmacology*, 86(8), 1063–1073.
<https://doi.org/10.1016/J.BCP.2013.06.023>

- Connolly, C. N. (2009). Trafficking of 5-HT3 and GABAA receptors (Review).
Http://Dx.Doi.Org/10.1080/09687680801898503, 25(4), 293–301.
<https://doi.org/10.1080/09687680801898503>
- Cooper, S. T., & Millar, N. S. (2002). Host Cell-Specific Folding and Assembly of the Neuronal Nicotinic Acetylcholine Receptor $\alpha 7$ Subunit. *Journal of Neurochemistry*, 68(5), 2140–2151. <https://doi.org/10.1046/j.1471-4159.1997.68052140.x>
- Cordero-Erausquin, M., Marubio, L. M., Klink, R., & Changeux, J. P. (2000). Nicotinic receptor function: new perspectives from knockout mice. *Trends in Pharmacological Sciences*, 21(6), 211–217. [https://doi.org/10.1016/S0165-6147\(00\)01489-9](https://doi.org/10.1016/S0165-6147(00)01489-9)
- Corringer, P. J., Bertrand, S., Galzi, J. L., Devillers-Thiéry, A., Changeux, J. P., & Bertrand, D. (1999). Mutational analysis of the charge selectivity filter of the $\alpha 7$ nicotinic acetylcholine receptor. *Neuron*, 22(4), 831–843. [https://doi.org/10.1016/S0896-6273\(00\)80741-2](https://doi.org/10.1016/S0896-6273(00)80741-2)
- Cory-Wright, J., Alqazzaz, M., Wroe, F., Jeffreys, J., Zhou, L., & Lummis, S. C. R. (2017). Aromatic Residues in the Fourth Transmembrane-Spanning Helix M4 Are Important for GABA ρ Receptor Function. *ACS Chemical Neuroscience*, acschemneuro.7b00315. <https://doi.org/10.1021/acschemneuro.7b00315>
- Crnjar, A., Mesoy, S., Lummis, S. C. R., & Molteni, C. (2021). A Single Mutation in the Outer Lipid-Facing Helix of a Pentameric Ligand-Gated Ion Channel Affects Channel Function Through a Radially-Propagating Mechanism. *Frontiers in Molecular Biosciences*, 8, 644720. <https://doi.org/10.3389/fmolb.2021.644720>
- Cunningham, B. C., & Wells, J. A. (1989). High-resolution epitope mapping of hGH-receptor interactions by alanine-scanning mutagenesis. *Science*, 244(4908), 1081–1085. <https://doi.org/10.1126/science.2471267>
- da Costa Couto, A. R. G. M., Price, K. L., Mesoy, S., Capes, E., & Lummis, S. C. R. (2020). The M4 Helix Is Involved in $\alpha 7$ nACh Receptor Function. *ACS Chemical Neuroscience*, acschemneuro.0c00027. <https://doi.org/10.1021/acschemneuro.0c00027>

DaCosta, C. J. B., & Baenziger, J. E. (2009). A lipid-dependent uncoupled conformation of the acetylcholine receptor. *Journal of Biological Chemistry*, 284(26), 17819–17825.

<https://doi.org/10.1074/jbc.M900030200>

Dacosta, C. J. B., Dey, L., Therien, J. P. D., & Baenziger, J. E. (2013). A distinct mechanism for activating uncoupled nicotinic acetylcholine receptors. *Nature Chemical Biology*, 9(11), 701–707. <https://doi.org/10.1038/nchembio.1338>

DaCosta, C. J. B., Medaglia, S. A., Lavigne, N., Wang, S., Carswell, C. L., & Baenzinger, J. E. (2009). Anionic lipids allosterically modulate multiple nicotinic acetylcholine receptor conformational equilibria. *Journal of Biological Chemistry*, 284(49), 33841–33849. <https://doi.org/10.1074/jbc.M109.048280>

Dämgen, M. A., & Biggin, P. C. (2021). State-dependent protein-lipid interactions of a pentameric ligand-gated ion channel in a neuronal membrane. *PLoS Computational Biology*, 17(2), e1007856. <https://doi.org/10.1371/JOURNAL.PCBI.1007856>

Dau, A., Komal, P., Truong, M., Morris, G., Evans, G., & Nashmi, R. (2013). RIC-3 differentially modulates $\alpha 4\beta 2$ and $\alpha 7$ nicotinic receptor assembly, expression, and nicotine-induced receptor upregulation. *BMC Neuroscience*, 14, 47. <https://doi.org/10.1186/1471-2202-14-47>

Davies, P. A., Pistis, M., Hanna, M. C., Peters, J. A., Lambert, J. J., Hales, T. G., & Kirkness, E. F. (1999). The 5-HT3B subunit is a major determinant of serotonin-receptor function. *Nature* 1999 397:6717, 397(6717), 359–363. <https://doi.org/10.1038/16941>

Dawaliby, R., Trubbia, C., Delporte, C., Noyon, C., Ruysschaert, J. M., Van Antwerpen, P., & Govaerts, C. (2016). Phosphatidylethanolamine is a key regulator of membrane fluidity in eukaryotic cells. *Journal of Biological Chemistry*, 291(7), 3658–3667. <https://doi.org/10.1074/jbc.M115.706523>

Dawes, M. A., Johnson, B. A., Ma, J. Z., Ait-Daoud, N., Thomas, S. E., & Cornelius, J. R. (2005). Reductions in and relations between “craving” and drinking in a prospective, open-label trial of ondansetron in adolescents with alcohol dependence. *Addictive Behaviors*, 30(9), 1630–1637. <https://doi.org/10.1016/J.ADDBEH.2005.07.004>

- Denning, G. M., Anderson, M. P., Amara, J. F., Marshall, J., Smith, A. E., & Welsh, M. J. (1992). Processing of mutant cystic fibrosis transmembrane conductance regulator is temperature-sensitive. *Nature* 1992 358:6389, 358(6389), 761–764.
<https://doi.org/10.1038/358761a0>
- Dineley, K. T., & Patrick, J. W. (2000). Amino Acid Determinants of $\alpha 7$ Nicotinic Acetylcholine Receptor Surface Expression. *Journal of Biological Chemistry*, 275(18), 13974–13985. <https://doi.org/10.1074/JBC.275.18.13974>
- Domville, J. A., & Baenziger, J. E. (2018). An allosteric link connecting the lipid-protein interface to the gating of the nicotinic acetylcholine receptor. *Scientific Reports*, 8(1), 3898. <https://doi.org/10.1038/s41598-018-22150-x>
- Dougherty, D. A. (2000). Unnatural amino acids as probes of protein structure and function. *Current Opinion in Chemical Biology*, 4(6), 645–652. [https://doi.org/10.1016/S1367-5931\(00\)00148-4](https://doi.org/10.1016/S1367-5931(00)00148-4)
- Eitner, K., Koch, U., Gaw, T., Eda, , & Edrzej Marciniak, J. . (2010). Statistical distribution of amino acid sequences: a proof of Darwinian evolution. *BIOINFORMATICS DISCOVERY NOTE*, 26(23), 2933–2935. <https://doi.org/10.1093/bioinformatics/btq571>
- Estrada-Mondragón, A., Reyes-Ruiz, J. M., Martínez-Torres, A., & Miledi, R. (2010). Structure-function study of the fourth transmembrane segment of the GABA $\rho 1$ receptor. *Proceedings of the National Academy of Sciences*, 107(41), 17780–17784.
<https://doi.org/10.1073/pnas.1012540107>
- Faerber, L., Drechsler, S., Ladenburger, S., Gschaidmeier, H., & Fischer, W. (2007). The neuronal 5-HT3 receptor network after 20 years of research - Evolving concepts in management of pain and inflammation. *European Journal of Pharmacology*, 560(1), 1–8. <https://doi.org/10.1016/J.EJPHAR.2007.01.028>
- Fakhfouri, G., Rahimian, R., Dyhrfjeld-Johnsen, J., Zirak, M. R., & Beaulieu, J. M. (2019). 5-HT3 receptor antagonists in neurologic and neuropsychiatric disorders: The iceberg still lies beneath the surface. *Pharmacological Reviews*, 71(3), 383–412.
<https://doi.org/10.1124/pr.118.015487>

- Faris, P. L., Eckert, E. D., Kim, S. W., Meller, W. H., Pardo, J. V., Goodale, R. L., & Hartman, B. K. (2006). Evidence for a vagal pathophysiology for bulimia nervosa and the accompanying depressive symptoms. *Journal of Affective Disorders*, 92(1), 79–90. <https://doi.org/10.1016/J.JAD.2005.12.047>
- Fiebich, B. L., Akundi, R. S., Seidel, M., Geyer, V., Haus, U., Müller, W., Stratz, T., & Candelario-Jalil, E. (2004). Expression of 5-HT3A receptors in cells of the immune system. *Scandinavian Journal of Rheumatology, Supplement*, 33(119), 9–11. <https://doi.org/10.1080/03009740410006952>
- Fitch, R. W., Xiao, Y., Kellar, K. J., & Daly, J. W. (2003). Membrane potential fluorescence: A rapid and highly sensitive assay for nicotinic receptor channel function. *Proceedings of the National Academy of Sciences of the United States of America*, 100(8), 4909–4914. <https://doi.org/10.1073/pnas.0630641100>
- Fonck, C., Cohen, B. N., Nashmi, R., Whiteaker, P., Wagenaar, D. A., Rodrigues-Pinguet, N., Deshpande, P., McKinney, S., Kwoh, S., Munoz, J., Labarca, C., Collins, A. C., Marks, M. J., & Lester, H. A. (2005). Novel seizure phenotype and sleep disruptions in knock-in mice with hypersensitive $\alpha 4^*$ nicotinic receptors. *Journal of Neuroscience*, 25(49), 11396–11411. <https://doi.org/10.1523/JNEUROSCI.3597-05.2005>
- Fong, T. M., & McNamee, M. G. (1986). Correlation between Acetylcholine Receptor Function and Structural Properties of Membranes. *Biochemistry*, 25(4), 830–840. <https://doi.org/10.1021/bi00352a015>
- Frank, B., Niesler, B., Nöthen, M. M., Neidt, H., Propping, P., Bondy, B., Rietschel, M., Maier, W., Albus, M., & Rappold, G. (2004). Investigation of the human serotonin receptor gene HTR3B in bipolar affective and schizophrenic patients. *American Journal of Medical Genetics Part B: Neuropsychiatric Genetics*, 131B(1), 1–5. <https://doi.org/10.1002/AJMG.B.30070>
- Fryer, J. D., & Lukas, R. J. (1999). Antidepressants Noncompetitively Inhibit Nicotinic Acetylcholine Receptor Function. *Journal of Neurochemistry*, 72(3), 1117–1124. <https://doi.org/10.1046/J.1471-4159.1999.0721117.X>

- García-Colunga, J., Awad, J. N., & Miledi, R. (1997). Blockage of muscle and neuronal nicotinic acetylcholine receptors by fluoxetine (Prozac). *Proceedings of the National Academy of Sciences of the United States of America*, 94(5), 2041. <https://doi.org/10.1073/PNAS.94.5.2041>
- Gee, V. J., Kracun, S., Cooper, S. T., Gibb, A. J., & Millar, N. S. (2007). Identification of domains influencing assembly and ion channel properties in a₇ nicotinic receptor and 5-HT 3 receptor subunit chimaeras. *British Journal of Pharmacology*, 152, 501–512. <https://doi.org/10.1038/sj.bjp.0707429>
- Gelman, M. S., & Prives, J. M. (1996). Arrest of Subunit Folding and Assembly of Nicotinic Acetylcholine Receptors in Cultured Muscle Cells by Dithiothreitol. *Journal of Biological Chemistry*, 271(18), 10709–10714. <https://doi.org/10.1074/JBC.271.18.10709>
- Graham, F. L., Smiley, J., Russell, W. C., & Nairn, R. (1977). Characteristics of a human cell line transformed by DNA from human adenovirus type 5. *Journal of General Virology*, 36(1), 59–72. <https://doi.org/10.1099/0022-1317-36-1-59/CITE/REFWORKS>
- Gu, S., Matta, J. A., Lord, B., Harrington, A. W., Sutton, S. W., Davini, W. B., & Bredt, D. S. (2016). Brain α₇ Nicotinic Acetylcholine Receptor Assembly Requires NACHO. *Neuron*, 89(5), 948–955. <https://doi.org/10.1016/J.NEURON.2016.01.018>
- Gunthorpe, M. J., Peters, J. A., Gill, C. H., Lambert, J. J., & Lummis, S. C. R. (2000). The 4'lysine in the putative channel lining domain affects desensitization but not the single-channel conductance of recombinant homomeric 5-MT(3A) receptors. *Journal of Physiology*, 522(2), 187–198. <https://doi.org/10.1111/j.1469-7793.2000.00187.x>
- Guo, T., Yang, C., Guo, L., & Liu, K. (2012). A comparative study of the effects of ABT-418 and methylphenidate on spatial memory in an animal model of ADHD. *Neuroscience Letters*, 528(1), 11–15. <https://doi.org/10.1016/J.NEULET.2012.08.068>
- Guros, N. B., Balijepalli, A., & Klauda, J. B. (2020). Microsecond-timescale simulations suggest 5-HT-mediated preactivation of the 5-HT3A serotonin receptor. *Proceedings of the National Academy of Sciences of the United States of America*, 117(1), 405–414.

<https://doi.org/10.1073/pnas.1908848117>

Haeger, S., Kuzmin, D., Detro-Dassen, S., Lang, N., Kilb, M., Tsetlin, V., Betz, H., Laube, B., & Schmalzing, G. (2010). An intramembrane aromatic network determines pentameric assembly of Cys-loop receptors. *Nature Structural and Molecular Biology*, 17(1), 90–99. <https://doi.org/10.1038/nsmb.1721>

Halevi, S., McKay, J., Palfreyman, M., Yassin, L., Eshel, M., Jorgensen, E., & Treinin, M. (2002). The C.elegans ric-3 gene is required for maturation of nicotinic acetylcholine receptors. *The EMBO Journal*, 21(5), 1012–1020.
<https://doi.org/10.1093/EMBOJ/21.5.1012>

Halevi, S., Yassin, L., Eshel, M., Sala, F., Sala, S., Criado, M., & Treinin, M. (2003). Conservation within the RIC-3 Gene Family: EFFECTORS OF MAMMALIAN NICOTINIC ACETYLCHOLINE RECEPTOR EXPRESSION. *Journal of Biological Chemistry*, 278(36), 34411–34417. <https://doi.org/10.1074/JBC.M300170200>

Hammer, V. A., Gietzen, D. W., Beverly, J. L., & Rogers, Q. R. (1990). Serotonin3 receptor antagonists block anorectic responses to amino acid imbalance.
Https://Doi.Org/10.1152/Ajpregu.1990.259.3.R627, 259(3 28-3).
<https://doi.org/10.1152/AJPREGU.1990.259.3.R627>

Hamouda, A. K., Chiara, D. C., Sauls, D., Cohen, J. B., & Blanton, M. P. (2005). Cholesterol Interacts with Transmembrane α -Helices M1, M3, and M4 of the Torpedo Nicotinic Acetylcholine Receptor: Photolabeling Studies Using [3 H]Azicholesterol†. *Biochemistry*, 45(3), 976–986. <https://doi.org/10.1021/BI051978H>

Han, L., Talwar, S., & Lynch, J. W. (2013). The Relative Orientation of the TM3 and TM4 Domains Varies between α 1 and α 3 Glycine Receptors. *ACS Chemical Neuroscience*, 4(2), 248–254. <https://doi.org/10.1021/cn300177g>

Harkness, P. C., & Millar, N. S. (2001). Inefficient cell-surface expression of hybrid complexes formed by the co-assembly of neuronal nicotinic acetylcholine receptor and serotonin receptor subunits. *Neuropharmacology*, 41(1), 79–87.
[https://doi.org/10.1016/S0028-3908\(01\)00042-9](https://doi.org/10.1016/S0028-3908(01)00042-9)

- Harkness, P. C., & Millar, N. S. (2002). Changes in Conformation and Subcellular Distribution of $\alpha 4\beta 2$ Nicotinic Acetylcholine Receptors Revealed by Chronic Nicotine Treatment and Expression of Subunit Chimeras. *Journal of Neuroscience*, 22(23), 10172–10181. <https://doi.org/10.1523/JNEUROSCI.22-23-10172.2002>
- Held, J. M. (2020). Redox Systems Biology: Harnessing the Sentinels of the Cysteine Redoxome. In *Antioxidants and Redox Signaling* (Vol. 32, Issue 10, pp. 659–676). <https://doi.org/10.1089/ars.2019.7725>
- Hénault, C. M., Govaerts, C., Spurny, R., Brams, M., Estrada-Mondragon, A., Lynch, J., Bertrand, D., Pardon, E., Evans, G. L., Woods, K., Elberson, B. W., Cuello, L. G., Brannigan, G., Nury, H., Steyaert, J., Baenziger, J. E., & Ulens, C. (2019). A lipid site shapes the agonist response of a pentameric ligand-gated ion channel. *Nature Chemical Biology*. <https://doi.org/10.1038/s41589-019-0369-4>
- Hénault, C. M., Juranka, P. F., & Baenziger, J. E. (2015). The M4 transmembrane α -helix contributes differently to both the maturation and function of two prokaryotic pentameric ligand-gated ion channels. *Journal of Biological Chemistry*, 290(41), 25118–25128. <https://doi.org/10.1074/jbc.M115.676833>
- Hénault, C. M., Sun, J., Therien, J. P. D., DaCosta, C. J. B., Carswell, C. L., Labriola, J. M., Juranka, P. F., & Baenziger, J. E. (2015). The role of the M4 lipid-sensor in the folding, trafficking, and allosteric modulation of nicotinic acetylcholine receptors. *Neuropharmacology*, 96(PB), 157–168. <https://doi.org/10.1016/j.neuropharm.2014.11.011>
- Hennings, E. C. P., Kiss, J. P., De Oliveira, K., Toth, P. T., & Vizi, E. S. (1999). Nicotinic Acetylcholine Receptor Antagonistic Activity of Monoamine Uptake Blockers in Rat Hippocampal Slices. *Journal of Neurochemistry*, 73(3), 1043–1050. <https://doi.org/10.1046/J.1471-4159.1999.0731043.X>
- Hibbs, R. E., & Gouaux, E. (2011). Principles of activation and permeation in an anion-selective Cys-loop receptor. *Nature*, 474(7349), 54–60. <https://doi.org/10.1038/nature10139>

- Holbrook, J. D., Gill, C. H., Zebda, N., Spencer, J. P., Leyland, R., Rance, K. H., Trinh, H., Balmer, G., Kelly, F. M., Yusaf, S. P., Courtenay, N., Luck, J., Rhodes, A., Modha, S., Moore, S. E., Sanger, G. J., & Gunthorpe, M. J. (2009). Characterisation of 5-HT3C, 5-HT3D and 5-HT 3E receptor subunits: Evolution, distribution and function. *Journal of Neurochemistry*, 108(2), 384–396. <https://doi.org/10.1111/j.1471-4159.2008.05775.x>
- Huang, X., Shaffer, P. L., Ayube, S., Bregman, H., Chen, H., Lehto, S. G., Luther, J. A., Matson, D. J., McDonough, S. I., Michelsen, K., Plant, M. H., Schneider, S., Simard, J. R., Teffera, Y., Yi, S., Zhang, M., Dimauro, E. F., & Gingras, J. (2017). Crystal structures of human glycine receptor α 3 bound to a novel class of analgesic potentiators. *Nature Structural and Molecular Biology*, 24(2), 108–113. <https://doi.org/10.1038/nsmb.3329>
- Ilegems, E., Pick, H. M., Deluz, C., Kellenberger, S., & Vogel, H. (2004). Noninvasive imaging of 5-HT3 receptor trafficking in live cells: From biosynthesis to endocytosis. *Journal of Biological Chemistry*, 279(51), 53346–53352. <https://doi.org/10.1074/jbc.M407467200>
- Ilegems, E., Pick, H. M., Dric Deluz, C., Kellenberger, S., & Vogel, H. (2004). *Noninvasive Imaging of 5-HT 3 Receptor Trafficking in Live Cells FROM BIOSYNTHESIS TO ENDOCYTOSIS** S. <https://doi.org/10.1074/jbc.M407467200>
- Imoto, K., Busch, C., Sakmann, B., Mishina, M., Konno, T., Nakai, J., Bujo, H., Mori, Y., Fukuda, K., & Numa, S. (1988). Rings of negatively charged amino acids determine the acetylcholine receptor channel conductance. *Nature*, 335(6191), 645–648. <https://doi.org/10.1038/335645a0>
- Jeanclos, E. M., Lin, L., Treuil, M. W., Rao, J., DeCoster, M. A., & Anand, R. (2001). The Chaperone Protein 14-3-3 η Interacts with the Nicotinic Acetylcholine Receptor α 4 Subunit: EVIDENCE FOR A DYNAMIC ROLE IN SUBUNIT STABILIZATION. *Journal of Biological Chemistry*, 276(30), 28281–28290. <https://doi.org/10.1074/JBC.M011549200>
- Jenkins, A., Andreasen, A., Trudell, J. R., & Harrison, N. L. (2002). Tryptophan scanning

- mutagenesis in TM4 of the GABA_A receptor $\alpha 1$ subunit: Implications for modulation by inhaled anesthetics and ion channel structure. *Neuropharmacology*, 43(4), 669–678.
[https://doi.org/10.1016/S0028-3908\(02\)00175-2](https://doi.org/10.1016/S0028-3908(02)00175-2)
- Jiang, J. C., & Gietzen, D. W. (1994). Anorectic response to amino acid imbalance: A selective serotonin3 effect? *Pharmacology, Biochemistry and Behavior*, 47(1), 59–63.
[https://doi.org/10.1016/0091-3057\(94\)90111-2](https://doi.org/10.1016/0091-3057(94)90111-2)
- Jumper, J., Evans, R., Pritzel, A., Green, T., Figurnov, M., Ronneberger, O., Tunyasuvunakool, K., Bates, R., Žídek, A., Potapenko, A., Bridgland, A., Meyer, C., Kohl, S. A. A., Ballard, A. J., Cowie, A., Romera-Paredes, B., Nikolov, S., Jain, R., Adler, J., ... Hassabis, D. (2021). Highly accurate protein structure prediction with AlphaFold. *Nature* 2021 596:7873, 596(7873), 583–589.
<https://doi.org/10.1038/s41586-021-03819-2>
- Kapoor, R., Peyear, T. A., Koeppe, R. E., & Andersen, O. S. (2019). Antidepressants are modifiers of lipid bilayer properties. *Journal of General Physiology*, 151(3), 342–356.
<https://doi.org/10.1085/jgp.201812263>
- Kelley, S. P., Bratt, A. M., & Hodge, C. W. (2003). Targeted gene deletion of the 5-HT3A receptor subunit produces an anxiolytic phenotype in mice. *European Journal of Pharmacology*, 461(1), 19–25. [https://doi.org/10.1016/S0014-2999\(02\)02960-6](https://doi.org/10.1016/S0014-2999(02)02960-6)
- Kelley, S. P., Dunlop, J. I., Kirkness, E. F., Lambert, J. J., & Peters, J. A. (2003). A cytoplasmic region determines single-channel conductance in 5-HT3 receptors. *Nature*, 424(6946), 321–324. <https://doi.org/10.1038/nature01788>
- Kracun, S., Harkness, P. C., Gibb, A. J., & Millar, N. S. (2008). Influence of the M3–M4 intracellular domain upon nicotinic acetylcholine receptor assembly, targeting and function. *British Journal of Pharmacology*, 153(7), 1474.
<https://doi.org/10.1038/SJ.BJP.0707676>
- Krzywkowski, K., Davies, P. A., Feinberg-Zadek, P. L., Bräuner-Osborne, H., & Jensen, A. A. (2008). High-frequency HTR3B variant associated with major depression dramatically augments the signaling of the human 5-HT3AB receptor. *Proceedings of*

the National Academy of Sciences of the United States of America, 105(2), 722.
<https://doi.org/10.1073/PNAS.0708454105>

Kuryatov, A., Mukherjee, J., & Lindstrom, J. (2013). Chemical Chaperones Exceed the Chaperone Effects of RIC-3 in Promoting Assembly of Functional $\alpha\beta\gamma\delta$ AChRs. *PLoS ONE*, 8(4), e62246. <https://doi.org/10.1371/journal.pone.0062246>

Kweon, H. J., Gu, S., Witham, E., Dhara, M., Yu, H., Mandon, E. D., Jawhari, A., & Bredt, D. S. (2020). NACHO Engages N-Glycosylation ER Chaperone Pathways for $\alpha 7$ Nicotinic Receptor Assembly. *Cell Reports*, 32(6), 108025.
<https://doi.org/10.1016/J.CELREP.2020.108025>

Labriola, J. M., Pandhare, A., Jansen, M., Blanton, M. P., Corringer, P. J., & Baenziger, J. E. (2013). Structural sensitivity of a prokaryotic pentameric ligand-gated ion channel to its membrane environment. *Journal of Biological Chemistry*, 288(16), 11294–11303.
<https://doi.org/10.1074/jbc.M113.458133>

Lansdell, S. J., Collins, T., Yabe, A., Gee, V. J., Gibb, A. J., & Millar, N. S. (2008). Host-cell specific effects of the nicotinic acetylcholine receptor chaperone RIC-3 revealed by a comparison of human and Drosophila RIC-3 homologues. *Journal of Neurochemistry*, 105(5), 1573–1581. <https://doi.org/10.1111/J.1471-4159.2008.05235.X>

Lansdell, S. J., Gee, V. J., Harkness, P. C., Doward, A. I., Baker, E. R., Gibb, A. J., & Millar, N. S. (2005). RIC-3 enhances functional expression of multiple nicotinic acetylcholine receptor subtypes in mammalian cells. *Molecular Pharmacology*, 68(5), 1431–1438.
<https://doi.org/10.1124/mol.105.017459>

Lasalde, J. A., Tamamizu, S., Butler, D. H., Vibat, C. R. T., Hung, B., & McNamee, M. G. (1996). Tryptophan substitutions at the lipid-exposed transmembrane segment M4 of *Torpedo californica* acetylcholine receptor govern channel gating. *Biochemistry*, 35(45), 14139–14148. <https://doi.org/10.1021/bi9615831>

Laverty, D., Desai, R., Uchański, T., Masiulis, S., Stec, W. J., Malinauskas, T., Zivanov, J., Pardon, E., Steyaert, J., Miller, K. W., & Aricescu, A. R. (2019). Cryo-EM structure of the human $\alpha 1\beta 3\gamma 2$ GABAA receptor in a lipid bilayer. *Nature*, 565(7740), 516–520.

- <https://doi.org/10.1038/s41586-018-0833-4>
- Lee, Y. H., Li, L., Lasalde, J., Rojas, L., McNamee, M., Ortiz-Miranda, S. I., & Pappone, P. (1994). Mutations in the M4 domain of *Torpedo californica* acetylcholine receptor dramatically alter ion channel function. *Biophysical Journal*, 66(3), 646–653.
[https://doi.org/10.1016/S0006-3495\(94\)80838-0](https://doi.org/10.1016/S0006-3495(94)80838-0)
- Levitan, I. (2017). *Sterol regulation of ion channels*. Current Topics in Membranes. <https://www.sciencedirect.com/bookseries/current-topics-in-membranes/vol/80/suppl/C>
- Li, G., Kakuda, S., Suresh, P., Canals, D., Salamone, S., & London, E. (2019). Replacing plasma membrane outer leaflet lipids with exogenous lipid without damaging membrane integrity. *PLoS ONE*, 14(10), 1–22. <https://doi.org/10.1371/journal.pone.0223572>
- Li, G., Kim, J., Huang, Z., Clair, J. R. St., Brown, D. A., & London, E. (2016). Efficient replacement of plasma membrane outer leaflet phospholipids and sphingolipids in cells with exogenous lipids. *Proceedings of the National Academy of Sciences*, 113(49), 14025–14030. <https://doi.org/10.1073/PNAS.1610705113>
- Li, L., Lee, Y. H., Pappone, P., Palma, A., & McNamee, M. G. (1992). Site-specific mutations of nicotinic acetylcholine receptor at the lipid-protein interface dramatically alter ion channel gating. *Biophysical Journal*, 62(1), 61–63.
[https://doi.org/10.1016/S0006-3495\(92\)81779-4](https://doi.org/10.1016/S0006-3495(92)81779-4)
- Lin-Moshier, Y., & Marchant, J. S. (2013). The Xenopus Oocyte: A Single-Cell Model for Studying Ca²⁺ Signaling. *Cold Spring Harbor Protocols*, 2013(3), 185–191.
<https://doi.org/10.1101/PDB.TOP066308>
- Lo, W. Y., Botzolakis, E. J., Tang, X., & Macdonald, R. L. (2008). A conserved Cys-loop receptor aspartate residue in the M3-M4 cytoplasmic loop is required for GABA_A receptor assembly. *Journal of Biological Chemistry*, 283(44), 29740–29752.
<https://doi.org/10.1074/jbc.M802856200>
- Lomazzo, E., MacArthur, L., Yasuda, R. P., Wolfe, B. B., & Kellar, K. J. (2010). Quantitative analysis of the heteromeric neuronal nicotinic receptors in the rat

- hippocampus. *Journal of Neurochemistry*, 115(3), 625. <https://doi.org/10.1111/J.1471-4159.2010.06967.X>
- Lummis, S. C. R., Thompson, A. J., Bencherif, M., & Lester, H. A. (2011). *Varenicline Is a Potent Agonist of the Human 5-Hydroxytryptamine 3 Receptor □ S.* <https://doi.org/10.1124/jpet.111.185306>
- Luo, Jiansong, Busillo, J. M., & Benovic, J. L. (2008). M3 Muscarinic Acetylcholine Receptor-Mediated Signaling Is Regulated by Distinct Mechanisms. *Molecular Pharmacology*, 74(2), 338–347. <https://doi.org/10.1124/MOL.107.044750>
- Luo, Jie, Taylor, P., Losen, M., de Baets, M. H., Shelton, G. D., & Lindstrom, J. (2009). Main Immunogenic Region Structure Promotes Binding of Conformation-Dependent Myasthenia Gravis Autoantibodies, Nicotinic Acetylcholine Receptor Conformation Maturation, and Agonist Sensitivity. *Journal of Neuroscience*, 29(44), 13898–13908. <https://doi.org/10.1523/JNEUROSCI.2833-09.2009>
- Madeira, F., Park, Y. M., Lee, J., Buso, N., Gur, T., Madhusoodanan, N., Basutkar, P., Tivey, A. R. N., Potter, S. C., Finn, R. D., & Lopez, R. (2019). The EMBL-EBI search and sequence analysis tools APIs in 2019. *Nucleic Acids Research*, 47(W1), W636–W641. <https://doi.org/10.1093/NAR/GKZ268>
- Maricq, A. V., Peterson, A. S., Brake, A. J., Myers, R. M., & Julius, D. (1991). Primary structure and functional expression of the 5HT3 receptor, a serotonin-gated ion channel. *Science*, 254(5030), 432–437. <https://doi.org/10.1126/science.1718042>
- Marubio, L. M., Arroyo-Jimenez, M. D. M., Cordero-Erausquin, M., Léna, C., Le Novère, N., De Kerchove d'Exaerde, A., Huchet, M., Damaj, M. I., & Changeux, J. P. (1999). Reduced antinociception in mice lacking neuronal nicotinic receptor subunits. *Nature* 1999 398:6730, 398(6730), 805–810. <https://doi.org/10.1038/19756>
- Matta, J. A., Gu, S., Davini, W. B., Lord, B., Siuda, E. R., Harrington, A. W., & Bredt, D. S. (2017). NACHO Mediates Nicotinic Acetylcholine Receptor Function throughout the Brain. *Cell Reports*, 19(4), 688–696. <https://doi.org/10.1016/j.celrep.2017.04.008>

- Mazzaferro, S., Whiteman, S. T., Alcaino, C., Beyder, A., & Sine, S. M. (2021). NACHO and 14-3-3 promote expression of distinct subunit stoichiometries of the $\alpha 4\beta 2$ acetylcholine receptor. *Cellular and Molecular Life Sciences : CMLS*, 78(4), 1565. <https://doi.org/10.1007/S00018-020-03592-X>
- McSpadden, L. C., Nguyen, H., & Bursac, N. (2012). Size and ionic currents of unexcitable cells coupled to cardiomyocytes distinctly modulate cardiac action potential shape and pacemaking activity in micropatterned cell pairs. *Circulation: Arrhythmia and Electrophysiology*, 5(4), 821–830. <https://doi.org/10.1161/CIRCEP.111.969329>
- Mesoy, S., Jeffreys, J., & Lummis, S. C. R. (2019). Characterization of Residues in the 5-HT 3 Receptor M4 Region That Contribute to Function. *ACS Chemical Neuroscience*. <https://doi.org/10.1021/acschemneuro.8b00603>
- Mesoy, S. M., & Lummis, S. C. R. (2021). M4, the Outermost Helix, is Extensively Involved in Opening of the $\alpha 4\beta 2$ nACh Receptor. *ACS Chemical Neuroscience*, 12(1), 133–139. <https://doi.org/10.1021/acschemneuro.0c00618>
- Mihalak, K. B., Carroll, F. I., & Luetje, C. W. (2006). Varenicline Is a Partial Agonist at $\alpha 4\beta 2$ and a Full Agonist at $\alpha 7$ Neuronal Nicotinic Receptors. *Molecular Pharmacology*, 70(3), 801–805. <https://doi.org/10.1124/MOL.106.025130>
- Mitra, A., Bailey, T. D., & Auerbach, A. L. (2004). Structural dynamics of the M4 transmembrane segment during acetylcholine receptor gating. *Structure*, 12(10), 1909–1918. <https://doi.org/10.1016/j.str.2004.08.004>
- Miyake, A., Mochizuki, S., Takemoto, Y., & Akuzawa, S. (1995). Molecular cloning of human 5-hydroxytryptamine3 receptor: heterogeneity in distribution and function among species. *Molecular Pharmacology*, 48(3).
- Monk, S. A., Williams, J. M., Hope, A. G., & Barnes, N. M. (2004). Identification and importance of N-glycosylation of the human 5-hydroxytryptamine 3A receptor subunit. *Biochemical Pharmacology*, 68(9), 1787–1796. <https://doi.org/10.1016/j.bcp.2004.06.034>

- Morales-Perez, C. L., Noviello, C. M., & Hibbs, R. E. (2016). Manipulation of subunit stoichiometry in heteromeric membrane proteins. *Structure (London, England : 1993)*, 24(5), 797. <https://doi.org/10.1016/J.STR.2016.03.004>
- Nashmi, R., Dickinson, M. E., Mckinney, S., Jareb, M., Labarca, C., Fraser, S. E., & Lester, H. A. (2003). *Assembly of 42 Nicotinic Acetylcholine Receptors Assessed with Functional Fluorescently Labeled Subunits: Effects of Localization, Trafficking, and Nicotine-Induced Upregulation in Clonal Mammalian Cells and in Cultured Midbrain Neurons.*
- Nemecz, Á., Prevost, M. S., Menny, A., & Corringer, P.-J. (2016). Emerging Molecular Mechanisms of Signal Transduction in Pentameric Ligand-Gated Ion Channels. *Neuron*, 90(3), 452–470. <https://doi.org/10.1016/j.neuron.2016.03.032>
- Nguyen, M., Alfonso, A., Johnson, C. D., & Rand, J. B. (1995). Caenorhabditis elegans mutants resistant to inhibitors of acetylcholinesterase. *Genetics*, 140(2), 527–535. <https://doi.org/10.1093/genetics/140.2.527>
- Niesler, B., Walstab, J., Combrink, S., Moller, D., Kapeller, J., Rietdorf, J., Bonisch, H., Gothert, M., Rappold, G., & Bruss, M. (2007). Characterization of the Novel Human Serotonin Receptor Subunits 5-HT3C, 5-HT3D, and 5-HT3E. *Molecular Pharmacology*, 72(1), 8–17. <https://doi.org/10.1124/mol.106.032144>
- Niesler, B., Weiss, B., Fischer, C., Nöthen, M. M., Propping, P., Bondy, B., Rietschel, M., Maier, W., Albus, M., Franzek, E., & Rappold, G. A. (2001). Serotonin receptor gene HTR3A variants in schizophrenic and bipolar affective patients. *Pharmacogenetics*, 11(1), 21–27. <https://doi.org/10.1097/00008571-200102000-00003>
- Niesler, Beate, Frank, B., Kapeller, J., & Rappold, G. A. (2003). Cloning, physical mapping and expression analysis of the human 5-HT3 serotonin receptor-like genes HTR3C, HTR3D and HTR3E. *Gene*, 310(1–2), 101–111. [https://doi.org/10.1016/S0378-1119\(03\)00503-1](https://doi.org/10.1016/S0378-1119(03)00503-1)
- Nievas, G. A. F., Barrantes, F. J., & Antolini, S. S. (2008). Modulation of nicotinic acetylcholine receptor conformational state by free fatty acids and steroids. *Journal of*

- Biological Chemistry*, 283(31), 21478–21486. <https://doi.org/10.1074/jbc.M800345200>
- Noviello, C. M., Gharpure, A., Mukhtasimova, N., Cabuco, R., Baxter, L., Borek, D., Sine, S. M., & Hibbs, R. E. (2021). Structure and gating mechanism of the $\alpha 7$ nicotinic acetylcholine receptor. *Cell*. <https://doi.org/10.1016/j.cell.2021.02.049>
- Opekarová, M., & Tanner, W. (2003). Specific lipid requirements of membrane proteins - A putative bottleneck in heterologous expression. In *Biochimica et Biophysica Acta - Biomembranes* (Vol. 1610, Issue 1, pp. 11–22). Elsevier. [https://doi.org/10.1016/S0005-2736\(02\)00708-3](https://doi.org/10.1016/S0005-2736(02)00708-3)
- Ortiz-Acevedo, A., Melendez, M., Asseo, A. M., Biaggi, N., Rojas, L. V., & Lasalde-Dominicci, J. A. (2004). Tryptophan scanning mutagenesis of the γ M4 transmembrane domain of the acetylcholine receptor from *Torpedo californica*. *Journal of Biological Chemistry*, 279(40), 42250–42257. <https://doi.org/10.1074/jbc.M405132200>
- Panicker, S., Cruz, H., Arrabit, C., & Slesinger, P. A. (2002). Evidence for a centrally located gate in the pore of a serotonin-gated ion channel. *Journal of Neuroscience*, 22(5), 1629–1639. <https://doi.org/10.1523/jneurosci.22-05-01629.2002>
- Patel, D., Zhang, X., & Veenstra, R. D. (2014). Connexin hemichannel and pannexin channel electrophysiology: How do they differ? *FEBS Letters*, 588(8), 1372. <https://doi.org/10.1016/j.febslet.2013.12.023>
- Polovinkin, L., Hassaine, G., Perot, J., Neumann, E., Jensen, A. A., Lefebvre, S. N., Corringer, P. J., Neyton, J., Chipot, C., Dehez, F., Schoehn, G., & Nury, H. (2018). Conformational transitions of the serotonin 5-HT3 receptor. In *Nature* (Vol. 563, Issue 7730, pp. 275–279). Nature Publishing Group. <https://doi.org/10.1038/s41586-018-0672-3>
- Pons, S., Sallette, J., Bourgeois, J. P., Taly, A., Changeux, J. P., & Devillers-Thiery, A. (2004). Critical role of the C-terminal segment in the maturation and export to the cell surface of the homopentameric alpha7-5HT3A receptor. *European Journal of Neuroscience*, 20(8), 2022–2030. <https://doi.org/10.1111/j.1460-9568.2004.03673.x>

- Potter, A., Corwin, J., Lang, J., Piasecki, M., Lenox, R., & Newhouse, P. A. (1999). Acute effects of the selective cholinergic channel activator (nicotinic agonist) ABT-418 in Alzheimer's disease. In *Psychopharmacology* (Vol. 142).
- Price, K. L., Hirayama, Y., & Lummis, S. C. R. (2017). Subtle Differences among 5-HT3AC, 5-HT3AD, and 5-HT3AE Receptors Are Revealed by Partial Agonists. *ACS Chemical Neuroscience*, 8(5), 1085–1091. <https://doi.org/10.1021/acschemneuro.6b00416>
- Price, K. L., & Lummis, S. C. R. (2004). The role of tyrosine residues in the extracellular domain of the 5-hydroxytryptamine3 receptor. *The Journal of Biological Chemistry*, 279(22), 23294–23301. <https://doi.org/10.1074/jbc.M314075200>
- Rankin, S. E., Addona, G. H., Kloczewiak, M. A., Bugge, B., & Miller, K. W. (1997). The cholesterol dependence of activation and fast desensitization of the nicotinic acetylcholine receptor. *Biophysical Journal*, 73(5), 2446–2455. [https://doi.org/10.1016/S0006-3495\(97\)78273-0](https://doi.org/10.1016/S0006-3495(97)78273-0)
- Raymond, C., Tom, R., Perret, S., Moussouami, P., L'Abbé, D., St-Laurent, G., & Durocher, Y. (2011). A simplified polyethylenimine-mediated transfection process for large-scale and high-throughput applications. *Methods*, 55(1), 44–51. <https://doi.org/10.1016/J.YMETH.2011.04.002>
- Reddi, R., Singarapu, K. K., Pal, D., & Addlagatta, A. (2016). The unique functional role of the C–H···S hydrogen bond in the substrate specificity and enzyme catalysis of type 1 methionine aminopeptidase. *Molecular BioSystems*, 12(8), 2408–2416. <https://doi.org/10.1039/C6MB00259E>
- Reeves, D C, Goren, E. N., Akabas, M. H., & Lummis, S. C. (2001). Structural and electrostatic properties of the 5-HT3 receptor pore revealed by substituted cysteine accessibility mutagenesis. *The Journal of Biological Chemistry*, 276(45), 42035–42042. <https://doi.org/10.1074/jbc.M106066200>
- Reeves, David C., Goren, E. N., Akabas, M. H., & Lummis, S. C. R. (2001). Structural and Electrostatic Properties of the 5-HT3 Receptor Pore Revealed by Substituted Cysteine Accessibility Mutagenesis. *Journal of Biological Chemistry*, 276(45), 42035–42042.

- <https://doi.org/10.1074/jbc.M106066200>
- Ren, X. Q., Cheng, S. Bin, Treuil, M. W., Mukherjee, J., Rao, J., Braunewell, K. H., Lindstrom, J. M., & Anand, R. (2005). Structural Determinants of $\alpha 4\beta 2$ Nicotinic Acetylcholine Receptor Trafficking. *Journal of Neuroscience*, 25(28), 6676–6686. <https://doi.org/10.1523/JNEUROSCI.1079-05.2005>
- Reyes-Ruiz, J. M., Ochoa-de la Paz, L. D., Martínez-Torres, A., & Miledi, R. (2010). Functional impact of serial deletions at the C-terminus of the human GABA $\rho 1$ receptor. *Biochimica et Biophysica Acta (BBA) - Biomembranes*, 1798(5), 1002–1007. <https://doi.org/10.1016/J.BBAMEM.2009.12.021>
- Richardson, B. P., Engel, G., Donatsch, P., & Stadler, P. A. (1985). Identification of serotonin M-receptor subtypes and their specific blockade by a new class of drugs. *Nature* 1985 316:6024, 316(6024), 126–131. <https://doi.org/10.1038/316126a0>
- Roccamo, A. M., Barrantes, F. J., Bouzat, C., & Garbus, I. (1998). Mutations at lipid-exposed residues of the acetylcholine receptor affect its gating kinetics. *Mol.Pharmacol.*, 54(1), 146–153. <https://doi.org/10.1124/MOL.54.1.146>
- Santiago, J., Guzmán, G. R., Rojas, L. V., Martí, R., Asmar-Rovira, G. A., Santana, L. F., McNamee, M., & Lasalde-Dominicci, J. A. (2001). Probing the Effects of Membrane Cholesterol in the Torpedo californica Acetylcholine Receptor and the Novel Lipid-exposed Mutation α C418W in Xenopus Oocytes. *Journal of Biological Chemistry*, 276(49), 46523–46532. <https://doi.org/10.1074/jbc.M104563200>
- Shaw, G., Morse, S., Ararat, M., & Graham, F. L. (2002). Preferential transformation of human neuronal cells by human adenoviruses and the origin of HEK 293 cells. *The FASEB Journal*, 16(8), 869–871. <https://doi.org/10.1096/FJ.01-0995FJE>
- Shen, X.-M. M., Deymeer, F., Sine, S. M., & Engel, A. G. (2006). Slow-channel mutation in acetylcholine receptor α M4 domain and its efficient knockdown. *Annals of Neurology*, 60(1), 128–136. <https://doi.org/10.1002/ana.20861>
- Sigel, E. (1990). Use of Xenopus Oocytes for the Functional Expression of Plasma

- Membrane Proteins. *J. Membrane Biol.*, 117, 201–221.
- Smit-Rigter, L. A., Wadman, W. J., & van Hooft, J. A. (2010). Impaired social behavior in 5-HT3A receptor knockout mice. *Frontiers in Behavioral Neuroscience*, 4(NOV), 169. [https://doi.org/10.3389/FNBEH.2010.00169/BIBTEX](https://doi.org/10.3389/FNBEH.2010.00169)
- Spurny, R., Debaveye, S., Farinha, A., Veys, K., Vos, A. M., Gossas, T., Atack, J., Bertrand, S., Bertrand, D., Danielson, U. H., Tresadern, G., & Ulens, C. (2015). Molecular blueprint of allosteric binding sites in a homologue of the agonist-binding domain of the $\alpha 7$ nicotinic acetylcholine receptor. *Proceedings of the National Academy of Sciences*, 112(19), E2543–E2552. <https://doi.org/10.1073/pnas.1418289112>
- Stewart, D. S., Hotta, M., Li, G. D., Desai, R., Chiara, D. C., Olsen, R. W., & Forman, S. A. (2013). Cysteine Substitutions Define Etomidate Binding and Gating Linkages in the α -M1 Domain of γ -Aminobutyric Acid Type A (GABA A) Receptors. *Journal of Biological Chemistry*, 288(42), 30373–30386. <https://doi.org/10.1074/JBC.M113.494583>
- Stith, B. J., Hall, J., Ayres, P., Waggoner, L., Moore, J. D., & Shaw, W. A. (2000). Quantification of major classes of Xenopus phospholipids by high performance liquid chromatography with evaporative light scattering detection. *Journal of Lipid Research*, 41(9), 1448–1454. [https://doi.org/10.1016/S0022-2275\(20\)33457-X](https://doi.org/10.1016/S0022-2275(20)33457-X)
- Sugai, T., Suzuki, Y., Sawamura, K., Fukui, N., Inoue, Y., & Someya, T. (2006). The effect of 5-hydroxytryptamine 3A and 3B receptor genes on nausea induced by paroxetine. *The Pharmacogenomics Journal* 2006 6:5, 6(5), 351–356. <https://doi.org/10.1038/sj.tpj.6500382>
- Sumikawa, K. (1992). Sequences on the N-terminus of ACh receptor subunits regulate their assembly. *Molecular Brain Research*, 13(4), 349–353. [https://doi.org/10.1016/0169-328X\(92\)90218-Z](https://doi.org/10.1016/0169-328X(92)90218-Z)
- Sun, J., Comeau, J. F., & Baenziger, J. E. (2017). Probing the structure of the uncoupled nicotinic acetylcholine receptor. *Biochimica et Biophysica Acta - Biomembranes*, 1859(2), 146–154. <https://doi.org/10.1016/j.bbamem.2016.11.009>

- Suzuki, R., Rahman, W., Hunt, S. P., & Dickenson, A. H. (2004). Descending facilitatory control of mechanically evoked responses is enhanced in deep dorsal horn neurones following peripheral nerve injury. *Brain Research*, 1019(1–2), 68–76. <https://doi.org/10.1016/J.BRAINRES.2004.05.108>
- Taly, A., Corringer, P. J., Guedin, D., Lestage, P., & Changeux, J. P. (2009). Nicotinic receptors: Allosteric transitions and therapeutic targets in the nervous system. In *Nature Reviews Drug Discovery* (Vol. 8, Issue 9, pp. 733–750). <https://doi.org/10.1038/nrd2927>
- Tamamizu, S., Guzmán, G. R., Santiago, J., Rojas, L. V., McNamee, M. G., & Lasalde-Dominicci, J. A. (2000). Functional effects of periodic tryptophan substitutions in the alpha M4 transmembrane domain of the *Torpedo californica* nicotinic acetylcholine receptor. *Biochemistry*, 39(16), 4666–4673. <https://doi.org/bi992835w> [pii]
- Tang, B., & Lummis, S. C. R. (2018). The roles of aromatic residues in the glycine receptor transmembrane domain. *BMC Neuroscience*, 19(1), 53. <https://doi.org/10.1186/s12868-018-0454-8>
- Tapper, A. R., McKinney, S. L., Nashmi, R., Schwarz, J., Deshpande, P., Labarca, C., Whiteaker, P., Marks, M. J., Collins, A. C., & Lester, H. A. (2004). Nicotine activation of $\alpha 4^*$ receptors: Sufficient for reward, tolerance, and sensitization. *Science*, 306(5698), 1029–1032. <https://doi.org/10.1126/science.1099420>
- Therien, J. P. D., & Baenziger, J. E. (2017). Pentameric ligand-gated ion channels exhibit distinct transmembrane domain archetypes for folding/expression and function. *Scientific Reports*, 7(1), 450. <https://doi.org/10.1038/s41598-017-00573-2>
- Theriot, J., & Ashurst, J. V. (2019). Antiemetic Serotonin-5-HT3 Receptor Blockers. In *StatPearls*. StatPearls Publishing. <https://www.ncbi.nlm.nih.gov/books/NBK513318/>
- Thompson, A J, & Lummis, S. C. R. (2013). Discriminating between 5-HT3A and 5-HT3AB receptors. In *British Journal of Pharmacology* (Vol. 169, Issue 4, pp. 736–747). Wiley-Blackwell. <https://doi.org/10.1111/bph.12166>
- Thompson, Andrew J., Sullivan, N. L., & Lummis, S. C. R. (2006). Characterization of 5-

- HT3 receptor mutations identified in schizophrenic patients. *Journal of Molecular Neuroscience*, 30(3), 273–281. <https://doi.org/10.1385/JMN:30:3:273>
- Thompson, M. J., & Baenziger, J. E. (2020). Structural basis for the modulation of pentameric ligand-gated ion channel function by lipids. *Biochimica et Biophysica Acta (BBA) - Biomembranes*, 183304. <https://doi.org/10.1016/j.bbamem.2020.183304>
- Thompson, M. J., Domville, J. A., & Baenziger, J. E. (2020). The functional role of the α M4 transmembrane helix in the muscle nicotinic acetylcholine receptor probed through mutagenesis and co-evolutionary analyses. *Journal of Biological Chemistry*, jbc.RA120.013751. <https://doi.org/10.1074/jbc.RA120.013751>
- Tobimatsu, T., Fujita, Y., Fukuda, K., Tanaka, K. ichi, Mori, Y., Konno, T., Mishina, M., & Numa, S. (1987). Effects of substitution of putative transmembrane segments on nicotinic acetylcholine receptor function. *FEBS Letters*, 222(1), 56–62. [https://doi.org/10.1016/0014-5793\(87\)80191-6](https://doi.org/10.1016/0014-5793(87)80191-6)
- Tong, A., Hsu, F. F., Schmidpeter, P. A., Nimigean, C. M., Sharp, L., Brannigan, G., & Cheng, W. W. (2019). Direct binding of phosphatidylglycerol at specific sites modulates desensitization of a Ligand-gated ion channel. *eLife*, 8. <https://doi.org/10.7554/eLife.50766>
- Tremblay, P. B., Kaiser, R., Sezer, O., Rösler, N., Schelenz, C., Possinger, K., Roots, I., & Brockmöller, J. (2003). Variations in the 5-hydroxytryptamine type 3B receptor gene as predictors of the efficacy of antiemetic treatment in cancer patients. *Journal of Clinical Oncology*, 21(11), 2147–2155. <https://doi.org/10.1200/JCO.2003.05.164>
- Vicente-Agulló, F., Rovira, J. C., Campos-Caro, A., Rodríguez-Ferrer, C., Ballesta, J. J., Sala, S., Sala, F., & Criado, M. (1996). Acetylcholine receptor subunit homomer formation requires compatibility between amino acid residues of the M 1 and M2 transmembrane segments. *FEBS Letters*, 399(1–2), 83–86. [https://doi.org/10.1016/S0014-5793\(96\)01291-4](https://doi.org/10.1016/S0014-5793(96)01291-4)
- Walsh, R. M., Roh, S. H., Gharpure, A., Morales-Perez, C. L., Teng, J., & Hibbs, R. E. (2018). Structural principles of distinct assemblies of the human α 4 β 2 nicotinic receptor.

- Nature*, 557(7704), 261–265. <https://doi.org/10.1038/s41586-018-0081-7>
- Walstab, J., Hammer, C., Lasitschka, F., Möller, D., Connolly, C. N., Rappold, G., Brüss, M., Bönisch, H., & Niesler, B. (2010). RIC-3 exclusively enhances the surface expression of human homomeric 5-hydroxytryptamine type 3A (5-HT3A) receptors despite direct interactions with 5-HT3A, -C, -D, and -E subunits. *Journal of Biological Chemistry*, 285(35), 26956–26965. <https://doi.org/10.1074/jbc.M110.122838>
- Walstab, J., Rappold, G., & Niesler, B. (2010). 5-HT3 receptors: Role in disease and target of drugs. *Pharmacology & Therapeutics*, 128(1), 146–169.
<https://doi.org/10.1016/j.pharmthera.2010.07.001>
- Wanamaker, C. P., & Green, W. N. (2005). N-Linked Glycosylation Is Required for Nicotinic Receptor Assembly but Not for Subunit Associations with Calnexin. *The Journal of Biological Chemistry*, 280(40), 33800.
<https://doi.org/10.1074/JBC.M501813200>
- Waterhouse, A. M., Procter, J. B., Martin, D. M. A., Clamp, M., & Barton, G. J. (2009). Jalview Version 2—a multiple sequence alignment editor and analysis workbench. *Bioinformatics*, 25(9), 1189–1191.
<https://doi.org/10.1093/BIOINFORMATICS/BTP033>
- Williams, M. E., Burton, B., Urrutia, A., Shcherbatko, A., Chavez-Noriega, L. E., Cohen, C. J., & Aiyar, J. (2005). Ric-3 promotes functional expression of the nicotinic acetylcholine receptor $\alpha 7$ subunit in mammalian cells. *Journal of Biological Chemistry*, 280(2), 1257–1263. <https://doi.org/10.1074/jbc.M410039200>
- Wilson, G. G., & Karlin, A. (1998). The Location of the Gate in the Acetylcholine Receptor Channel M2, and M3), a large cytoplasmic loop, a fourth mem-brane-spanning segment (M4), and a short, extracellular tail. The two ACh binding sites are formed in the extracel. *Neuron*, 20, 1269–1281.
- Xiu, X., Puskar, N. L., Shanata, J. A. P., Lester, H. A., & Dougherty, D. A. (2009). Nicotine binding to brain receptors requires a strong cation- interaction. *Nature*, 458(7237), 534–537. <https://doi.org/10.1038/nature07768>

- Xu, M., & Akabas, M. H. (1996). Identification of channel-lining residues in the M2 membrane-spanning segment of the GABA(A) receptor alpha1 subunit. *The Journal of General Physiology*, 107(2), 195–205. <https://doi.org/10.1085/jgp.107.2.195>
- Yamada, K., Hattori, E., Iwayama, Y., Ohnishi, T., Ohba, H., Toyota, T., Takao, H., Minabe, Y., Nakatani, N., Higuchi, T., Detera-Wadleigh, S. D., & Yoshikawa, T. (2006). Distinguishable Haplotype Blocks in the HTR3A and HTR3B Region in the Japanese Reveal Evidence of Association of HTR3B with Female Major Depression. *Biological Psychiatry*, 60(2), 192–201. <https://doi.org/10.1016/J.BIOPSYCH.2005.11.008>
- Zeitz, K. P., Guy, N., Malmberg, A. B., Dirajlal, S., Martin, W. J., Sun, L., Bonhaus, D. W., Stucky, C. L., Julius, D., & Basbaum, A. I. (2002). The 5-HT3 Subtype of Serotonin Receptor Contributes to Nociceptive Processing via a Novel Subset of Myelinated and Unmyelinated Nociceptors. *The Journal of Neuroscience*, 22(3), 1010. <https://doi.org/10.1523/JNEUROSCI.22-03-01010.2002>